Analysing nuclear import of Parvoviruses - Effects of parvovirus H-1 on the nuclear envelope (NE)

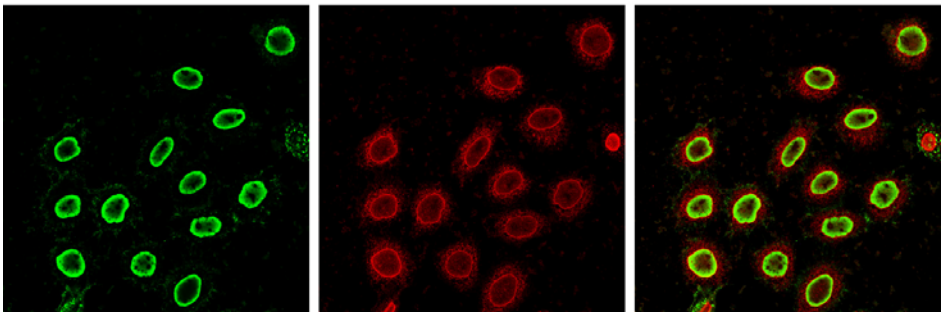

Inauguraldissertation

Zur Erlangung des Grades
Doktor der Naturwissenschaften
Dr. rer. nat.
des Fachbereiches Biologie und Chemie
der Justus-Liebig-Universität Gießen

vorgelegt von M.Sc. **Manvi Porwal**
aus Indien

Gießen
2007

This project was funded by DFG (Deutsche Forschungsgemeinschaft) with in the Graduiertenkolleg, Biochemie von Nucleoproteinkomplexen and the Universite Victor Segalen Bordeaux 2.

Aus dem Institute für Medizinische Virologie
am Fachbereich Humanmedizin
der Justus-Liebig-Universität Gießen

Analysing nuclear import of Parvoviruses - Effects of parvovirus H-1 on the nuclear envelope (NE)

Inauguraldissertation

Zur Erlangung des Grades
Doktor der Naturwissenschaften
Dr. rer. nat.
des Fachbereiches Biologie und Chemie
der Justus-Liebig-Universität Gießen

vorgelegt von M.Sc. **Manvi Porwal**
aus Indien

Gießen
2007

Mit Genehmigung des Fachbereichs der Justus-Liebig-Universität Gießen

Dean: Prof. Dr. Wolfgang Weidner

Supervisor: Prof. Dr. Michael Kann

Reviewer: Prof. Dr. Alfred M Pingoud

DECLARATION

I, Manvi Porwal, certify that the work presented in the thesis is original work conducted by myself, unless otherwise specified, under the supervision of Prof. Dr. Michael Kann. All sources of information have been specifically acknowledged. No part of this thesis has been submitted for a degree at any other university.

Date: **(Manvi Porwal)**

Place:

Abbreviations

°C	Degree centigrade
aa	Aminoacids
ATP	Adenosine triphosphate
bp	Base pair
BSA	Bovine serum albumin
CPV	Canine Parvovirus
C-terminal	Carboxy terminal
DMEM	Dulbecco's Modified Eagle Medium
DMSO	Dimethylsulfoxide
DNA	Deoxyribonucleic Acid
DTT	Dithiothreitol
E.coli	Escherichia coli
ECL	Enhanced Chemiluminescence
EDTA	Ethylene-diamintetraaceticacid
EGTA	(Ethylenebis(oxyethylennitrilo))tetraaceticacid
ER	Endoplasmic reticulum
FCS	Fetal calf serum
FG repeat	Phenylalanine glycine repeat
FITC	Fluorescein Isothiocynate
kDa	Kilo-Dalton
Min	Minute
MVM	Minute virus of mice
NE	Nuclear envelope
NEBD	Nuclear envelope breakdown
NES	Nuclear export signal
NLS	Nuclear localization signal
NP-40	Nonidet P-40
NPC	Nuclear pore complex
NS Proteins	Non structural proteins
N-terminal	Amino-terminal
Nup	Nucleoporin
PAGE	Polyacrylamide gel electrophorosis
PBS	Phosphate buffer saline
PFA	Paraformaldehyde
PKC	Protein kinase C
POD	Peroxidase
PV	Parvovirus
PVDF	Polyvinylidene fluoride
RNA	Ribonucleic acid
rpm	Rotations per minute
RRL	Rabbit reticulate lysate
RT	Room temperature
SDS	Sodium dodecylsulphate
ss-DNA	Single-stranded DNA
SV40	Simian virus 40
TB	Transport buffer
Tris	Trishydroxymethyl aminomethane
VP	Viral proteins
WGA	Wheat germ agglutinin

Index

1. Introduction 1
2. Review of the literature 3
2.1 Overview:- How viruses enter into animal cells 3
2.1.1 Attachment 3
2.1.2 Penetration 3
2.1.3 Viral uncoating 4
2.1.4 Entry 4
2.1.5 Assembly, maturation and release of progeny virus 4
2.2 Overview:- Parvovirus H-1 5
2.2.1 Parvovirus infection and diseases 5
2.2.2 Taxonomy 5
2.2.3 Virus structure 5
2.2.3.1 Morphology 5
2.2.3.2 The virion 5
2.2.3.3 Genome 6
2.2.3.4 Proteins 6
2.2.4 Virus life cycle 6
2.2.5 Genome organization and gene expression 7
2.2.6 Use of parvoviruses in medicines 9
2.2.7 Parvovirus in gene therapy 10
2.3 Overview:- Mechanisms of nuclear transport 11
2.3.1 Endocytosis 11
2.3.2 Acidification 13
2.3.3 Signal- mediated nuclear import 15
2.3.4 The Nuclear Pore Complex (NPC) 15
2.3.5 Nuclear localisation signal (NLS) receptors and import factor recycling 16
2.3.6 Nuclear envelope (NE) and nuclear envelope breakdown (NEBD) 17
2.3.6.1 Mitosis 17
2.3.6.2 Apoptosis 18
3. Aim of the project 22
4. Material and Methods 23
4.1 Materials 23
4.1.1 Antibiotics, Chemicals and Enzymes 23
4.1.2 Inhibitors 24
4.1.3 Antibodies and Beads 24
4.1.4 Cell Lines 24
4.1.5 Primers 25
4.1.6 Plasmid 25
4.1.7 Equipments 25
4.1.8 Kits and Extras 25
4.1.9 Buffers and Solutions 26
4.2 Methods 28
4.2.1 Cell Culture 28
4.2.2 Virus preparation and Virus purification 28
4.2.3 Localization of capsids 28
4.2.4 pH treated capsids 28
4.2.5 Indirect immunofluorescence 29
4.2.6 Confocal Laser Scanning microscopy 29
4.2.7 Co-immune precipitation 29
4.2.7.1 Co-immune precipitation of nups by progeny H-1 and vice-versa 29

4.2.7.2 Co-immune precipitation of importin α and anti capsid antibody 30
4.2.8 SDS gel electrophoresis 30
4.2.9 Western blot 30
4.2.9.1 Western blot (I) 30
4.2.9.2 Western blot (II) 30
4.2.10 Agarose gel electrophoresis 31
4.2.11 S7 Nuclease digestion of Parvovirus H-1 31
4.2.12 Gradient passed pH treated capsids 31
4.2.13 Proteinase K digestion 31
4.2.14 Phenol-chloroform-extraction 31
4.2.15 Determination of Parvovirus H-1 DNA with Real-Time-PCR 32
4.2.16 Permeabilized and non-permeabilized HeLa cells treated with H-1 virus 34
4.2.17 Phase contrast microscopy 34
4.2.18 Live cell microscopy 34
4.2.19 Confocal analysis and quantification of nuclear fluorescence 35
5. Results 36
5.1 Localisation of H-1 capsids 36
5.2 Time and dose dependent process 37
5.3 Effect of mRNA translocation inhibitors on nuclear capsids 37
5.4 To exclude the cross-talk of antibodies and overlapping of NPC and capsid stain 40
5.5 Interaction of nucleoporins with H-1 capsids 41
5.6 Effect of pH on H-1 capsids 42
5.7 Role of importin α on pH treated capsids 43
5.8 Detection of pH treated H-1 capsids by immunofluorescence 44
5.9 Kinetics of H-1 at different time course 45
5.10 Live cell microscopy with mock purified virus 47
5.11 Live cell microscopy of different parvoviruses 49
5.12 Release of substrate after H-1 induction 50
5.13 Analysis of nuclear degradation by EYFP lamin B receptor NRK cell line 51
5.14 Analysis by wide field microscopy 53
5.15 Effect of permeabilized YEFP lamin B receptor expressing cells upon H-1 56
5.16 H-1 treatment of non-permeabilized HeLa cells 57
5.17 Effect of NS1 protein on nuclear disruption 57
5.18 Kinetics of nuclear degradation at different temperatures 59
5.19 Role of ATP/ or GTP in NEBD 60
5.20 Role of apoptosis and mitosis in NEBD 61
5.21 Involvement of cytosolic proteins in live cell microscopy 63
5.22 Role of WGA at NEBD process 63
5.24 Live cell microscopy of phosphorylated HBV capsid 66
5.25 Role of apoptotic and mitotic markers on H-1 infected HeLa cells 67
5.26 Effect of apoptotic and mitotic inhibitors on synthesis and transport of progeny H-1 capsid 70
6. Discussion 72
7. Summary 78
8. Zusammenfassung 79
9. References 81
10. Acknowledgements 96
11. Curriculum Vitae 97

1. Introduction

Parvoviruses (PV) are small, non-enveloped DNA viruses that infect vertebrates and insects. They enter via endosomes and require low pH for penetration and productive infection (Basak.S and Tuner.H, 1992, Parker.JS and Parrish.CR, 2000). Following entry into the cell, the majority of the viruses appear to be retained in a perinuclear location (Bartlett.JS, et al, 2000 and Vihinen-Ranta.M, et al, 2000), possibly in perinuclear recycling endosomes.

Parvoviruses are classified into three genera, *Parvoviruses* (autonomous parvoviruses), *Erythrovirus* (human parvovirus, B19), and *Dependovirus* (adeno-associated virus, AAV). Autonomous parvoviruses infect a wide varity of mammalian and avian hosts (minute virus of mice, canine parvovirus, Feline parvovirus, Aleutian mink disease virus and Parvovirus H-1). Parvoviruses are lytic viruses, i.e necessary for leaving the cells. This lytic activity has been ascribed, at least in part, to the non-structural (NS) viral proteins (Caillet-Fauquet.P, et al, 1990 and Rayet.B, et al, 1998).

Parvovirus H-1 and Kilham rat virus (KRV) were first identified in the late 1950s and belong to the rodent family which infects hamster/rat. Infection with rat H-1 virus can be lethal in fetal or perinatal animals, probably due to high numbers of mitotically active cells that serve as targets for cytolytic viral replication (Ball-Goodrich.LJ, et al, 2002). Entry of viruses into host cells starts by binding to the cell surface receptors, followed by penetration across the cellular membrane. Although cell entry of enveloped viruses is well characterized, but the mechanisms of viral entry and nuclear targeting of non-enveloped viruses are still poorly understood.

Parvoviruses exhibit an icosahedral structure formed by the two capsid proteins VP1 and VP2. 80% of the capsid proteins consists of VP2 and 20% of the larger VP1. VP1 comprises the entire amino acids sequence of VP2 and plus an additional terminal domain of 150-230 amino acids. Due to the mode of genome replication a viral protein termed NS1 is covalently linked to the viral DNA genome (Cotmore.SF, et al, 1998). NS1 is exposed to the surface of the virus (Cotmore.SF, et al, 1989) but consistent with its function in replication – only in DNA containing capsids and not in empty ones. Parvoviruses (PVs) replicate with in the cell nuclei using the eukaryotic DNA polymerases α or δ. PVs require cell division for replication but they enter the nucleus independent upon the disintegration of the nuclear envelope (NE) that occurs upon mitosis. As numerous other viruses, (e.g. influenza and adeno viruses (Whittaker.GR, et al, 2000) all parvoviruses being investigated infect the cells by endocytosis requiring acidification (Bartlett.JS, et al, 2000, Basak.S, et al, 1992 and Parker.JS, 2000). The decreasing pH causes structural changes as the cleavage of some VP2 proteins by cellular proteases. Furthermore the initially hidden N terminal domain of VP1 (VP1 unique part, VP1up) becomes exposed (Suikkanen.S, et al, 2003). This region exhibits a phospholipase A_2 (PLA_2) domain that catalyzes the hydrolysis of phospholipids at the 2-acyl ester position (Zadori.Z, et al, 2001). It was shown that PLA_2 is involved in the release of the capsid from the endosomal compartment into the cytosol (Suikkanen.S, et al, 2003, Zadori.Z, et al, 2003, Farr.GA and Zhang.LG, et al, 2005). This process is apparently inefficient as the vast majority of capsids end in the lysosomal compartment (Mani.B, et al, 2002) explaining the low ratio of virions to infectious units (~1:1000).

Escaping the endosome parvoviruses use the microtubule network for the centripetal transport (Suikkanen.S, et al, 2003 and Vihinen-Ranta.M, et al, 1998). The following step of nuclear import is a controversial topic. VP1up contains clusters of basic amino acids similar to “classical” nuclear localization signals (NLS). One of these clusters showed a nuclear import capacity when being fused to BSA (Vihinen-Ranta.M, et al, 1997). Consequently it was assumed that the entire capsid

pass the nuclear pore complex (NPC) as described for the capsid of the hepatitis B virus (Kann.M, et al, 1999, Rabe.B, et al, 2003). Being of small diameter, the parvovirus falls below the 39 nm transport limit of the pore (Pante.N and Kann.M, 2002).

However, others propose that the basic amino acids only form an NLS when being arranged in a trimeric form of one VP1 and two VP2 (Riolobos.L, et al, 2006) being dependent upon phosphorylation (Riolobos.L and Reguera.J 2006). This trimer however, is not result of acidification during parvovirus entry but is an assembly intermediate during synthesis of progeny virions. It was thus assumed that the exposure of this NLS contributes to the transport of the progeny capsid subunits into the nucleus where viral assembly occurs. Consistent with idea that another protein facilitates nuclear import of the viral genome are findings of Mani.B et al, who observed that genome and capsid proteins already dissociates in the endosomal / lysosomal compartment (Mani.B, et al, 2006). Following this scenario and considering that nucleic acids per se are not karyophilic, the genome attached NS1 should mediate the import. A corresponding NLS was identified on NS1 (Nuesch.JP, et al, 1993). Seemingly contradictory is a report that describes the removal of NS1 from the viral genome upon endocytosis (Cotmore.SF, et al, 1989) but it remains open whether this observation is related to capsids that are successfully infecting the cell or to those capsids ending in the lysosomal compartment.

A third pathway was described by Zadori et al, who assumed that the PLA_2 activity enables the parvoviral capsid to pass the nuclear envelope without using the NPC (Zadori.Z, et al, 2001). Seemingly consistent with this idea, MVM damages the NE after microinjection into the cytosol of *Xenopus laevis* oocytes (Cohen.S, et al, 2005). However, it must be considered, as these capsids have not undergone the pH induced structural change, they not exhibit the PLA_2 domain strongly suggesting a yet unknown mechanism of parvoviral nuclear entry. Infact this assumption is in agreement with the observation that the parvoviral PLA_2 induces only small pores into membranes allowing the diffusion of molecules of 3 kDa but retaining molecules of 10 kDa (Suikkanen.S, 2003).

The review literature of this thesis will briefly describe the features of cellular elements and their role in viral entry into the nucleus of the cell, as well as the processes of the viruses. The aim of my project is to investigate the mechanisms of the parvovirus H-1 entry since parvoviruses along with adenoviruses widely used as a major tool for gene therapy applications.

2. Review of the literature

2.1 Overview:- How viruses enter into animal cells

Replication of virus occurs within living cells and uses the cellular machinery for the synthesis of their genome and other components. To gain access, they have evolved a variety of mechanisms to deliver their genes and accessory proteins into the host cells. In brief, virions must attach to the cell surface, penetrate the cell, and become sufficiently uncoated to make its genome accessible to viral or host machinery for transcription or translation.

2.1.1 Attachment

Attachment constitutes the specific binding of a viral protein (the ligand) to a component of the cell surface (the receptor). The viral cellular receptors are mainly glycoproteins. Binding site of the viral receptor varies depending on the virus. Enveloped viruses bind to cell surface receptors by their envelope glycoproteins (Grewe.C, et al, 1990) while non-enveloped viruses have been described to use grooves, depressions, loops or spikes of the virion surface as their receptor binding sites (Marsh.M and Helenius.A, 1989). In addition to the direct binding of virus to the plasma membrane, viruses might bind to the cell surface through soluble proteins intermediates such as antibodies or β2-microglobulin (Marsh.M and Helenius.A, 1989). Attachment of the viruses to the cells in many instances leads to irreversible changes in the surface of the virion. However, when penetration does not take place, the virus can detach and adsorb to a different cell as shown by orthomyxoviruses and paramyxoviruses, which carry a neuraminidase (receptor destroying enzyme) on their surface. Elution of these viruses from their receptors takes place by cleaving the terminal neuraminic acid from the polysaccharide chains of the receptors (Mahon.PJ, et al, 1995).

2.1.2 Penetration

Viral penetration is an energy-dependent process. Some of the viruses surf on the surface until they reach to the confined zone after that attachment occurs and involves one of the three mechanisms: **(a)** translocation of the entire virus across the plasma membrane, **(b)** endocytosis of the virus particle resulting in accumulation of the virus particles inside cytoplasmic vesicles, and **(c)** fusion of the viron envelope with the cellular membrane. Non-enveloped viruses penetrate by the first two mechanisms.

Many viruses require exposure to an acidic pH during infectious entry (Marsh.M, et al, 1993). For example, influenza virus and semliki forest virus are well known example of enveloped viruses. They require the low pH (< 6) in the endosome to cause their glycoprotein spike complexes to undergo conformational changes needed for fusion of the viral envelope with endosomal membranes (Bullough.PA, et al, 1994, Kielian.M and Helenius.A, 1985). In the presence of drugs disrupting endosomal acidification processes, the infection caused by these viruses is blocked (Matlin.KS, et al, 1981, Kielian.M, 1995). Many non-enveloped viruses are also affected by these drugs. For example adenoviruses, rhinoviruses, reoviruses and parvoviruses require a low pH step for their productive infection. Infection by some pH-dependent viruses may be inhibited by indirect effects of these drug treatments on endosomal protease activation or on endosomal trafficking of viral particles (Clague.MJ, et al, 1994, Authier.FB, et al, 1996). Generally, viruses that require exposure to low pH for penetration enter their host cells by clathrin-mediated endocytosis to ensure the delivery to acidic organelles (Marsh.M and Pelchen- Matthews.A,

2000). Most viruses using endocytosis are adapted to escape from the early endosomes or the late endosomes to avoid the delivery to lysosomes, which would cause inactivation and degradation (Marsh.M and Helenius.A, 1989).

2.1.3 Viral uncoating

Penetrating into the cytoplasm in not merely enough for replication of many viral species, because most DNA viruses (except poxviruses), as well as some RNA species (influenza virus) replicate in the nucleus. The nucleus provides cellular factors needed for the amplification and transcription of their genomes as well as for the post transcriptional processing of viral mRNA. Therefore, these viruses have to transverse through the cytoplasm and enter the nucleus after penetrating the cellular membranes (Cullen.BR, 2001). Trafficking of cytoplasm depends on cytosolic filaments such as microtubules, actin filaments (Sodeik.B, 2000). The functional participation of the microtubules in cytoplasmic traffic has been reported for a number of viruses, and dynein-mediated transport has been described for adenoviruses (Leopold.PL, et al, 2000).

2.1.4 Entry

After reaching to the nucleus, viruses can wait until the cell undergoes mitosis, when the nuclear envelope is temporarily lost, allowing the viral genome to become part of newly assembled nucleus. Viruses using this strategy (many retroviruses) are able to replicate only in dividing cells. More commonly, the genome of incoming viruses is transported to the nucleus, through the nuclear envelope of the interphase nucleus allowing replication also in non-dividing cells (Whittaker.GR, et al, 2000). Nuclear pore complex (NPC) plays a critical and vital role in viral nuclear import processes. Active nuclear import is mediated by different nuclear transport receptors (importins or karyopherins). Only few viruses are small enough to pass through the NPCs with their capsid shells. Viruses have different strategies to circumvent this size limitation. Many of the viruses undergo partial or full disassembly before nuclear entry such as adenoviruses.

2.1.5 Assembly, maturation and release of progeny virus

Viruses choose different fundamental strategies for their assembly, maturation and to release the progeny capsids. In case of picornaviruses, reovirus, adenoviruses and parvoviruses, involves intracellular assembly and maturation. Adeno-and parvoviruses assemble in the nucleus. The releasing mechanism of progeny virus from the infected cell depends on the structure of the virus. It has been accepted in the parvoviruses that non-enveloped viruses are released by the lysis of the cells. However, there are few evidence exists for the release of some non-enveloped viruses without cell lysis, and one report indicates, polarised release of SV40 from the epithelial cells. In addition, few other examples like poliovirus, where cellular mechanisms used by viruses for the active release of non-enveloped viruses that are not the result of lysis of the host cell. Once the progeny viruses released, they can initiate infection in new cells, and a whole new round of virus replication and interaction with a host cell can begin.

2.2 Overview:- Parvovirus H-1

2.2.1 Parvovirus infection and diseases

Parvoviruses are wide spread throughout humans and animals including dogs and mice. Based on their lytic activity that facilitates progeny virus release they evoke a variety of different disease. The canine parvovirus (CPV) for instance causes enteric and mycardial diseases in dogs, the minute virus of mice (MVM) targets small intestine, lymphoid tissue, kidneys and cerebellum with sometimes devastating consequences as fetal death. There are two parvoviruses known to infect humans: B19 and the adeno-associated virus (AAV). While AAV is not related to any disease (Srivastava.A, 1994, Rabinowitz.JE, 2000), B19 causes a variety of different ailments.
The seroprevalence of B19 infections is 40 to 60% and most infections occur during childhood. At this stage of infection the most common illness is the erythema nodosum with rashes. Adults develop additional symptoms as joint pain or swelling, which may last several months. Due to the tropism of B19 for erythroid progenitor cells, fatal consequences occur when parvovirus B19 infection will happen to pregnant women. In 10% the unborn baby will develop severe anaemia resulting in a miscarriage. Haemolytical crises have been observed in patients with different forms of anaemia and in immune compromised patients, as HIV infected individuals. Here, B19 is an opportunistic pathogen causing not only severe anaemia but focal encephalitis (Gyllensten.K, et al, 1994). Today there is no vaccine or medicine that prevents parvovirus B19 infection.

2.2.2 Taxonomy

Viruses of parvoviridae family are divided in to two subfamilies 1. Parvovirinae, which infect vertebrates. 2. Densovirinae, infect insects. Both subfamilies are further divided into three genera (Berns.KI and Giraud.C, 1996). Parvovirinae have three genera *Parvovirus, Erythrovirus,* and *Dependovirus.* In case of AAVs (Adeno-associated virus) need helper virus (adenovirus, herpes virus) co-infection for their replication (Janik.JE, et al, 1981). In the absence of helper virus AAV virion is able to infect the host cell efficiently but the genome undergoes an incomplete replication and integrates into the host genome to establish latency (Kotin.RM, et al, 1990, Samulski.RJ, et al, 1991). Viruses of the genera *Parvovirus* and *Erythrovirus* are autonomous viruses replicating without helper virus infection. However, members of both genera needs functions of host cells supplied during cellular S phase for their DNA replication (Cotmore.SF and Tattersall.P, 1987).

2.2.3 Virus structure

2.2.3.1 Morphology

The three dimensional structures of several parvoviruses have been determined to atomic resolution by using X-ray crystallography. These studies revealed the presence of (i) spike protrusions at the icosahedral threefold axes, (ii) a cylindrical structure surrounded by a canyon like depression at about the five fold axes, and (iii) a dimple- like depression at the two fold axes (McKenna.R, et al, 1999). The analysis of these structures allowed several functional implications to be postulated, in particular regarding tissue tropism, antigenicity and DNA packaging.

2.2.3.2 The virion

The parvovirus virion has a relatively simple structure composed of only three proteins and a linear, single-stranded DNA molecule. The particle has icosahedral symmetry and a diameter of 18 to 26 nm. There are 60 protein subunits, consisting primarily of VP2. The main structural motif is 8 stranded β barrel composed of VP2, but much of the protein is present as large loops

connecting the strands in the β barrel structure (Kaufmann.B, et al, 2004). The particle has a molecular weight of 5.5 to 6.2 x 10^6. Approximately 50% of the mass protein and the remainder is DNA. Because of relatively high DNA-to-protein ratio, the buoyant density of the intact virion in CsCl is 1.39 to 1.42 g/cm^2. Due to the structurally simplicity, the virion is extremely resistant to inactivation. It is stable between pH 3 and 9 and at 56° C for 60 min. The virus can be inactivated by formalin, β-propriolactone, hydroxylamine and oxidizing agents (Cotmore.SF and Tattersall.P, 1987).

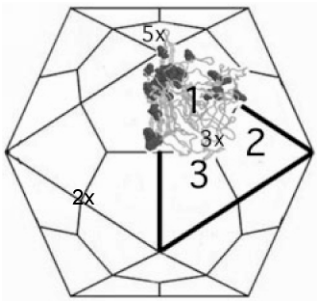

Figure 1: Schematic representation of parvovirus capsid. (Reguera.J, et al, 2004): Thick lines delimit 1 of the 20 identical trimeric subunits, and the three VP2 subunits within this trimer are numbered 1, 2, and 3. A ribbon model of the structure of one VP2 subunit has been superimposed.

2.2.3.3 Genome

The genome is a linear, single-stranded poly-deoxynucleotide chain. Several parvovirus DNAs have been completely sequenced. H-1 and MVM DNAs contain 5,176 and 5,084 bases. In general, autonomous parvoviruses encapsidate primarily strands of one polarity, which is complimentary to mRNAs. While AAV encapsidates strands of both polarities with equal frequency.

All parvovirus genomes have palindromic sequences at both the 5' and 3' termini of the virion strand. The palindromic sequence at the orientation of the 3' end of the virion strand of the most murine autonomous parvovirus DNAs is approximately 115 bases long. In the human parvovirus B19, these sequences appear to be more than 300 nucleotides in length.

2.2.3.4 Proteins

NS1 protein acts as a transactivator, covalently bound to a viral DNA, and believed to be release during endocytosis. NS2 protein is essential for viral replication and required for sufficient protein synthesis. VP1 comprises 15% of virion, and its coding sequence contains all of VP2 plus 140 additional N-terminal amino acids.VP2, is the predominant capsid protein, accounting for approximately 85% of the virion. VP3, a cleavage product of VP2, is present in small, varying amounts in DNA- containing virions (Ball-Goodrich.LJ, et al, 2002). VP2 and VP3 constitute the majority of capsid proteins in full virions, whereas empty capsids do not contain VP3 (Tattersall. P, et al, 1976).

2.2.4 Virus life cycle

The parvovirus H-1 and MVM bind to ubiquitous N- acetylneuraminic acid (sialyl)- containing glycoproteins located at the cell surface. So far, the cellular receptors were only identified for the human parvovirus B19 and for the related canine and feline parvoviruses (transferring receptor) (Brown. KE, et al, 1993 and Parker. JS, et al, 2001).

In the nucleus, single-stranded DNA is converted into a duplex replication form, a reaction that does not require virus-encoded proteins. This conversion reaction is strictly S-phase dependent, and it requires cyclin A and/or associated cdk2 kinase activities that are induced in late G1 and early S phases (Bashir.T, et al, 2000). Moreover, conversion was followed by the amplification of the duplex intermediate via multimeric forms (Cotmore. SF, et al, 1987). Duplex parvoviral DNA serves as a template for the synthesis of mRNAs and progeny single-stranded DNA to be packaged into empty capsids form in the nucleolus.

The observation that the mature virion is redistributed from the nucleolus into the nucleoplasm suggests that nucleolus function, perhaps cellular chaperon protein(s), is needed for genome packaging. Although parvovirus structure and composition are simple, its packaging pattern appears to have evolved along with that of adenovirus. The mature MVM virion has one molecule of NS1 covalently attached to the 5' end of the MVM genome, with the NS1 outside of the nucleocapsid.

The release of progeny virions of replicated parvovirus is usually associated with cell death. H-1 virus infection was shown to induce apoptosis in human promonocytic leukemic and hepatocellular carcinoma cells, in rat glioblastoma cells, and in the cerebellum of infected rats (Rayet. B, et al, 1998 and Moehler. M, et al, 2001).

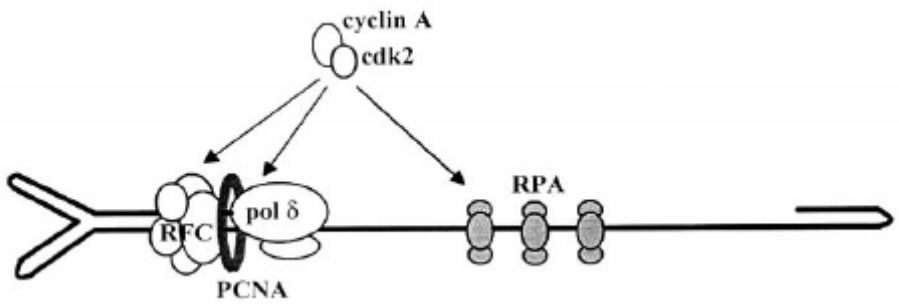

Figure 2: Life cycle of parvoviruses (Bashir.T, et al, 2000). Schematic representation of the cellular factors assembled at the MVM virion DNA primer-template junction and thought to be involved in complementary strand elongation. Cyclin A or the cyclin A cdk2 complex may regulate the conversion reaction by forming part of the elongation machinery and/or phosphorylating some of its constituents.

2.2.5 Genome organization and gene expression

Both ends of the viral genome consist of palindromic sequences that can form hairpin structures and serve as self-priming origins of DNA replication (Cotmore.SF, et al, 1987). Most of the autonomous parvovirus genome consists of two large open reading frames (ORFs) and two promoters (figure 3) (Maxwell.IH, et al, 2002). The left-and right-hand ORFs code for the non-structural (NS) polypeptides and viral capsid proteins (VP), respectively.

Generally, Parvovirus capsid contains 60 protein subunits, encoded by alternative splicing of mRNA. The P38 promotor (at map unit 38) programs R3 transcripts of approximately similar size that are generated by differential splicing and encode the capsid proteins (structural proteins) VP1 and VP2 (Cornelis.JJ, et al, 1990). Overlapping of two transcription units produce three major cytoplasmic mRNA species. The transcripts R1 and R2 are both initiated from the left handed promoter (P4) at map unit 4 and translated into non-structural proteins NS1 and NS2, respectively. The right-hand promoter (P38) directs the transcription of the genes encoding the structural proteins. The capsid proteins VP1 and VP2 are translated using two distinct initiation codons as a

result of differential splicing of the precursor messenger RNA (Cotmore.SF, et al, 1987). Most abundant protein VP2 comprises the C-terminal 64 kDa region of the 83 kDa VP1. VP2 can be processed to VP3 by proteolytic cleavage of approximately 25 amino acids and form it N-terminus, can be seen only in DNA containing virions (Tattersall.P, et al, 1977). The N-terminal domain of VP2 is essential for the nuclear export of full particles. The proteolytic cleavage of VP2 may occur at the stage of virus binding to the host cells; however, role of VP2 during the virus cycle remains unclear. The VP1-specific N-terminal domain is highly basic, contains a number of putative nuclear localisation signals (Lombardo.E, et al, 2002) as well as highly conserved PLA_2 domain (Zadori.Z, et al, 2001). This domain is protruded out of the capsid shell without disassembly (Cotmore.SF, et al, 1999). The later process might be required for the transport of the virions from the late endosomes/lysosomes to the nucleus (Zadori. Z, et al, 2001), explaining why capsids devoid of VP1 can be assembled but lack infectivity (Tullis.GE, et al, 1993). The capsid VP2 is necessary for capsid formation and packaging of the viral genome (Tullis. GE, et al, 1993 and Willwand.K, et al, 1993).

The strong left-hand promoter (P4) controls the expression of the NS1 and NS2 polypeptides. NS1 is a phosphorylated protein that is required for replication of the viral genome after the incoming single- stranded DNA has been converted into a duplex form. To exert its replication function in the nucleus, NS1 contains a nuclear localization signal and is endowed with helicase, endonuclease, ATPase, and site-specific DNA binding activities. Beside its functions in viral DNA replication, NS1 is a transcription factor by virtue of its ability to transactivate the P38 promotor (Rhode.SL III, 1985). Importantly, it was already described that, NS1 exhibit cytotoxic properties (Caillet-Fauquet.P, et al, 1990, Li.X and Rhode.SL III, 1990). Thus the lytic outcome of a parvovirus infection may be due, at least in part, to the overexpression of this viral protein. Phosphorylation of the NS1 polypeptide also plays an important role in this regard, as it was shown to control both the replicative and cytotoxic functions of the viral product (Nüesch.JP, et al, 1998, Corbau.R, et al, 2000).

The small non-structural protein NS2 plays an important role and it is required at various steps of the parvoviral life-cycle in a host specific manner (Naeger.LK, et al, 1990). In mouse cells infected with MVM mutants unable to express NS2, (i) the synthesis of DNA replication forms (RF) severely impaired, (ii) progeny single-stranded DNA is undetectable, and (iii) the VP1 and VP2 proteins that are synthesized do not become assembled into capsids (Cotmore.SF, et al, 1997). NS2 may be non-essential in cells from other species such as the SV40- transformed human fibroblasts NBK-324 (Naeger.LK, et al, 1990), even though NS2 may still play a role in the release of virions from these cells (Cotmore.SF, et al, 1997). It was also shown that functional NS2 is also needed for the efficient nuclear egress of progeny virions, and may therefore participate in virus spread (Eichwald.V, et al, 2002).

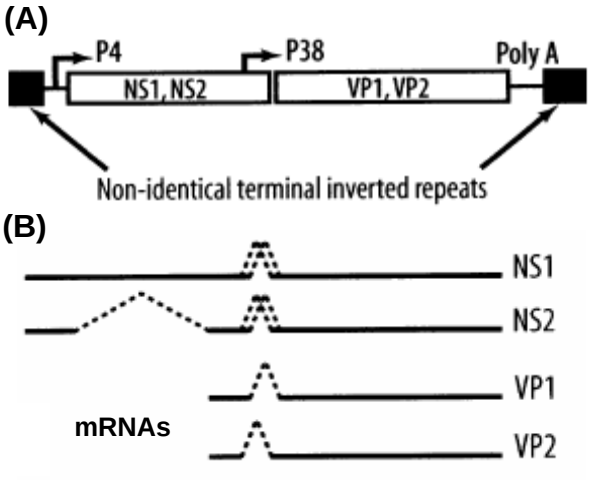

Figure 3: Structure of the LuIII parvovirus genome (Maxwell.IH, et al, 2002). (A) Major mRNAs present in infected cells. (B) DNA is single stranded (having both polarities, in contrast with MVM and H-1), with the termini having hairpin structure. (A) In the infectious plasmid and the replicative form DNA, the termini form inverted repeat sequences which contain origins of replication and packaging signals. These black bars termini must be retained in gene transfer vectors. P4 promoter is alternatively spliced by the primary transcript. (B) The small alternative splices shown just before where the translation of NS1 terminates. NS2 proteins share an N-terminal amino acid sequence with NS1 but their translation continues, followed by the large splice, in a different reading frame and the small splices give rise to C-terminal variants of NS2. The p38 promoter, on transactivation by NS1, give rise to a primary transcript that is subject to the same alternative small splices, generating the mRNAs for the capsid proteins, VP1 and VP2. In the more abundant mRNA, encoding the major protein, VP2, the splice removes the VP1 initiation codon, allowing translation to initiate at the appropriate downstream AUG.

2.2.6 Use of parvoviruses in medicines

Several ways of in vitro transformation of human and rodent cells, including viral and cellular oncogenes, was found to correlate with an increase in their capacity to sustain certain steps of the productive parvovirus (H-1 and MVM) cycle, in particular amplification of DNA, gene expression and killing the cells. Parvovirus H-1 exhibit oncotropic nature and thus could be visualized at the individual level in human fibroblast cultures. Indeed, the proportion of these cells that were able to accumulate nuclear NS1 proteins in amounts detectable by immunostaining were considerably higher in transformed than in non-transformed parental cultures. It is noteworthy that normal cells take up parvovirus particles as efficiently as their transformed derivatives in the cell systems analyzed so far, indicating that in the former virus replication and cytotoxicity are blocked at an intracellular step manner (Rommelaere.J, et al, 1991).

Similar findings about oncotropic and oncolytic behaviour of rodent parvoviruses were observed by using various cultures of tumor derived cells, as compared with normal cells of the same tissue origin (Rommelaere.J, et al, 1991). Therefore, it appears that some cancer cells provide these viruses with an environment that are beneficial to their multiplication. This feature was recently exploited for the isolation of the new rat parvovirus (RPV-1). Indeed, by implantation tumour cells in rats suspected of being parvovirus-infected, a previously unknown parvovirus could be recovered from the developing tumors (Ball-goodrich.LJ, et al, 1998). A parallel may be drawn between this oncotropism of parvoviruses and their known predilection for highly proliferating and generally poorly differentiated cells (Cotmore.SF and Tattersall.P, 1987). Since oncogenic transformation is accompanied by cell cycle and differentiation dysregulations (Hanahan.D, et al, 2000 and Harbour.JW, et al, 2000), it can be assumed that some of these changes are advantage to

the parvovirus, e.g., by extending the timeframe during S-phase-coupled virus replication and expression.

2.2.7 Parvovirus in gene therapy

Replication of parvoviruses do not occur in resting cells, and the permissiveness of cycling cells to parvovirus infection is much restricted by their differentiation state, thus the safety of H-1 and MVMp-based vectors is expected to be high. (Cotmore.SF and Tattersall.P, 1987). Further, these viruses failed to induce significant inflammatory reactions even after repeated injections in animal models (Giese.N, et al, 2002). In agreement with this assumption, two phase I clinical studies showed no adverse reactions in patients suffering from osteosarcoma or other solid tumors after infection with wild-type H-1 virus, despite the fact that virus amplification and seroconversion took place in most cases (Toolan.HW, et al, 1965). However, these pilot studies should be extended by including more parameters of virus infection and host immune and inflammatory reactions (Lang.S, et al, 2002). In particular, potential targets for H-1 virus infection and pathogenicity, such as leukocytes (Moehler.M, et al, 2003), endothelial cells and high cell-turnover tissues, should be evaluated for their susceptibility to parvovirus infection. Cellular immune responses triggered by the virus also need to be investigated in infected patients. Neutralising antibodies are readily formed after parvovirus infections in animals (Jacoby.RO, et al, 1996 and Lang.S, et al, 2002). These antibodies have been shown to reduce the efficiency of subsequent therapeutic administrations of wild-type or recombinant viruses, but can be circumvented by the further use of pseudotypes in which the virus/vector genome of interest is packaged within the capsid of a related parvovirus (Lang.S, et al, 2002). This strategy may be applied to humans who also appear to develop neutralizing antibodies against inoculated H-1 virus (Lang.S, et al, 2002).

2.3 Overview:- Mechanisms of nuclear transport

2.3.1 Endocytosis

Endocytosis is an important process and endocytic entry is an advantangeous pathway for viruses. Firstly, the viral particles are directed only into cells that have active membrane transport and not into erythrocytes, a dead end. Secondly, a particle can bind anywhere on the cell surface and rely on the endocytic processes to ferry it not only into the cell but also to carry the past cortical actin filaments and other cytoplasmic barriers to the perinuclear region (Marsh.M and Bron.R, 1997). In this process, a virus avoids diffusion through the cytoplasm by itself. Thirdly, penetration from cytoplasmic organelles decreases the risk for immunodetection because viral proteins are not exposed on the plasma membrane. Fourthly, in the endocytic organelles, local cues such as low pH help the virus undergo its penetration programme (Falnes.PO, et al, 2000).

Endocytosis is the essential process used by the cell to internalize the extracellular ligands in plasma membrane derived vesicles. Endocytic processes can be occurred by different pathways such as lipid-raft-mediated endocytosis, macropinocytosis, calveolae-mediated endocytosis and clathrin-mediated endocytosis. Apparently the most common pathway for viral entry in different viruses, enveloped and non-enveloped, have been shown to use a clathrin-mediated pathway with penetration in early or late endosomes.

Clathrin-mediated endocytosis is the major pathway for selective internalization of plasma membrane receptors and the ligands bound to them (Simonsen.A, et al, 2001). A cargo selection by clathrin coated vesicles is attributed to endocytic signals present on the cytoplasmic tails of the plasma membrane receptors. The binding of the extra cellular ligands to receptors is followed by interactions of adaptor proteins (AP2s) and accessory proteins with lipids and receptors. These interactions mediate the recruitment of the receptors into the coated areas of plasma membrane and cause the clathrin lattice to force vesicle invagination of the membrane. Invaginated pits undergo vesicle fission with the help of dynamin (a GTPase) and other effector proteins (Marsh.M, 2000). In addition to clathrin-dependent pathway, cells have also other mechanisms to internalize (macro) molecules bound to their receptor. For instance macropinocytosis, this is the characteristic feature for macrophages and dendritic cells. Many authors have reported that the clathrin-independent pathways may integrate with clathrin-dependent pathway (Montesano.R, 1982, Tran.D, et al, 1987, Vilhardt.F, et al, 1999). Furthermore, in many cases, molecules enter cells both by clathrin-dependent and independent routes (Marsh.M, 2000).

Ligands taken into cells by clathrin-mediated endocytosis are transported to early endosomes (EEs). Slightly acidic environment (pH 5.9-6.0) in early endosomes causes many ligands to dissociate from their receptors (Mukherjee.S, et al, 1997). These receptors contain specific signals on their cytoplasmic tail may cause them to be sorted and returned back to the plasma membrane for reuse, while others are transported together with dissociated ligands to the lysosomes for the degradation (Mellman.I, 1996 and Riezman.H, et al, 1997). Recycled molecules, targeted back to the plasma membrane, are rapidly shuttled back to the plasma membrane from EEs or from the tubulovesicular compartment near the nucleus, known as recycling endosomes or perinuclear recycling endosomes (RE) (Gruenberg.J and Maxfield.FR, 1995). The transitition through RE is slow and requires an intact microtubular network. However, early endosomal membranes contain the small GTPases Rab4 (Daro.E, et al, 1996), Rab5 (Bucci.C, et al, 1992) and the early endosomal antigen-1 (EEA1) as specific marker proteins. These molecules thought to confer directionality for endocytic transport (Simonsen.A, et al, 2001). In addition, EEs contain special proteins destined for recycling as well as degradation (Yamashiro.DJ, et al, 1984), whereas REs have Rab11 and proteins destined specifically for recycling (Yamashiro.DJ, et al, 1984). REs also

possess more alkaline pH EEs (Yamashiro.DJ, et al, 1984, Sipe.DM, and Murphy.RF, 1987 and Mukherjee.S, et al, 1997). Late endosomes (Les) are considered as an intermediate structure in the transport of endocytosed molecules, lysosomal hydrolases and membrane proteins to lysosomes. They differ from EEs by their lower luminal pH (pH 5-6), different protein composition and association with different small GTPases of the Rab family (Rodman.JS and Wandinger-Ness.A, 2000). LEs and lysosomes (LYs) have lysosomal membrane proteins (LAMPs or Lgps) associated in their membranes and both LEs and LYs have properties expected of functional degradative compartments including a low luminal pH and contents of acid hydrolases. Unlike lysosomes, LEs are enriched in mannose 6-phosphate receptors (MPRs) (Griffiths.G, et al, 1990, Griffiths.G and Gruenberg.J, 1991). In addition, LYs has a slightly lower pH (pH 5-5.5) than LEs (Mukherjee.S, et al, 1997). It has been reported that there is also retrograde traffic from terminal lysosomes to LEs suggesting dynamic equilibrium between LEs and lysosomes (Jahraus.A, et al, 1994). In addition, receptor bound ligands can be transported from clathrin coated pits to ER (Gruenberg.J and Maxfield.FR, 1995, Mallard.F, et al, 1998). After binding to its receptors on the cell surface toxin-receptor complex is internalized in clathrin coated pits and transported via EEs and REs to the trans golgi network (TGN) of the golgi and the finally to the ER (Mallard.M, et al, 1998).

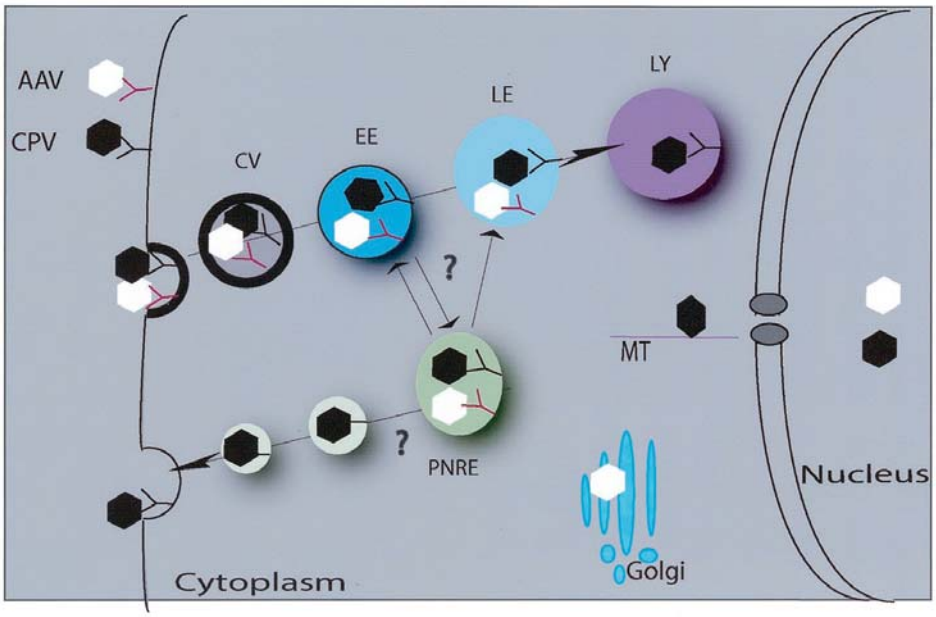

Figure 4: A schematic cell entry mechanisms utilized by parvoviruses within the host cell is shown (Vihinen-Ranta. M, et al, 2004). After binding to their cell surface receptors, viruses are internalized into clathrin-coated vesicles (CV), followed by transport to early (EE), late (LE), or perinuclear recycling endosomes (PNRE). Later in entry, in the case of AAV, capsids are found in golgi compartments, whereas CPV can be found in lysosomes (LY). The site of the capsid escape from endocytic vesicles into the cytosol is still unclear. CPVs make use of microtubules (MT) during the traffic through the cytosol toward the nucleus. Viral capsids are able to enter the nucleus in intact form without apparent deformation.

Although the receptor-ligand complex has a certain intracellular multivalent ligands such as multivalent transferrin (composed of more than 10 transferrin molecules) may result redirecting of a ligand-receptor complex. Transferrin is transported to the REs and receptor-bound multivalent transferrin is rerouted to the degradative pathway. In addition, apo-B, E-receptor (Tabas.I, et al, 1990, 1991), M glycoprotein (as coronavirus receptor) and Fc-receptors (Mellman.I and Plutner.H, 1984) have also reported to be rerouted by the binding of multivalent ligands. All in all, the basic organisation of the endocytic pathway has been elucidated, particularly in the case of the internalization of protein ligands bound to the cell surface receptors (Kornfeld.S and Mellman.I,

1989, Trowbridge.IS, et al, 1993, Gruenberg.J and Maxfield.FR, 1995, Mellman.I, 1996), there remains much to be studied to fully understand the complex processes of the endocytosis.

During recent years, lipids found to contribute to the organization and functions of the vacuolar system (Gruenberg.J, 2001). The membrane phospholipids phosphatidylinositol can be phosphorylated in different ways to produce distinct second messengers known as phosphoinositides. Localised changes of phosphoinositides are mediated by kinases and phosphatases providing temporal and spatial regulation of the membrane budding, motility and fusion (Simonsen.A, et al, 2001). Phosphoinoitides seem to be rather well organized the organelles of the endocytic pathways (Gruenberg.J, 2001). Clathrin coated vesicle (CCVs) are enriched in phosphatidylinositol 4, 5-phosphates (PI (4, 5) P_2), that seems to have the key role of regulating formation, scission and uncoating of CCVs (Jost.M, et al, 1998). Phosphoinoitides, in particular (PI 4, 5) P_2 and phosphatic acid, have been reported to participate in CCV formation as regulators of dynamin membrane activity (Lin.FT, et al, 1997, Burger.KN, et al, 2000). Phosphatidylinositol 3-phosphate, which interacts with proteins containing a FYVE or PX domain, is concentrated in early endosomal membranes, where it is suggested to regulate the fusion events of EEs through Rab5-GTP (Simonsen.A, et al, 1998, Gillooly et al, 2000, Rubino.M, et al, 2000, Simonsen.A, et al, 2001). Furthermore, lysophosphatidic acid and phosphatidylinositol 3, 5-bi phosphate (PI (3,5) P_2) are suggested to be typical lipids for endosomal carrier vesicles, multi vesicular bodies and late endosomes (Shisheva.A, et al, 2001), while sphingolipids and sulfatide are abundant in recycling endosomes (Holtta-Vuori.M, et al, 2002). However, the roles of these lipids on membrane trafficking have not yet been clarified.

2.3.2 Acidification

Acidification is an important property for endocytic sorting. One of the major functions of endosomes is to dissociate ligands from their receptors. After dissociation, many receptors are recycled to the cell surface and the ligands are degraded (Davis.CG, et al, 1987, DiPaola.M and Maxfield. FR, 1984). Receptors release their ligands at low pH could result from a pH- dependent conformational change in the receptors. This was also demonstrated for the EGF and the asialoglycoprotein receptors (DiPaola.M, et al, 1984). Additionally, neutralizing the endosomal pH with the proton ionophore monensin prevents ligand-receptor dissociation (Kaiser.J, et al, 1988, Nunez.MT and Glass.J, 1985). A separate function that is also a consequence of pH-dependent conformational change is the release of iron from transferring. Sorting of endosomes at the acidic pH, iron is released from transferrin, and apo-transferrin remains bound to its receptors in the acidic endosomes. (Dautry-Varsat.A, et al and 1983, Rao.K, et al, 1983).

Endosomal acidity is maintained by ATP-dependent proton pump (vacuolar H^+ ATPase), which is a member of a family of multi-subunit proton pumps (AL-Awqati.Q, 1986, Gluck.SL, 1993, Nelson.N, 1987). This family includes the proton pump in adrenal chromaffin granules and other secretory vesicles and is similar to proton pumps in the membranes of plant vacuoles. These proton pumps are electrogenic in that the movement of a proton results in translocation of the net charge that is not directly coupled with the transport of another ion to maintain electroneutrality. The mechanism for maintaining the different acidities in endosomes is not certain, although several hypotheses have been put forth. Early endosomes, but not late endosomes, contain the Na^+-K^+-ATPase (Cain.CC, et al, 1989, Fuchs.R, et al, 1989, vanWeert.AW, et al, 1995). The Na^+-K^+-ATPase would generate an inside positive membrane potential that would make it more difficult to pump protons into the endosome. Its presence in early sorting endosomes thought to be required for their relatively low acidification (Sato.SB and Toyama.S, 1994). Other ion transporters such as chloride channels may also affect and regulate the pH of endosomes (AL-Awqati.Q, 1986, Nelson.N, 1987). A suggested mechanism by which changes in the membrane

potential can affect the steady-state pH of an endosome involves changes in the coupling between proton translocation and ATP hydrolysis by the vacuolar proton pump as the proton concentration and or positive charge in the compartment builds up (Nelson.N, 1987).

The control of the internal pH of endosomes plays an important role in membrane traffic. For example, inhibition of the vacuolar H^+-ATPase causes slows delivery to late endosomes or lysosomes in different cell types (Clague.MJ, et al, 1994 and van Weert.AW, et al, 1995), and it slows receptor recycling in CHO cells (Johnson.LS, et al, 1993). Similarly, the movement of TGN38 along the endocytic pathway was inhibited after neutralization of the endosomal pH (Chapman.RE and Munro.S, 1994). However, the mechanisms by which internal pH alter properties such as the maturation of endosomes or the rate of recycling remains unclear. The problem is that most of the affected properties require changes on the cytoplasmic side of the vesicle. One possibility is that pH-induced conformational changes in the luminal domains to transmembrane proteins are transmitted across the membrane and affect the cytoplasmic domain. Many receptors and other membrane proteins have been shown to have pH-dependent conformational changes over the range from pH 5 to 7 (Diapola.M and Maxfield.FR, 1984, Turkewitz.AP, et al, 1988), including changes in their ability to self-associate (Turkewitz.AP, et al, 1988). For asialoglycoprotein receptor, biophysical studies have shown that changes in pH or transmembrane electrical potential can cause gross changes in the disposition of the protein in the bilayer (Blumenthal.R, et al, 1983 and Blumenthal.R, et al, 1980).

The mechanisms of viral entry of non-enveloped viruses into the cytoplasm and nuclear targeting of the virus or its genome prior to replication are still poorly understood. However, the use of certain members of the parvovirus family as vectors for gene therapy has prompted research in this field. A common uptake principle of these viruses involves receptor-mediated endocytosis. However, cell surface attachment differs among parvoviruses. Authors reported that, MVM and parvovirus H-1 use sialic acid moieties of cell surface glycoproteins as the receptor (Cotmore.SF, and Tattersall.P, 1987). Canine parvoviruses (CPV) and feline parvoviruses use the transferrin receptor (Parker.JS, et al, 2001). For B19, one glycolipid, globotetraosylceramide or globocide is the receptor (Brown.KE, et al, 1993, Chipman.PR, et al, 1996). Bovine parvovirus binds to sialated erythrocyte membrane glycoproteins and attaches to the major membrane glyprotein, glycophorin A (Thacker.TC, and Johnson.FB, 1998). Adeno-associated viruses (AAVs), of the *Dependovirus* genus of parvoviruses, were reported to employ membrane-associated heparan sulfate proteoglycans as cellular receptors (AAV-2) (Summerford.C and Samulski.RJ, 1998) or sialic acid (AAV-4 and -5) (Kaludov.N, et al, 2001 and Walters.RW, et al, 2001). Acidification is known to be essential for the entry of AAV and CPV, since drugs that interfere with the endosomal pH are able to block the infection (Bartlett.JS, et al, 2000, Basak.S and Turner.H, 1992, Douar.AM, et al, 2001, Parker.JS and Parrish.CR, 2000, Vihinen-Ranta.M, et al, 1998). The infectious entry of CPV could also be blocked by the disruption of microtubules and by low temperatures, suggesting the involvement of microtubule dependent transport (Vihinen-Ranta.M, Kalela.A, et al, 1998). For AAV translocation to the nucleus, functional microtubules and microfilaments are needed (Sanlioglu.S, et al, 2000). The release of these viruses may be directly linked to the acidification of the vesicle. However, the exact mechanism and time course of this release from the endosomal compartments remain unclear. Sequence analysis of the VP1 revealed phospholipase A_2 motifs in the capsid proteins of parvoviruses, an activity that was not known to exist in viruses and that might be responsible for parvovirus entry (Dorsch.S, et al, 2002, Li.Y, et al, 2001, Zadori.Z, et al, 2001). However, the mechanism and time course by which the viral particles, once released into the cytoplasm, translocate to the nucleus is not known.

2.3.3 Signal- mediated nuclear import

The nucleus and cytoplasm are separated by the double membrane of the nuclear envelope. The outer membrane is continuously connected with the membrane of the endoplasmic reticulum. Transport between the cytoplasm and the nucleoplasm is highly regulated and occurs through protein-lined aqueous channels called nuclear pore complexes.

The NPC physically allows for the signal-mediated passage of large, charged molecules across the nuclear envelope. Theoretically, proteins could transverse back and forth across the nuclear envelope but be specifically retained in the nucleus by a nuclear retention signal. Alternatively, trafficking across the nuclear envelope could be restricted to those proteins that carry an NLS to target them for active nuclear import. The first NLS identified was a basic stretch of amino acids (KKKRK) from the SV40 large T-antigen. This sequence has been named the classical NLS. A second class of NLS, the bipartite signal, is characterized by the sequence from the Xenopus nucleoplasmin protein in which the classical NLS is broken into two halves by an intervening group of 5 to 20 amino acids (KRPAATKKAGQAKKKK). The hnRNP A1 proteins contain a third class of NLS, termed the M9 sequence. Unlike the other NLSs, M9 is not rich in basic amino acids, but functions as both a nuclear import and export signals.

2.3.4 The Nuclear Pore Complex (NPC)

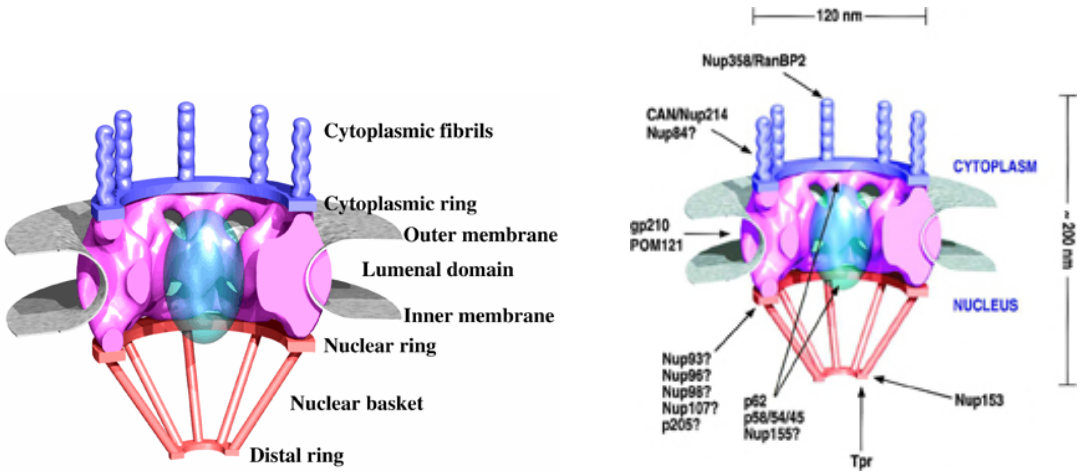

Figure 5: Structure of the nuclear pore complex (Hinshaw.JE, et al, 1992, Pante.N and Aebi.U, 1996). **(A)** A 3-D reconstruction of detergent extracted and negatively stained nuclear pore complexes, revealing the central framework which exhibits strong 822 symmetry and thus consists of two identical halves relative to the central plane of the nuclear envelope (NE). **(B)** Higher eukaryotic NPC, based on electron microscopic structural studies. The symmetrical membrane-spanning portion contains an aqueous, possibly gated, central channel through which translocation occurs, and a central plug of unclear composition and function. The cytoplasmic filaments and nuclear basket are involved in the initial and terminal stages of translocation. The location of some nucleoporins (nups) as determined by electron microscopy, are indicated.

In vertebrates, the NPC is a large 125 MDa multiprotein structure that completely spans across the nuclear envelope (NE) and extends into cytoplasm and nucleoplasm. It contains about 30 different proteins that are present in at least 8 fold redundancies. The NPC consists of a membrane-embedded framework (the spoke complex), which is formed by 8 multidomain spokes with two rings on each face (Figure 5). The ring facing the cytoplasm is connected with eight 50 nm long fibrils extending into the cytoplasm. The nuclear ring is capped with a basket like assembly of eight thin, 50-100 nm filaments joined distally by a 30-40 nm diameter terminal ring. The centre

of the channel harbours a hydrophobic framework through which the signal-mediated bi-directional transport of macromolecules occurs. The proteins that form the NPC are called nucleoporins (nups). Nucleoporins have been localised to discrete regions of the NPC and are often used as markers for this compartment. Approximately half of the nucleoporins contain a phenylalanine-glycine repeat motif (FG repeat) which play an important role in the nuclear transport of protein. During each cell division, higher eukaryotes go through an open mitosis characterized by dissolution of the nuclear envelope. In a coordinate fashion, the NPC is also disassembled. Notably, some nups play important roles during or after mitotic remodeling of the pore itself (Salina.D, et al, 2003).

2.3.5 Nuclear localisation signal (NLS) receptors and import factor recycling

Nuclear import of NLS-containing proteins is mediated by a family of transport molecules collectively known as karyopherins or importins. Proteins with the classical NLS present in the cytoplasm are bound by importin α, which recognizes the highly basic PKKKRV amino acids (Nadler.SG, et al, 1997). Importin α acts as an adaptor molecule, binding both the NLS of the cargo protein and via its importin β binding domain (IBB) to importin β. Nucleoplasmin and other proteins with a bipartite NLS use the same importin α/β import machinery. It was later discovered that β homologoues can directly bind to various IBB -like domains (Lange.A, et al, 2007). These α/β/NLS or β/NLS multiprotein complexes localize to the NE as importin β binds to cytoplasmic fibres that protrude from the NPC (Gorlich.D, et al, 1996). Dissociation occurs via Ran GTP, once the import complex reaches the nucleus. Binding of Ran GTP to importin β causes a confirmational change that result in the release of the importin α-cargo complex (Lee.SJ, et al, 2005 and Weis.K, et al, 1996). The importin β binding (IBB) domain of importin α (Kobe.B, 1999), nucleoporin nup2 (nup 50 or Npap 60 in vertebrates) (Gilchrist.D, et al, 2002, Matsuura.Y, et al, 2003, Matsuura.Y and Stewart.M, 2005) and the export receptor for importin α, Cse1/Ran GTP (CAS/Ran GTP in vertebrates) (Matsuura.Y and Stewart.M, 2004) then work together to deliver the cargo into the nucleus. Finally, Cse1/RanGTP recycles importin α back to the cytoplasm to repeat another round of import (Hood.JK and Silver.PA, 1998, Kutay.U, et al, 1997).

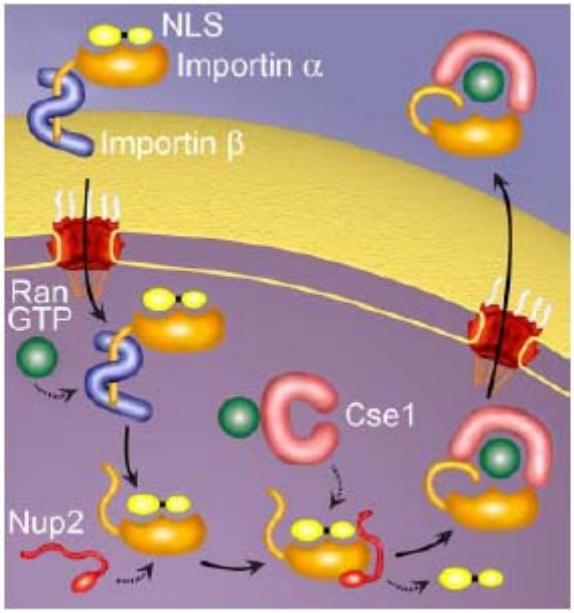

Figure 6: The classical nuclear import cycle (Lange.A, et al, 2007). In the cytoplasm, cargo containing NLS bound by the import receptor, importin α/β. Importin α recognises the NLS, and the importin β mediates interaction with the nuclear pore during translocation. Inside the nucleus, RanGTP binding causes a conformational change in importin β, which release the IBB region of importin α. This domain,

nucleoporin and Cse1, facilitates the NLS dissociation and the delivery of the NLS cargo in the nucleus. At last, importin α recycles back to the cytoplasm to take for another round of import.

2.3.6 Nuclear envelope (NE) and nuclear envelope breakdown (NEBD)

In eukaryotic cells, NE (nuclear envelope) separates the nucleoplasmic and cytoplasmic activities. The NE is mainly composed of two lipid bilayer membranes: 1) Outer nuclear membrane (ONM) 2) inner nuclear membrane (INM). Outer nuclear membrane is continuous with the endoplasmic reticulum (ER), decorated with ribosomes and is a site for protein translation and modifications. The ONM and the inner nuclear membrane (INM) are separated by a 25-45 nm thick lumen and are fused at sites where the nuclear pore complexes (NPC) are embedded. Underlying the INM and bordering the peripheral chromatin, there is a protein meshwork called the nuclear lamina (Gruenbaum.Y, et al, 2005).

Key events in the early stages of mitosis in metazoans are hallmarked by nuclear envelope breakdown (NEBD) and release of condensed chromosomes into the cytoplasm. NEBD involves the disassembly of all major structural elements of the nuclear envelope, including nuclear pore complexes (NPCs), and the dispersal of nuclear membranes components. In NEBD, minus-end directed motion started to create pulling force on the NE surface towards the centrosome. These forces become stronger with increasing length and number of spindle microtubules and push NE materials towards to centrosomes, creating folds. Distal from centrosome, creates stretching and disruption of nuclear lamina. After NEBD, NE fragments pulled away from chromosomes by dynein. In this model NEBD is caused by tearing a nuclear lamina, which is shown to correspond the site of permeabilization (Beaudouin.J, et al, 2002).

2.3.6.1 Mitosis

The NE (nuclear envelope) completely disassembles during mitosis in a process called “open mitosis in higher eukaryotes”. Nuclear membranes, nuclear lamina, and NPCs disassemble between prophase and prometaphase stages of the cell cycle allowing engagement of the chromosomes with the cytoplasmic mitotic spindle. The dynamics of NE are best examplified, when nuclear membranes disassemble from chromatin and the break down of nuclear lamina. Irrespective of whether lamins, integral proteins of the INM, NPC proteins or all of these play important roles in driving the disassembly of NE at mitosis, it is generally agreed that their cell cycle-dependent phosphorylation is critical in these processes. Many authors reported that several integral proteins of the INM, including LBR (Lamin B receptor), LAP2β (Lamin associated proteins) and emerin, are also phosphorylated at mitosis (Courvalin.JC, et al, 1992, Ellis.JA, et al, 1998, Foisner.R and Gerace.L, 1993, Dreger.M, et al, 1999). In contrast to lamins, however, there is no evidence for a role and involvement of multiple kinases in phosphorylation of INM integral proteins. In addition, specific residues phosphorylated by CDK1 have been identified for LBR in the N-terminal nucleoplasmic domain (Courvalin.JC, et al, 1992, Ellis.JA, et al, 1998, Foisner.R and Gerace.L, 1993, Nikolakaki.E, et al, 1997). Nucleoporins are also phosphorylated in a cell-cycle-dependent manner (Favreau.C, et al, 1996), as are chromatin protein HP1 variants, which are ligands for LBR (Minc.E, et al, 1999). This suggests the detachment of the INM from peripheral structures may result from phosphorylation of a large number of integral and peripheral proteins of NE. From *in vivo* and *in vitro* studies performed in mammalian somatic cells and in *Xenopus* eggs, it appears that protein kinases promote membrane release from chromatin (Foisner.R and Gerace.L, 1993, Pfaller.R and Newport.JW, 1995, Pyrpasopoulou.A, et al, 1996), whereas protein phosphatases stimulate binding (Pfaller.R, et al, 1991, Vigers.GP and Lohka.MJ, 1992). When disassembled, membranes containing LBR, LAP2β and gp210 are excluded from the mitotic spindle, suggesting that they are contained in membrane sheets too large to enter the microtubule network (Buendia.B and Courvalin.JC, 1997, Chaudhary.N and Courvalin.JC, 1993).

Therefore, except for a fraction of emerin which is apparently localised within the spindle (Dabauvalle.MC, et al, 1999, Haraguchi.T, et al, 2000), chromosomes and membranes are segregated during metaphase inside and outside of the spindle, respectively.

Caspase activation is required for T cell proliferation (Kennedy.NJ, et al, 1999) and that activated caspases can cleave the substrates in the non-apoptotic cells during T lymphocyte stimulation (Alam.A, et al, 1999). Current study showed caspase 3 is upregulated and activated during the G2/M transition. At present, it is not known how caspase 3 participates in the network of the mitotic checkpoint. Nevertheless, the pre-activated caspase 3 may enable the system to response rapidly when cells were seriously damaged (Hsu.SL, et al, 2006).

2.3.6.2 Apoptosis

Apoptosis or programmed cell death, results in several morphological changes in cell. In addition to cytoskeletal alterations and plasma membrane blebbing, the nucleus undergoes remarkable remodelling during apoptosis. Chromatin condensation and fragmentation of nuclei were also reported (Strasser.A, et al, 2000). Underlying the hallmark changes in morphology and cell function is a cascade of proteases, termed caspases. Caspases undermine normal elements of cell structure by targeting specific proteins for cleavage (Strasser.A, et al, 2000). Active phase of apoptosis is characterized by nuclear modification i.e chromatin condensation (Wyllie.AH, et al, 1980). This process is secondary to DNA cleavage (Enari.M, et al, 1998 and Sakahira.H, et al, 1998) and to proteolysis of some specific nuclear proteins by proteases of the caspase family that are selectively activated during apoptosis (Thornberry.NA and Lazebnik.Y, 1998, Villa.P, et al, 1997). In contrast to the precocity of chromatin condensation, nuclear envelope (NE) ultrastructure is preserved until the late stages of apoptosis (Wyllie.AH, et al, 1980), despite the early cleavage of A-type and B-type lamins, the major peripheral proteins of the envelope (Lazebnik.YA, et al, 1993, Weaver.VM, et al, 1996). The dramatic changes in nuclear periphery – including nuclear pore clustering (Buendia.B, et al, 1999, Falcieri.E, et al, 1994) as well as the importance of nucleocytoplasmic trafficking during apoptosis.

Molecular properties of caspases

Caspases are the interleukin-1β-converting enzyme family proteases, are highly homologous *to Caenorhabditis elegans* cell death gene CED-3. So far, fourteen caspases have been identified and all of which share some common properties. All Caspases are aspartate-specific cysteine proteases, by having a conservative pentapeptide active site 'QACXG' (X can be R, Q or D). Additionally, their precursors are all zymogens known as procaspases. The N-terminal of the prodomain in procaspases contains highly diverse structure required for caspases activation; and they all are capable of autoactivating as well as activation of other caspases, to produce a heterodimer with a big and small subunit, and two heterodimers form and enzymatic active heterotetramer (Launay.S, et al, 2005), caspases are divided into three subfamilies basing on their homology in amino acids sequences, as shown in table below (Fan.TJ, et al, 2005).

Subfamily	Role	Members
I	Apoptosis activator	Caspase-2
		Caspase-8
		Caspase-9
		Caspase-10
II	Apoptosis executioner	Caspase-3
		Caspase-6

III	Inflammatory mediator	Caspase-7 Caspase-1 Caspase-4 Caspase-5 Caspase-11 Caspase-12 Caspase-13 Caspase-14

Table : Subfamily members of caspase family

At least 14 caspases have been identified in mammals (Alnemri.ES, et al, 1996, Kumar.S and Lavin.MF, 1996, Nicholson.DW and Thornberry.NA, 1997) (figure 7). These enzymes recognize tetrapeptide motifs and cleave their substrates on the carboxyl side of an aspartate residue. Individual caspases have distinct substrate specificities that are determined by the pattern of amino acids upstream of the cleavage site (the P2–P4 positions) (Nicholson.DW and Thornberry NA, 1997). Caspases are synthesized as zymogens, which have very low intrinsic enzymatic activity. The fully active enzymes are heterotetramers composed of two identical subunits of 20 kDa plus two identical subunits of 10 kDa (Walker.NP, et al, 1994, Wilson.KP, et al, 1994, Rotonda.J, et al, 1996). These sub-units can be produced by caspase-mediated cleavage. There is evidence that aggregation of at least some caspase zymogens is sufficient to promote self-processing (Muzio.M, et al, 1998, Martin.DA, et al, 1998, Srinivasula.SM, et al, 1998). So called initiator caspases (e.g. caspase-8 and caspase-9) start an increasing of caspase activity by processing and activating so-called effector caspases (Nicholson.DW and Thornberry.NA, 1997). However, some caspases, particularly effector caspases, cleave and inactivate certain vital cellular proteins, such as DNA repair enzymes, lamin, gelsolin, MDM2 (an inhibitor of p53), and protein kinase C δ (Thornberry.NA and Lazebnik.Y, 1998, Nicholson.DW and Thornberry.NA, 1997). There are also enzymes that can be activated directly or indirectly by caspase-mediated proteolysis. Certain caspases (e.g. caspase-3) can remove a negative regulatory domain from the kinase p21-activated protein kinase 2, and this is thought to trigger plasma membrane blebbing (Rudel.T and Bokoch.GM, 1997). The caspase-activated DNase (CAD) is normally inactivated by binding to an inhibitor, iCAD (also called DNA fragmentation factor (DFF) (Enari.M, et al, 1998, Sakahira.H, et al, 1998). During apoptosis, iCAD is cleaved by caspases, and this leads to release of the active endonuclease, which produces the characteristic internucleosomal DNA cleavage.

Caspase-3, a key factor in apoptosis execution, is the active form of procaspases-3. The latter can be activated by caspases-3, caspases-8, caspases-9, caspase-10, CPP32 (32kDa cysteine protease) activating protease, granzyme B (Gran B), and others (Yuan.CQ, et al, 2005). minocycline inhibits the proliferation of microglial cells and NMDAR (N-methyl-D aspartate induced activation of p38 mitogen-activated protein kinase, inhibition of caspase1 and 3 and the inducible form of nitric oxide synthase and a decrease in mitochondrial permeability transition mediated cytochrome *C* release (Baptiste.DC, et al, 2004). Through alternative splicing, caspases-3 pre-mRNA can be translated into a short caspases-3 (caspases-3S), which lacks the conservative 'QACXG' sequence in the catalyzing site, and is co-expressed with caspases-3 in all human tissues, overexpression of caspases-3S could protect cells from apoptosis induced by proteosome inhibition was observed in HEK293 cells (Yuan.CQ, et al, 2005). Experiments performed by using electrospray MS and N-terminal sequence analysis revealed the active enzyme site composed of two subunits of 17 kDa and 12 kDa, derived from the precursor protein by cleavage at Asp-28-ser-29 and Asp-175-Ser-176 (Nicholson.DW, et al, 1995). While the initial cleavage is probably between the large and small subunits, it has been suggested that processing with in the prodomain occurs initially at Asp-9, not at Asp-28 (Fernandes-Alnemri.T, et al, 1996, Srinivasula.SM, et al, 1996).

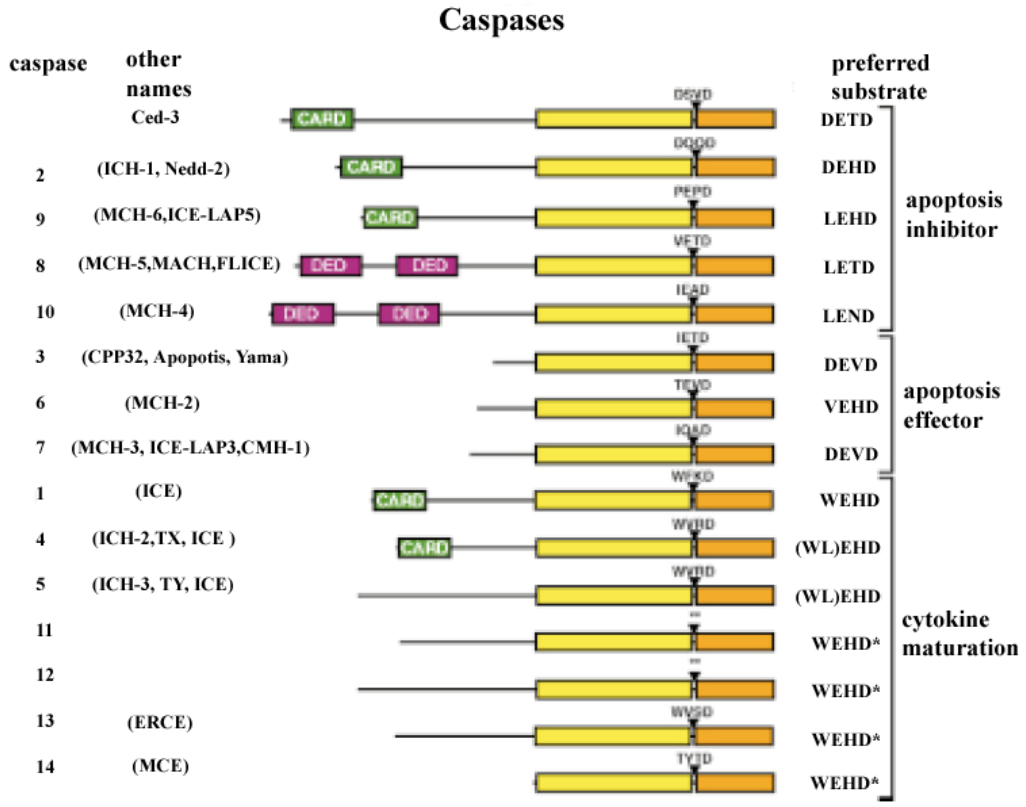

Figure 7: Structural comparison of the caspase pro-enzymes and substrate specificity of the caspases (Strasser.A, et al, 2000). The aspartate cleavage sites between the large (*open bars*) and small (*tinted bars*) subunits are indicated. **, Aspartate cleavage site is not known. Death effector domains (DED) and caspase recruitment domains (CARD) are shown. Human caspases 1–10, mouse caspases 11–14, and *C. elegans* Ced-3 are shown.

Apoptosis induced in cultured cells or in cell-free extracts generates stereotyped NE alterations. These alterations include budding, detachment of membranes from chromatin and clustering of NPCs (Lazebnik.YA, et al, 1993, Rao.L, et al, 1996, Buendia.B, et al, 1999). Despite these NE alterations, the NE persists and *in vivo* and *in vitro* until the late stages of apoptosis, and the ultrastructure of chromatin-detached nuclear membranes and NPCs is conserved (Buendia.B, et al, 1999, Falcieri.E, et al, 1994). First biochemical modification was observed at the NE after apoptosis induction was the cleavage of lamins 1-3 h (Rao. L, et al, 1996, Buendia. B, et al, 1999, Oberhammer. FA, et al, 1994, Neamati.N, et al, 1995). The caspases 6 cleavage site of A- and B-type lamins has been mapped to a conserved aspartic residue located in a hinge region upstream of coil 2 (Rao.L, et al, 1996, Neamati.N, et al, 1995, Orth.K, et al, 1996, Lazebnik.YA, et al, 1995). This cleavage generates a carboxy-terminal proteolytic fragment of 46 kDa containing coil 2, which is necessary for the formation of stable B-type lamin homodimers and for their lateral interactions in filaments. The feature of this proteolytic fragment may explain the persistent association of lamina remnants with nuclear membranes until late stages of apoptosis (Weaver.VM, et al, 1996, Duband-Goulet.I, et al, 1998). In addition to lamins, other proteins of the INM and NPCs are also selectively cleaved during apoptosis, although with a short delay (~ 1 h) compared with lamin B.

Major nuclear changes occurring simultaneously with NE alterations during apoptosis are chromatin condensation and DNA cleavage. Downstream pathway of the effector caspases 3 are responsible for oligonucleosomal DNA cleavage (Enari.M, et al, 1998) and chromatin

condensation (Sahara.S, et al, 1999), although some factors may also induce peripheral chromatin condensation in a caspase-independent manner (Susin.SA, et al, 2000). Chromosome condensation is independently facilitated by the loss of integrity of the nuclear matrix secondary to the cleavage of some of its components such as NuMA, topoisomerase II, and SnRNP and hnRNP proteins. Chromatin condensation process is enhanced by cleavage of lamina network and nucleoporin filaments, which are integral parts of the nuclear skeleton.

3. Aim of the project

The aim of the project is to evaluate the nuclear entry pathway of parvovirus H-1. Firstly, we evaluated the homology results obtained from the published data of the minute virus of mice (MVM) and the canine parvovirus (CPV). The incoherent of the reported unclear import pathways focussed the research in this thesis to search for the mechanisms that are unrelated to the previously assumed classical import pathways.

4. Material and Methods

4.1 Materials

4.1.1 Antibiotics, Chemicals and Enzymes

Agarose	Amersham (Freiburg)
Anamed gels (10-20% Tris glycine gels)	Apelex (Massy-France)
ATP	Roche (Mannheim)
Bovine serum albumin	Sigma-Aldrich (Taufenkirchen)
Collagen	BD Biosciences (Heidelberg)
Creatine phosphate	CalBiochem (Damstadt)
Creatine phosphokinase	CalBiochem (Damstadt)
DABCO (1,4-Diazabicyclo-(2.2.2) octane	Sigma-Aldrich (Steinheim)
Digitonin	Fluka Biochemika (Taufenkirchen)
DTT	Sigma-Aldrich (Taufenkirchen)
EDTA	Sigma-Aldrich (Taufenkirchen)
EGTA	Sigma-Aldrich (Taufenkirchen)
Fetal calf seurm	GIBCO-BRL (Karlsruhe)
FITC-Albumin	Sigma-Aldrich (Taufenkirchen)
Gentamycin	GIBCO (Invitrogen)
G-418	GIBCO (Invitrogen)
Glycerin	Merck (Damstadt)
Lectin from *Triticum vulgaris* (WGA)	Sigma-Aldrich (Taufenkirchen)
Moviol	Sigma-Aldrich (Taufenkirchen)
Nonindet P-40 (NP-40)	Fluka (Buchs)
Normal goat serum	JI- Research, Dianova (Hamburg)
Nupage bis-tris gel (4-12%)	Invitrogen (Karlsruhe)
Nupage tris-acetate gel (4-8%)	Invitrogen (Karlsruhe)
Optiprep density gradient medium	Sigma- Aldrich (Taufenkirchen)
Paraformaldehyde	Merck (Damstadt)
Phenol	Roth (Karshule)
Phenol red	Merck (Damstadt)
PLA_2 enzyme	Sigma-Aldrich (Taufenkirchen)
Propidium iodide	Sigma-Aldrich (Taufenkirchen)
Proteinase K	Roche (Mannheim)
Rabbit reticulate lysate	Promega (Mannheim)
Radiochemicals	Amersham (Braunschweig)
S7 nuclease	Roche (Mannheim)
TritonX-100	Serva (Heidelberg
t-RNA (*S. cerevisiae*)	Sigma-Aldrich (Taufenkirchen)
Tryphane blue	Feinbiochemika (Heidelberg)
Trypsin 10X	GIBCO-BRL (Karlsruhe)
Tween 20	Merck (Damstadt)

4.1.2 Inhibitors

AACOCF3	Merck Biosciences (Damstadt)
Cycloheximide	Sigma-Aldrich (Taufenkirchen)
H-89 dihydrochloride	Calbiochem Merck (Damstadt)
Hygromycin B	Sigma-Aldrich (Taufenkirchen)
Manoalide	Mol.Bio.Tech (Gottingen)
Roscovitine	Sigma-Aldrich (Taufenkirchen)
Z-VAD-FMK (Z-Val-Ala-DL-Asp-fluoromethylketone)	A.G Scientific (Göttingen)

4.1.3 Antibodies and Beads

Alexa fluor 594 donkey anti-mouse	Molecular probes (Heidelberg)
Alexa fluor 488 donkey anti-rabbit	Molecular probes (Heidelberg)
Antibody against NS1 anti-mouse	Kind gift from Jan Cornelis, DKFZ, Heidelberg
Cy5- conjugated goat anti-mouse	Dianova (Hamburg)
Cy5- conjugated goat anti-rabbit	Dianova (Hamburg)
FITC-conjugated goat anti-mouse	Dianova (Hamburg)
FITC-conjugated goat anti-rabbit	Dianova (Hamburg)
Karyopherin α/Rch-1 anti-mouse	BD Biosciences (Heidelberg)
Monoclonal Ab against NPC anti-mouse	Hiss Diagnostic (Freiberg)
Antibody against VP1 anti-rabbit	Kind gift from Jan Cornelis, DKFZ, Heidelberg
POD-conjugated donkey anti-mouse	Dianova (Hamburg)
POD-conjugated donkey anti-rabbit	Dianova (Hamburg)
Texas red-conjugated goat anti-mouse	Dianova (Hamburg)
Texas red-conjugated goat anti-rabbit	Dianova (Hamburg)
Dynabeads M280 sheep anti-mouse	Dynal Biotech (Hamburg)
Dynabeads M280 sheep anti-rabbit	Dynal Biotech (Hamburg)

4.1.4 Cell Lines

EYFP-Lamin B receptor cell line	Kind gift from Jan Ellenberg, EMBL, Heidelberg, Germany. (Ellenberg.J, et al, 1997)
HeLa cell line	Human cervical carcinoma cell line with epithelial morphology. The original HeLa cells came from Henrietta Varnish, died in 1951 in Baltimore, USA.
Huh-7 cell line	Human Hepatoma cell line, established from a hepatocellular carcinoma of 57 year old Japanese.
NBK cell line	Simian virus 40-transformed human newborn kidney cells (Shein and Enders 1962)

4.1.5 Primers

H-1 3479f	The 5' and 3' end of the primers correspond the positions (5'-3') 3479-3485 in the genome of parvovirus H-1	TIB MOLBIOL, Berlin
H-1 3732r	The 5' and 3' end of the primers correspond the positions (5'-3') 3732-3707 in the genome of parvovirus H-1	TIB MOLBIOL, Berlin
H-1 3´FL Probe	The 5' and 3' end of the Hy- probe correspond the positions (5'-3') 3642-3669 in the genome of parvovirus H-1	TIB MOLBIOL, Berlin
H-1 3´LC Probe	The 5' and 3' end of the Hy- probe correspond the positions (5'-3') 3671-3698 in the genome of parvovirus H-1	TIB MOLBIOL, Berlin

4.1.6 Plasmid

H-1 Plasmid (5176+2686bp)	Plasmid coding for the Parvovirus H-1 cloned with restriction sites in the basic vector PUC 19 (2686) (New England Biolabs), were kind gift from Jan Cornelis, DKFZ, Heidelberg.

4.1.7 Equipments

Binocular microscope	Leitz (Wetzlar)
Centrifuge biofuge 15R	Heraeus (Hanau)
Confocal laser scan microscope	Leica Lasertech (Heidelberg)
Confocal Leica SP-5	Leica (Mannheim)
Desk centrifuge 5415 C	Eppendorf (Hamburg)
Light Cycler PCR	Roche (Manheim)
Petridishes	Greiner (USA)
Phase contrast microscope	Zeiss (Heidelburg)
Rotors for ultracentrifuge	Bechmann (Munich)
Ultracentrifuge L5-50	Bechmann (Munich)
Ultrasonic sonicator UW-70	Bendelin Electro (Berlin)
24 well dishes	Nunc Inc. (USA)

4.1.8 Kits and Extras

DNA ladder marker	Promega (France)
Hyper film MP (X-Ray films)	Amersham Biosciences (Freiburg)
Molecular weight marker (Rainbow marker)	Amersham Biosciences (Freiburg)
Western lightning chemiluminescence Reagent	Perkin Elmer (Rodgau)

4.1.9 Buffers and Solutions

DMEM media (ready to use)
4500 mg/L glucose
GlutaMax
Pyruvate

PBS (pH 7.4)
171 mM NaCl
3.4 mM KCl
10 mM Na_2HPO_4
1.9 mM KH_2PO_4

PBS-MK
500 ml 1X PBS
500 µl 1 M-$MgCl_2$
500 µl 2.5 M-KCl
Do not autoclave, only sterilize by sterile filter.

3% PFA
6 g Paraformaldehyde
150 ml D/W + 3-4 drops of 3 M KOH
Dissolve PFA at 55°C for 10 min
20 ml 10X PBS and make final volume of 200 ml D/W.

Mowiol/DABCO
2.4 g Mowiol
6.0 g in glycerin,
6 ml Distill water
6 ml 200 mM Tris-buffer pH 8.5
stored at -20°C. Add 100 mg DABCO in 1 ml mowiol just before the use.

10X Transfer buffer
30 g Tris
144 g Glycine
15% Methanol
Add 1000 ml of distill water and make the pH 8.5

10X Transport buffer
200 mM Hepes (pH 7.3)
20 mM Magnesium acetate
100 mM Potassium acetate
50 mM Sodium acetate
10 mM EGTA
Add 1 M DTT just before the use.

50X TAE buffer (pH 7.8)	242 g Tris-base 57.1 g Acetic acid 0.5 M EDTA (pH 8.0) (100 ml) add distill water to make up the volume 1000 ml.
Agarose sample buffer with SDS (6X)	50% (w/v) Saccharose 0.25% (w/v) Bromophenol blue 6X TAE 1.2% (w/v) SDS
PAGE running buffer (20X)	97.6 g MES 60.6 g Tris Base 10 g SDS 3 g EDTA
PAGE sample buffer (4X)	4 g Glycerol 0.682 g Tris Base 0.666 g Tris HCl 0.8 g LDS 0.006 g EDTA 0.75 ml 1% Serva blue G250 0.25 ml 1% Phenol Red add 10 ml of H_2O.
2x Proteinase K-buffer	200 mM Tris-HCl (pH 7,5) 25 mM EDTA (pH 8,0) 300 mM NaCl 2% SDS

4.2 Methods

4.2.1 Cell Culture

NBK-324 (New Born Kidney) and HeLa cells (Human Cervical Carcinoma) cell lines were maintained in DMEM (Dulbecco's Modified Eagle Medium) supplemented with 5% Fetal calf serum (FCS) and grown at 37°C in 5% CO_2. Huh-7 (Human Hepatoma) cells and EYFP lamin B receptor NRK cells were maintained in same above mentioned medium but were supplemented with 10% FCS.

4.2.2 Virus preparation and Virus purification

Virus stock was prepared by infection (H-1 virus) of NBK cells with 0.1 PFU of virus per cell and incubated at 37°C for 2.5 days. After freezing and thawing for 5 times, the cells were harvested at 10,500 rpm for 15 min at 4°C. Again 5 times freezing and thawing cycles of the supernatant was repeated and aliquots were stored at -20°C. Cell lysates were further purified with iodoxinal gradient, which was formed by underlying and displacing the less dense cell lysate with iodoxinal, prepared using 60% (w/v) sterile solution of optiprep 10 ml of the crude virus extracts were transferred into quick-seal ultra-clear centrifuge tubes (Beckmann, Munich) using a spinal needle. This step performed to avoid air bubbles, which would interfere with subsequent filling and sealing of the tube. Then 7.5 ml of 15% iodoxinal and 1 M NaCl in PBS-MK buffer (1X Phosphate Buffer Saline, 1 mM $MgCl_2$ and 2.5 mM KCl), 2.5 ml of 25% iodoxinal in PBS-MK buffer containing phenol red (2.5 µl of a 0.5% stock solution/ml of iodoxinal solution), 2 ml of 40% iodoxinal in PBS-MK buffer, and finally, 2 ml of 60% iodoxinal in PBS-MK containing phenol red (0.01 µg/ml) were added in this order. Tubes were sealed and centrifuged by using rotor TST 41.14 at 36,000 rpm for 4.5 h at 10°C. The purpose of the phenol red was to distinguish the alternating density steps. The purified virus was collected from the visible clear 40% phase. Empty capsids were collected from the 25% phase and cell debris collected from 15% phase.

4.2.3 Localization of capsids

NBK and HeLa cells (1 x 10^3 cells) were grown on collagenised cover slips in DMEM medium which was complimented with 5% FCS and incubated overnight at 37°C. Removed the old media and FCS free DMEM media (500 µl) was added to the cells and incubated for 10 min at 37°C. Cells were infected with different concentrations of H-1 virus and timepoints, which were mentioned in each experiment. According to the experiment requirement, cells were treated with different inhibitors cycloheximide (50 µg/ml), hygromycin B (300 µg/ml), H89 (10 µm), roscovitine (50 µm) and ZVAD-fmk (50 µm) for overnight at 37°C. In another experiment, cells were treated with cycloheximide (50 µg/ml) in the presence of H-1 virus for 10 h at 37°C. Cells were washed two times carefully with FCS free DMEM media and incubate at 37°C for 30 min later H89, roscovitine and ZVAD-fmk inhibitors were added in the DMEM medium supplemented with 5% FCS for overnight at 37°C. Cells were washed two times with 500 µl of 1x PBS and fixed with 400 µl of 3% paraformaldehyde (PFA) at 4°C for 2 h. Later indirect immunostaining and confocal analysis were performed.

4.2.4 pH treated capsids

After growing HeLa cells on collagenised coverslips, acidified the H-1 capsids by treating with pH 5.2 (potassium acetate buffer) for 10 min at 37°C and followed by neutralisation with 0.5 M Tris (1.5 µl). Cells were infected with pH treated and untreated H-1 capsids for overnight at 37°C. Two times cells were washed with 1x PBS (500 µl) and fixed with 3% PFA.

4.2.5 Indirect immunofluorescence

After fixation, cells were washed three times with 1x PBS (500 µl) at RT before each well was filled with 500 µl 0.1% Triton X-100. The dish incubated at room temperature for 10 min in order to permeabilize the cell membranes. After that, the wells were washed three times with 1x PBS (500 µl). In the primary antibody mixture, mAb 414 (mouse) was diluted in 1:200 in antibody solution (1x PBS, 5% BSA, 5% goat serum), whereas the anti-capsid (rabbit) antibody was diluted 1:100. For each coverslip, 20 µl antibody mixture was spotted on parafilm in a humid box. The coverslips were placed with their cell side on the drop of antibody mixture. The humidified box was incubated at 37°C. After 1.5 h, the down side of the coverslips (where cells were attached) were rinsed with 100 µl 1x PBS before replaced in the 24 well dishes. The 24 well dishes was washed three times with 500 µl of 1x PBS. For secondary antibody reaction, a goat Texas Red-labelled anti-mouse antibody and goat FITC labelled anti- rabbit antibody were diluted (1:100) in antibody solution. In few experiments, texas red-labelled anti-mouse antibody was replaced by goat Cy-5 labelled anti-mouse antibody dilution (1:100) or donkey alexa 594 labelled anti-mouse antibodies (1:200), Alexa 488 anti-rabbit (1:200) and propidium iodide (chromosomal stain 1:1000) were added. This antibody mixture was spotted on parafilm in the humidified box followed by transfer of the cover slips as described before. The box was incubated at 37°C for 45 minutes, the cover slips were rinsed, replaced and washed as described. Drops of DABCO-Moviol were spotted on microscopical glass slides and the cover slips placed on them. The glass slides were kept overnight in the darkness at room temperature.

4.2.6 Confocal Laser Scanning microscopy

The cells were analysed using a 63X or 40X an apochromat objective by a LEICA DM IRBE. For the confocal analysis, the cells were scanned by laser power of 30% a signal of 85 % and a pinhole size of 1.0 with two folds magnification. Eight pictures were merged. For the representation of FITC, the FITC filter setting was used, for depicting texas red, the TRITC filter were used. The z position in all pictures was adjusted to the equatorial level of the cell. The pictures were arranged by using the Adobe-Photoshop software program version (8.0.1) on Microsoft Windows platform.

4.2.7 Co-immune precipitation

20 µl of dynabeads were taken for each sample and washed two times with 0.1% of BSA in 1x PBS (1 ml). Dynabeads coated with anti-VP1 (10 µl) and mAb 414 antibodies (10 µl), rotate on rotating wheel at 1000 rpm at 4°C for overnight. Dynabeads were washed four times with 0.1% BSA in 1x PBS (1 ml), resuspended in 150 µl of washing buffer and incubated the beads for 1 h at RT and 3 h at 4°C. Rest protocol defined separately. Later Anti-VP1 or mAb 414 coated dynabeads were added to the samples and reaction was followed by incubating for O/N at 4°C at 1000 rpm. Samples were washed three times with washing buffer (0.1% BSA in 1x PBS (1 ml)), one time with 0.1% NP-40 in PBS followed by three times with washing buffer. Finally, pellet was spinned down at 4°C, for 10 min at 8200 rpm. Supernatant was removed and the pellet was dissolved in 15 µl of 1X SDS loading buffer followed by SDS PAGE and western blot.

4.2.7.1 Co-immune precipitation of nups by progeny H-1 and vice-versa

HeLa cells were grown overnight at 37°C. Cells infected by full and empty H-1 capsids for 48 h at 37°C. Later HeLa cells treated with full and empty capsids, thereafter cells were washed with PBS and removed the cells ($1x10^{10}$ cells) carefully with rubber police. Cell pellet was obtained at 1200 g for 15 min at 4°C. Pellet was collected and resuspended in 200 µl of PBS and sonified for 15 s at

least five times. Final concentration of 0.1% Triton 100X and Protease A were added and incubated for 30 min at 37°C.

4.2.7.2 Co-immune precipitation of importin α and anti capsid antibody

Dynabead coating and washing procedure was same as mentioned before. For sample preparation, untreated and pH treated H-1 virus was used (pH treatment: 4.6, 5.2 and 6.0 for 10 min at 37°C and neutralized with 0.5 M Tris (1.5 µl)). In all samples, importin α (50 ng) and importin β (90 ng) was added and incubated for 2 h at RT. Later, dynabeads were mixed with coated VP1 antibody to the samples for overnight at 4°C. Rest procedure was same as described in 4.2.7 paragraph.

4.2.8 SDS gel electrophoresis

For proteins, SDS-PAGE was performed according to ready to use gels (4-12% bis-tris gel and 4-8% Tris-acetate-gel from Invitrogen and Anamed gels (Aplelex). Each sample was dissolved in 15 µl of 1X SDS loading buffer (Invitrogen) and 1.5 µl of DTT (1M). Samples were heated at 95°C for 10 min before loading. The electrophoresis assembly was connected with power supply; a voltage of 8 V/cm was applied to the gel. Later, the voltage was increased to 15 V/cm and the gel was run until the bromophenol blue dye reaches to the bottom of the resolving gel.

4.2.9 Western blot

4.2.9.1 Western blot (I)

Firstly, activate the PVDF (poly vinylidene fluoride, VWR International, Frankfurt main) membrane with methanol for 2 min followed by 2 min with distill water treatment and then 10 min incubation with 1X transfer buffer at RT. Proteins were blotted on to the membrane using a wet blot chamber from Invitrogen (40mA volts at RT for overnight). Membrane was blocked with 5% fat free skim milk in 1x PBS for 1h at RT and followed by incubation for 3 h at RT with primary antibodies (anti-capsid, anti-mAb 414 and anti-importin α (1:1000). Membrane was washed three times for 10 min with washing buffer (0.5% skim milk and 0.1% tween 20 in PBS) at RT. Membrane was incubated with corresponding secondary antibodies (peroxidase anti-rabbit (1:5000) / mouse antibody (1:3000)) for 1 h. Membrane was washed three times for 10 min with washing buffer and finally, membrane was washed with one time with 1x PBS for 15 min. Antigen-antibody immunoreactive reaction was visualized with ECL system (Enhanced chemiluminescence system from Perkin Elmer, Rodgau) according to the company instructions.

4.2.9.2 Western blot (II)

Activation of PVDF membrane and running conditions were same as described above. Membrane was blocked with 5% skim milk and 0.2% tween 20 in PBS for 1 h at RT followed by primary antibody (TAT 1, specific to tubulin) was diluted 1:50 in PBS + 0.2% tween 20 + 0.5 M NaCl + 0.02% NaN3 at 4°C for overnight. Membrane was washed three times with 1 M NaCl. Membrane was incubated with the corresponding secondary peroxidase anti-mouse antibody with 5% skim milk and 0.2% tween 20 in PBS for 1 h at RT. After secondary antibody treatment, washing was done with 0.2% Tween 20 in PBS at least four times. Later membrane was visualized for antigen-antibody complex as described before.

4.2.10 Agarose gel electrophoresis

DNA was separated by agarose gel electrophoresis. 1 % agarose in 1x TAE buffer was placed in the microwave till the agarose was completely dissolved, allowed to cool slowly, mixed and poured into a taped gel tray. Thereafter, the 13 well combs were inserted and the gel allowed solidifying. Afterwards, the comb was removed, DNA was loaded along with loading buffer. The DNA was electrophoretically separated at a voltage of 75 V. After proper separation, gel was placed in 0.5 µl of ethidium bromide (1 mg/ml stock solution) solution for 20 min. Ethidium bromide was a fluorescent dye that intercalates between bases of nucleic acids and allows very convenient detection of DNA fragments. Ethidium bromide intercalates DNA and this complex becomes fluorescent viewed under UV-light (260 nm wave lengths, UV-25, MarcoVue, Hoefer, Germany). Photographs were taken with a gel camera (RS-1, Kaiser, Clara Vision) by using Gel smart V 7.3 software program. To determine the size of the DNA present in the fragment of interest, a DNA ladder marker (Promega, Mannheim, Germany) of similar size and known concentration was applied and the amount of DNA present in the band of interest estimated by comparing it to appropriate marker.

4.2.11 S7 Nuclease digestion of Parvovirus H-1

Parvovirus H-1 was digested with S7 Nuclease at 2 U/µl in the presence of 5 mM $CaCl_2$ for 3 h at 37°C. S7 nuclease digests both single stand as well as double strand of DNA. The digestion process was stopped by adding supplements of 6 mM EGTA and released the protected viral DNA by digestion with proteinase K out of the H-1 capsid.

4.2.12 Gradient passed pH treated capsids

Capsids were treated with pH 4.6 (potassium acetate buffer) for 10 min at 37°C and neutralised by 0.5 M Tris (1.5 µl) and pH untreated capsids were used as control. Iodoxinal gradient were ran as described before at 36,000 rpm for 4.5 h at 10°C (SW 41 Beckmann). Fractions were collected and aliquoted 500 µl per vial. All fractions were treated with proteinase K.

4.2.13 Proteinase K digestion

Viral DNA was digested with proteinase K (Roche, Mannheim) to release the viral capsids. For the proteinase K digestion, 1 sample volume of proteinase K in 2X proteinase K buffer was mixed. Digestion of the viral DNA and proteinase K mixture was performed by incubating at 65°C for overnight. After the digestion process, Phenol-chloroform extraction carried out in order to elute the protein contained in the solution.

4.2.14 Phenol-chloroform-extraction

The proteinase K digested samples were transferred with a volume of phenol, vortex for a min and centrigued for 10 min by the table centrifuge (5415 Eppendorf) at 14,000 rpm. In this manner, debris denatured and collected itself in the organic phase, while the nuclei acids remain in the liquid phase. The upper liquid phase transported into a new eppendorf tube. After the centrifugation if, an interphase appeared that contains a mixture of proteins and nuclei acids, this had to transfer together with the phenol (1time of sample volume), vortexed and follow the same centrifugation process as described above.

The resulting upper phase was taken out and added with a pipette to the first DNA phase. The step was repeated until no more interphase seen. To remove the rest of the phenol in the DNA phase, a

volume of chloroform was transferred, vortexed for a min and centrifuged for 10 min at 14,000 rpm in the table centrifuge. The upper water phase was transported into a new Eppendorf reaction tube. The last step was repeated to develop the interphase. Subsequently the precipitation of the nucleic acids obtained through ethanol precipitation. 96% ethanol added to 2.5 sample volume of the hydrophilic DNA-containing supernatant and vortexed. The mixture freezed at least for 20 min at -70°C. Then centrifugation was performed for 15 min at 4°C and 15,000 rpm. After the centrifugation, the obtained supernatant discarded and the DNA pellet dried at RT to remove the additional ethanol. The purified nucleic acids further used for PCR.

4.2.15 Determination of Parvovirus H-1 DNA with Real-Time-PCR

All samples applied for PCR reaction must digested with proteinase K digestion, extraction with phenol-chloroform and concentration of DNA with ethanol in the presence of tRNA (50 ng) co-precipitation with nucleic acids. After purification, nucleic acids resuspended in H_2O and directly used for the PCR. 10 µl of the sample volume was used for the PCR. H-1 plasmid was used to create the standard curve. The H-1 plasmid concentration was quantified with UV-spectrophotometer Du-70 (Bechmann, Munich, Germany). The plasmids (~1,65 x 10^{11} copies/µl ds DNA) were diluted in H_2O. Standard serial dilutions were generated using 1.5 dilution steps for a concentration of 5x10^7 till 1.6 x10^3 single stranded DNA genome. In Light Cycler, the reaction was performed in a glass capillary tube with a volume of 20 µl. 10 µl of template free water was used as a negative control. Before the capillaries loaded with the standard curve and the examining samples, 10 µl of master mix, necessary primers, probes and enzymes were added.

Following list of the primers were used for the detection of Parvovirus H-1 with Real-Time-PCR (Besselsen.DG, et al, 1995)

H-1 3479f: 5′ – CTA GCA ACT CTG CTG AAG GAA CTC – 3′

The 5′ and 3′ end of the primers from 24 nucleotides corresponds to the positions (5′- 3′) 3479-3502 in H-1 parovirus genome.

H-1 3732r: 5′ – TAG TGA TGC TGT TGC TGT ATC TGA TG – 3′

The 5′ and 3′ end of the primers from 26 nucleotides corresponds the positions (5′- 3′) 3732-3707 in H-1 parovirus genome.

The designed primers amplified 254 bp fragments from the 5176 bp of the parvovirus H-1 genome. Following sequence of the H-1 genome was selected in this work for the hybridization probes.

H-1 probe 3′FL 5′ – ACT TAC TCA CAC ATG GCA AAC CAA CAG A – 3′ - Fluorescein

The 5′ and 3′ end of the hybridization probe corresponds to the positions (5′- 3′) 3642-3669 in H-1 parvovirus genome

H-1 probe 5′LC 5′ - LC Red640 – ACT TGG CAT GCC TCC AAG GAA TAA CTG A – 3′

The 5′ and 3′ end of the hybridization probe corresponds to the positions (5′- 3′) 3671-3698 in H-1 parvovirus genome

All the preparations were performed on ice to avoid the degradation of hybridization probes. Since the probes are photosensitive, all probes were kept in the dark during preparations.

The master mix consists of 20 µl volume including following reagents:

1 µl primer H-1 3479f [10 pmol/µl]

1 µl primer H-1 3732r [10 pmol/µl]

0,5 µl H-1 probe 3´FL [8 pmol/µl]

0,5 µl H-1 probe 5´LC [8 pmol/µl]

1,6 µl $MgCl_2$ [25 mM]

3,4 µl H_2O

2 µl LC-FastStart Reaction Mix (Roche diagnostics, Mannheim), contains *Taq* polymerase enzyme.

Master Mix was prepared with the above described reagents, mixed well and distributed to Light-Cycler capillaries tubes with a volume of 10 µl. Then after, 10 µl of the sample added. Filled capillaries were subjected for a short centrifugation with a speed of 1000 rpm in the table centrifuge and carefully placed in the Light-Cycler carrousel. PCR-software program used to run the machine with the following conditions.

Denaturing: 1 cycle	Temperature	Incubation period
	95°C	10 min
Increase of temparature	20°C/sec	

Amplification: 45 cycles	Temperature	Incubation period	2. temperature
Denaturation	95°C	10 sec	
Annealing	62°C	8 sec	53°C
(Decrease of temperature from 1°C for a cycle till reached the 2.temparature)			
Elongation	72°C	10 sec	
Increase in temperature	20°C/sec		

Cooling: 1 cycle	Temperature	Incubation period
	40°C	30 sec
Increase in temperature	20°C/sec	

Real-Time-PCR conditions for the Light Cycler were established in this work for the Parvovirus H-1. After denaturing step at 95°C for a period a 10 min, that was necessary for the activation of the relative ducks "almost start Taq" Polymerase.

The PCR was carried out as a "touch down PCR". In the first amplification cycle, the annealing temperature was set to the goal temperature of 62°C. In every amplification cycle, annealing temperature was sunken 1°C until it reaches the second goal temperature at 53°C.

In the PCR program, the sample amount and the standard dilutions of known concentrations were stored. After completing the PCR cycles, the samples were evaluated. The measurement canal was placed on "Ch 2/1"that measures the light of the wave lengths 640 nm and 530 nm. Through blocking the basic line ("Noise volume"), genome concentrations of the samples were calculated in different intensities of the fluorescence.

4.2.16 Permeabilized and non-permeabilized HeLa cells treated with H-1 virus

HeLa cells were grown on collagenised coverslips with 5% FCS containing DMEM media for overnight at 37°C**.** Media was removed and cells were washed three times with FCS free media. In permeabilzed cells, permeabilization buffer (DMEM media without FCS + digitonin (20 mg/ml) 1:500, propidium iodide 1:1000) were added for 5 min at 37°C. Cells were washed two times with 1X transport buffer at RT. H-1 virus was added to the required samples for 30 min at 37°C followed by the two times washing with 1X transport buffer. In another set, restained the cells with propidium iodide (1:1000) in transport buffer for 5 min at 37°C .Wash the cells two times with 1X transport buffer. In non-permeabilized cells, H-1 virus was added in required samples for different time points (15 and 30 min) at 37°C. Cells were washed and staining was performed by propidium iodide (1:1000) in 1X transport buffer for 5 min at RT. In both cases, cells were mounted with one or two drop of DABCO/moviol as described before. Results were determined by phase contrast microscopy.

4.2.17 Phase contrast microscopy

Samples were examined by phase contrast microscope (Zeiss, Heidelberg), by using 63X phase-3, an apochromat objective with immersion oil was dripped on each of cover slips. 25-50% laser intensity used. Pictures were taken by using Micromax camera and captured by Metamorph software program.

4.2.18 Live cell microscopy

HeLa cells (1 x 10^{10} cells) were grown on collagenised petridishes (Falcon, Heidelberg, Germany) at 37°C for overnight. Cells were washed two times with FCS free DMEM media at RT, followed by the permeabilization (permeabilization buffer: FCS free media, digitonin (20 mg/ml) 1:500 and propidium iodide (1 mg/ml) 1:1000) for 5 min at 37°C (prewarmed the permeabilization buffer at 37°C). Chromatin was stained with propidium iodide. Then after, 2 times washed with 2 ml of 1X transport buffer. After permeabilization, 1X transport buffer (100 µl) was added as a negative control. Release of chromatin was initiated by addition of H-1 (1.6 x10^8 capsids) in transport buffer (100 µl). Mock purified virus from non H-1 infected cell line (NBK) was purified as same as given in section 4.2.2. Cells were pre-incubated with hexokinase (1 U/ml)/glucose (7 mM) of final concentration for 10 min at 37°C. In control samples, hexokinase/glucose treatment was not given. To see the effect of lamin B receptor, instead of HeLa cells EYFP lamin B expressed cell line was used. In negative control, 1X tranport buffer was added. To know the involvment of NS1 protein, H-1 virus was pre-incubated with NS1 antibody (10 µl) at 4°C for overnight. In enzymatic experiment, in required samples (transport buffer/H-1 virus) was added in the petridish at RT and 37°C. (pictures were taken for every 5 min till 60 min for RT samples and for every 2 to 5 min till 30 min). Apoptotic and mitotic cells were observed by pre-incubation with H-89 (10 µm), roscovitin (50 µM) and ZVAD-fmk (50 µM) inhibitors for 2 h at 37°C. These inhibitors were present through out the experiment later H-1 (1.6 x10^8 capsids) were added. In WGA experiment, (first low concentrations of WGA were used but did not show any effect to used high concentrations) cells were treated with 1mg/ml WGA (lectin from *Triticum vulgaris*). WGA was present through out the experiment. In PLA_2 experiment, after permeabilization PLA_2 molecules

(1.6×10^8 PLA_2 molecules, Bovine pancreas) were added. To see the effect of NPC on NEBD, cells were permeabilized and pre-incubated with phosphorylated HBV capsids (1.2 µg) in the presence of cytosol RRL (rabbit reticulysate 21 mg/ml) for 15 min at 37°C. Cells were washed carefully with 2 ml of 1X transport buffer and, H-1 was added. In control samples, instead of P-rHBV capsids 1X transport buffer was added and incubated for 15 min at 37°C. Pictures were taken by confocal microscopy (pinhole size 1.0, 40 X objectives) for every 2 to 5 min.

4.2.19 Confocal analysis and quantification of nuclear fluorescence

A drop of immersion oil was dripped on each of cover slips/petridishes. The cover slips/ petridishes were put on the microscope (Confocal Leica SP-5). The cells were analysed using a 63X (aperture size 1.4) or 40X (aperture size 1.25) an apochromat objective by a HCX PLAPO CS. For the confocal analysis the cells were scanned by laser power of 20% a signal of 85% and a pinhole size of 1.0, zoom size of 1.5 and all antibodies setting were given below. Pictures were taken by LAS AF (Leica Application System Advanced Fluorescence) software program. The z position in all pictures was adjusted to the equatorial level of the nuclei. The pictures were arranged by using the Adobe-Photoshop software program. Image J software program was used for the quantification of the stained nuclei and graphs were prepared in excel data sheets.

Antibody	Laser	Excitation (nm)	Emission (nm)
Alexa 488	Ar 488	499	520
Alexa 594	He Ne 543	580	618
Cy-5	He Ne 633	650	670
EYFP	Ar 514	514	527
FITC	Ar 488	495	519
Propidium iodide	Ar 514	538	617
Texas-red	He Ne 543	595	616

5. Results

5.1 Localisation of H-1 capsids

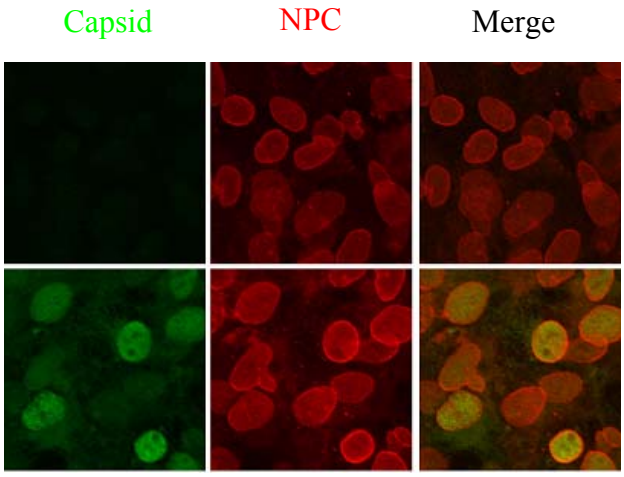

Figure.1A. Immunostaining of NBK cells infected by H-1

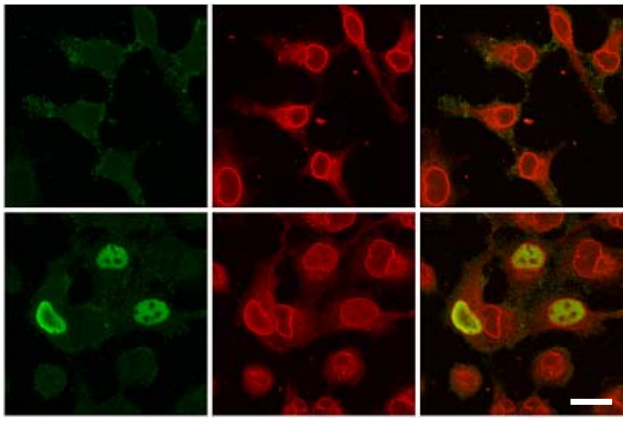

Figure.1B. Immunostaining of HeLa cells infected by H-1

Figure 1: Localization of H-1 parvovirus capsids after overnight infection in NBK (figure 1A) and HeLa (figure 1B) cells by confocal laser scanning microscopy after immune staining. Capsid (green) and NPC (red). Bar 10 µm.

Most studies on parvoviruses were performed using MVM and CPV. H-1 was choosen as it allows investigations without safety precautions incontrast to the before mentioned ones. Despite of its ability to infect basically all cell lines but not showing any diseases, is related to H-1 infection. For allowing to draw parallels between H-1 and other autonomous parvoviruses we first investigated the infection process by monitering the viral capsid using microscopy.

Indirect immunofluorescence analysis was performed with two different cell lines NBK (newborn kidney human) which are lytic to H-1 and non-lytic HeLa (cervical cancer cell line, *Helenus lactinus*). These two cell lines were used to localize H-1 viral capsids after infection. Uninfected NBK and HeLa cells did not show any capsid fluorescence (figure 1) but the rim-like NPC stain (red). Over night infection of the both cell lines with H-1 (100 genome-containing capsids/cell) showed a capsid fluorescence (green) indicating specificity of capsid detection and the

susceptibility of both cell lines. Localization of the capsids was exclusively intranuclear with no detectable transport intermediates within the cytoplasm. This finding might indicate a very rapid transport through the cytoplasm into the nucleus. Instead, the amount of incoming capsids may not be sufficient to cause a visible signal but the strong intranuclear stain is derived from capsid multiplication after successful infection. For differentiation dose and time dependent infection experiments on HeLa cells were performed.

5.2 Time and dose dependent process

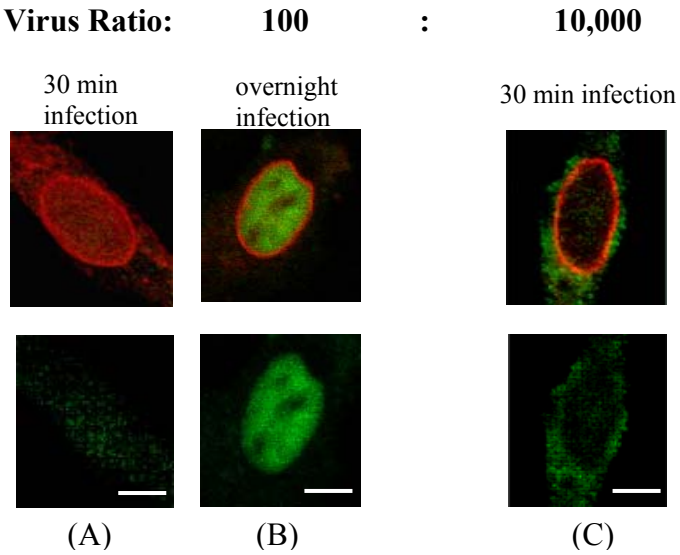

Figure 2: Localization of H-1 capsids at different time points after infection (HeLa), (A) no binding (green) only NPC stain (red) after 30 min infection at low dose, (B) intra-nuclear capsids (green) NPC (red) after overnight infection. (C) binding (green) NPC (red) after 30 min infection at high doses. Bar 10 µm.

HeLa cells were infected with a low and a high MOI of H-1 (ratio 100:10,000 capsids). Cells were fixed after 30 min to visualize incoming virus and after over night incubation, thought to allow the synthesis of progeny capsids. No capsids were observed in the HeLa cells that were infected with low dose of H-1 after 30 min (figure 2A) but upon infection with 100 times higher dose (figure 2C). This finding indicates that at low doses of H-1 the signal remained below the detection limit. In high dose infection, the capsids stayed cytoplasmic.

However, after over night incubation after low dose infection a strong intranuclear capsid signal was achieved (figure 2B), indicating capsid amplification. It must be thus concluded that intranuclear capsids represent progeny capsids.

5.3 Effect of mRNA translocation inhibitors on nuclear capsids

For confirmation, two different inhibitors blocking protein synthesis at different steps were used. First NBK cells were infected in the presence of hygromycin. This inhibitor blocks protein synthesis by disrupting translocation and promoting mistranslation of the ribosome. The results were confirmed by cycloheximide which interferes with the peptidyl transferase activity of the 60S ribosome, thus blocking translational elongation.

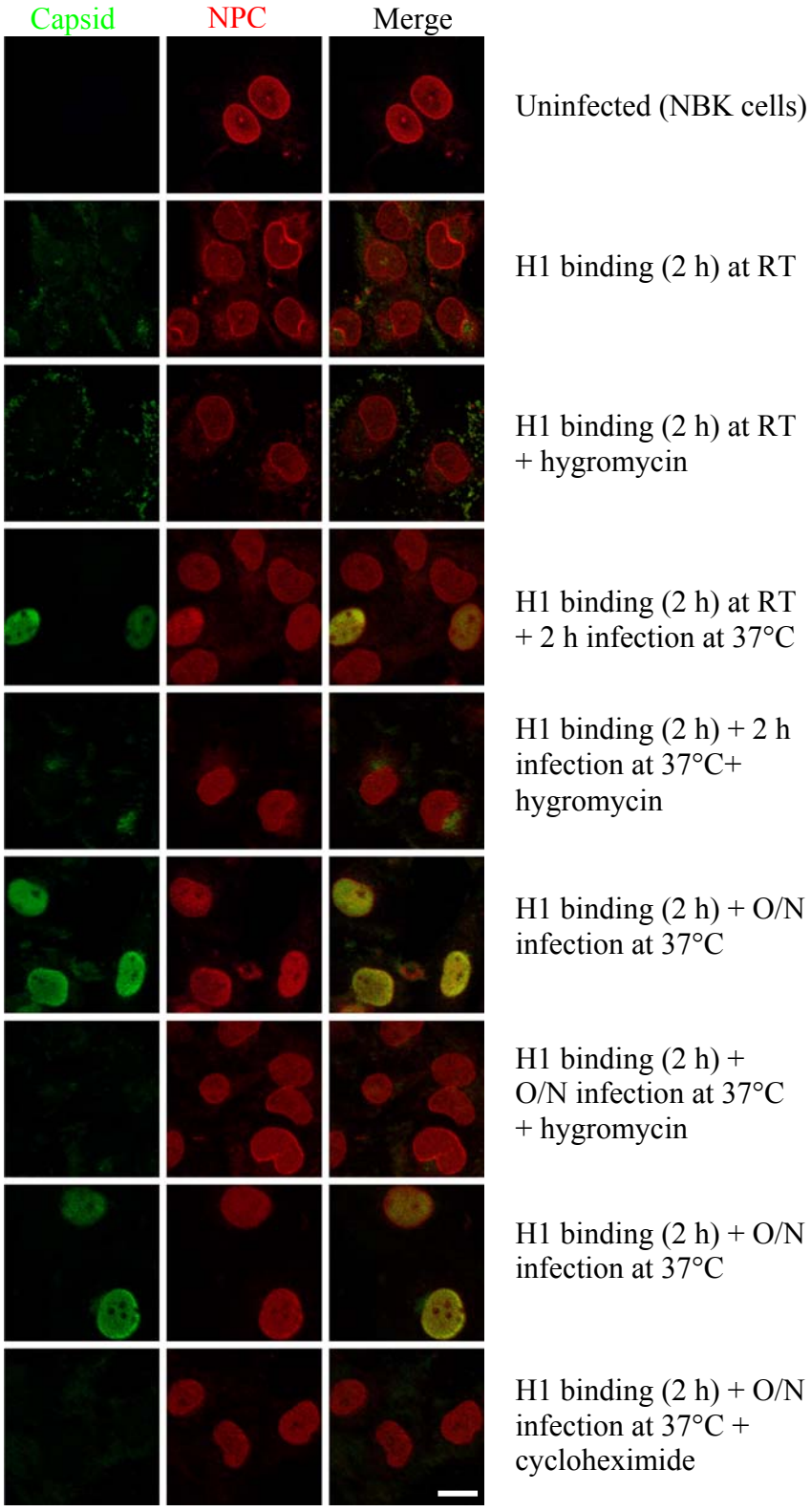

Figure 3A: Influence of mRNA translocation inhibitor on the generation of nuclear capsids (NBK), binding of capsid at RT (green), after 2 h and overnight post infection at 37°C intra-nuclear capsid observed, binding and intra-nuclear capsids formation was blocked by adding the hygromycin (250 µg/ml) and cycloheximide (50 µg/ml), this experiment shows that intra-nuclear capsids are progeny capsids not the incoming virus. Bar 10 µm.

Overview picture

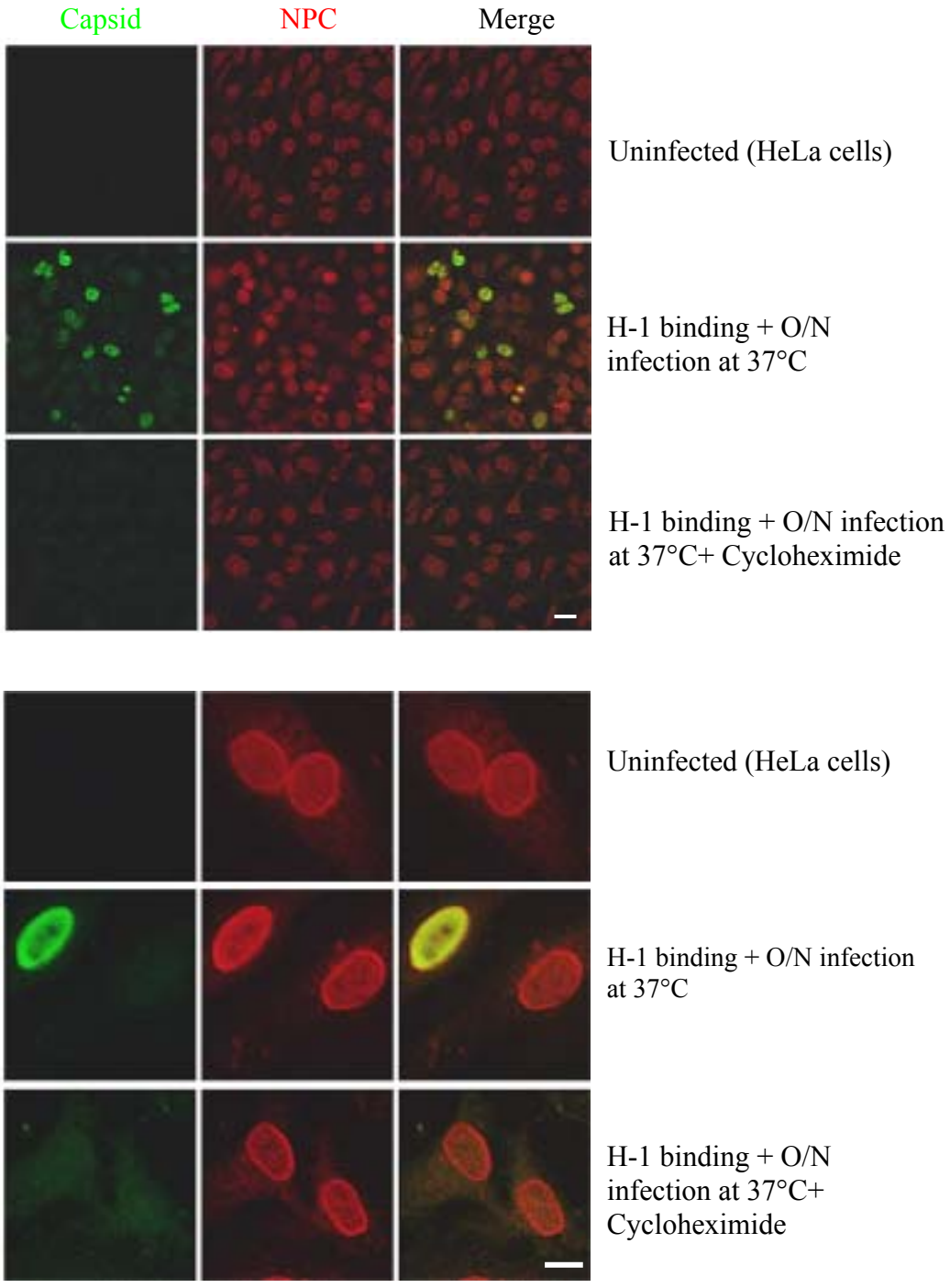

Figure 3B: Influence of translational elongation inhibitor on the generation of nuclear capsids (HeLa), overview picture showed the quantification. Bar 5 µm. Negative control no capsid stain. Overnight H-1 post infection showed intra-nuclear capsid and cycloheximide (50 µg/ml) treated cells. Bar 10 µm.

Infection was performed by adding the 150 capsids/cell together with inhibitor for 2 h at RT followed by incubation for 2 h or O/N at 37°C. Incubations at RT are known to allow receptor binding of the virus but active transport processes as endocytosis does not take place as it was shown in canine parvovirus (CPV) and feline parvovirus (FPV) (Hueffer.K, et al, 2003).

After 2 h at RT faint capsid signals were obtained in the presence and absence of the inhibitors (figure 3A), indicating that the inhibitors did not alter the binding activity of H-1. Further incubation at 37°C for 2 h showed a strong signal of intranuclear capsids in some cells of the untreated control but no intranuclear capsids in hygromycin treated cells (figure 3A). Consistently, an extended incubation at 37°C over night showed intranuclear capsids only in the untreated cells. Noteworthy, capsid and NPC stain overlapped intranuclear. Taken together, hygromycin B inhibits the intranuclear capsid formation, but did not interfere with the H-1 binding and uptake. In the absence of hygromycin B, rapid generation of nuclear capsids formed which supports the idea that intranuclear capsids are progeny capsids (figure 3A). Same observation shown incase of cycloheximide treated cells (figure 3A).

For excluding a cell line-dependent phenomenon, HeLa cells were infected in the presence of cycloheximide. Consistent with the infection of NBK cells, cycloheximide prevented intranuclear capsid formation even after over night incubation (figure 3B). As depicted in the magnification, same overlap of intranuclear capsid and NPC stain was observed.

5.4 To exclude the cross-talk of antibodies and overlapping of NPC and capsid stain

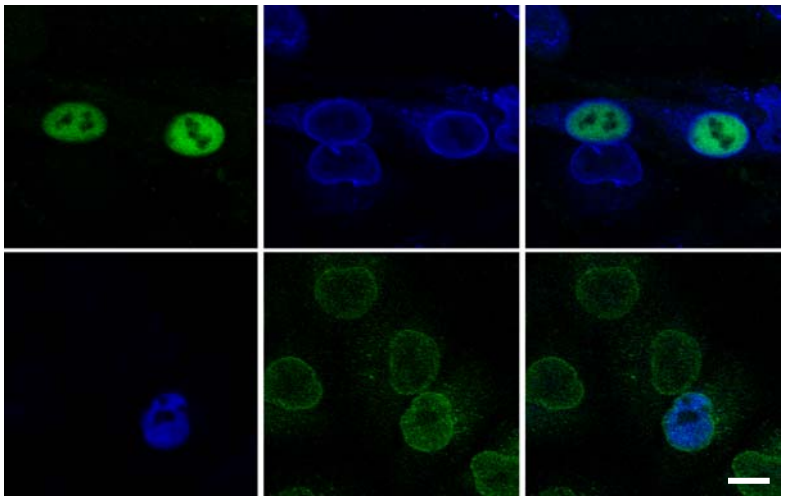

Figure 4: Analysing the overlapping stain of NPC and progeny H-1 capsids. (A) Capsids are depicted in green the NPCs in blue, in (B) vice-versa. This analysis showed the co-localization of the capsid staining. Bar 10 µm.

The overlap of capsid and NPC stain could be derived from (i) a co-localization of capsids with proteins of the NPC that are recognized by the anti-NPC antibody (FXFG containing nups e.g nup62, 358 and 153) (DavisLI and Blobel.G, 1986, Wu.J, et al, 1995, Shah.S, et al, 1998), (ii) a cross reactivity of the primary antibodies or (iii) a "bleed through" of the strong capsid fluorescence into the filter used for detection of the texas red-labelled secondary antibody that indicates the NPC (595- 616 nm).

To exclude the latter phenomenon, which is a technical artefact, a different secondary antibody for detection of the NPC was used. Cy5 was chosen as the emitted light is detected by a filter of 652-775 nm. At this long wave length FITC fluorescence (495-519 nm) can practically not be detected. In another experiment the second antibodies were exchanged, meaning that the capsids were visualized by Cy5 and the NPC by FITC. Figure 4 depicts that both detections after over night infection showed a significant co-stain, indicating that either the primary antibodies cross-reacted or that in fact progeny H-1 and NPC proteins were associated within the nucleus. It must be considered however that in the previous experiments no co-stain was observed for intracytosolic capsids, making cross-reactivity unlikely. Consistently, an interaction of the capsids with one or more antibody-reactive proteins of the NPC so called nucleoporins must be assumed.

5.5 Interaction of nucleoporins with H-1 capsids

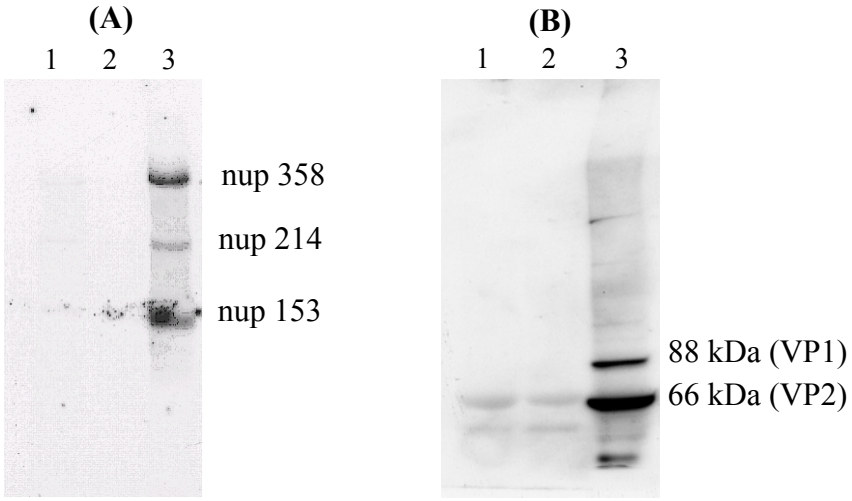

Figure 5: (A) Co-immune precipitation of nups by progeny H-1. Nucleoporins Nup 358, 218 and 153 were co-precipitated with the full capsids. **(B) Co-immune precipitation of H-1 by nups**. Full H-1 infected lysate as indicated by the 88 kDa band of VP1 and the 66 kDa band of VP2. Lane 1: HeLa cells (uninfected), Lane 2: HeLa cells + empty capsid, Lane 3: HeLa cells + full capsids.

For obtaining physical evidence for a capsid nucleoporins interaction (nup 358, 214, 153 and 62 complex). Lysates from HeLa cells, infected with empty and full capsids for 24 h was used. As negative control non-infected cells were used. After SDS PAGE and blotting the nucleoporin-bound capsids were detected with anti-VP1 antibodies. In the *vice versa* reaction, nucleoporins bound to capsids were visualized using the mAb 414 (after co-precipitation with the anti-capsid antibody).

Figure 5 depicts that both precipitations were specific in that no signal was obtained when the lysate of uninfected cells were subjected to the co-precipitation. Using the lysate from cells infected with full H-1, the nucleoporins Nup 358, 218 and 153 were co-precipitated. No signal was obtained using lysates from HeLa cells infected with empty capsids (figure 5A).

Consistently, mAb 414 co-precipitated capsids out of the full H-1 infected lysate as indicated by the 88 kDa band of VP1 and the 66 kDa band of VP2 (figure 5B). The missing band of VP3 that is a cleavage product of VP1 upon viral entry implies that these bands are derived from progeny capsid proteins. This assumption is in accordance with the missing capsid bands in the infection experiment to which empty capsids were added. In this sample no multiplication of capsids proteins took place.

5.6 Effect of pH on H-1 capsids

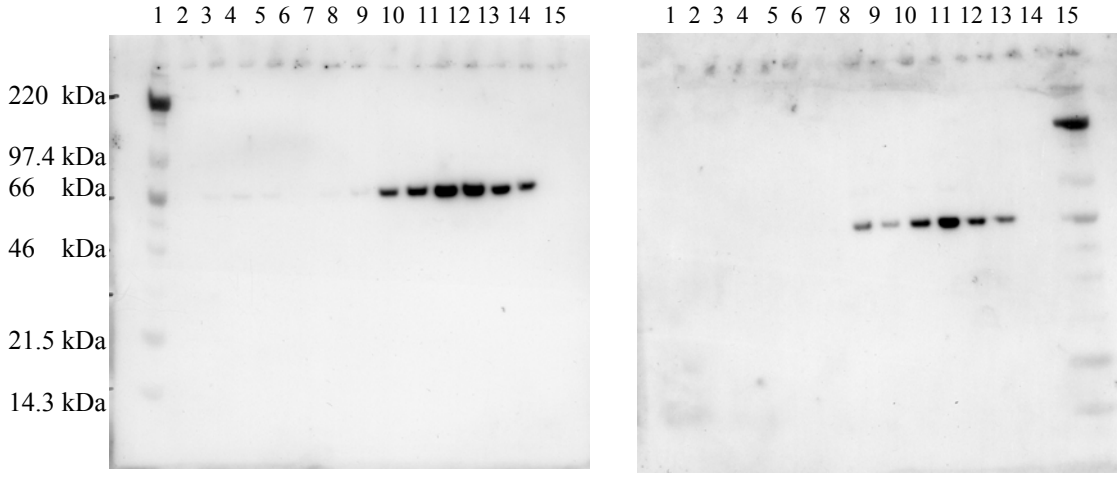

H-1 **H-1 pH4.6 treated with Tris**

Lanes	Samples	Lanes	Samples
1	Marker	1	X
2	X	2	15% fraction 1
3	15% fraction 1	3	15% fraction 2
4	15% fraction 2	4	15% fraction 3
5	15% fraction 3	5	25% fraction 1
6	25% fraction 1	6	25% fraction 2
7	25% fraction 2	7	25% fraction 3
8	25% fraction 3	8	40% fraction 1
9	40% fraction 1	9	40% fraction 2
10	40% fraction 2	10	40% fraction 3
11	40% fraction 3	11	60% fraction 1
12	60% fraction 1	12	60% fraction 2
13	60% fraction 2	13	60% fraction 3
14	60% fraction 3	14	X
15	X	15	Marker

Figure 6A: Effect of acidification on parvoviral entry. pH 4.6 treated and untreated capsids after neutralization tris (0.5 M). Passed with iodoxinal gradient (15%, 25%, 40% and 60%), centrifugation done for 2.5 h at 10°C. Aliquoted the different fractions. SDS PAGE (Bis Tris gel 4-12%) and western blot was performed and developed with anti-capsid antibody.

Parvoviruses enter the cell by endocytosis, requiring acidification (Bartlett.JS, et al, 2000, Basak.S and Turner.H, 1992, Parker.JS and Parrish.CR, 2000). At low pH the hidden N terminal domain of VP1 (VP1 unique part, VP1up) become exposed (Suikkanen.S, 2003). To analyse whether capsid (proteins) and genome dissociated upon acidification, we performed an experiment in which H-1 pH 4.6 treated and untreated capsids were subjected to gradient centrifugation analysis. Before giving the pH treatment H-1 was digested with S7 nuclease that was inhibited after the degradation reaction. After centrifugation fractions were analyse for VP1, density and viral DNA. In both preparations viral DNA was found in the fast migrating, heavy fractions (density 1.16). This effect was slightly move pronounced in the pH treated capsids. pH treated and untreated capsids were not showing difference in density between the capsid proteins in both cases the density peak is at 1.24

(figure 6B). Modification of viral capsids may thus allow the exposure of NLS which is needed for nuclear targeting and transport of viral particles, but did not show any sign of disintegration of the capsids.

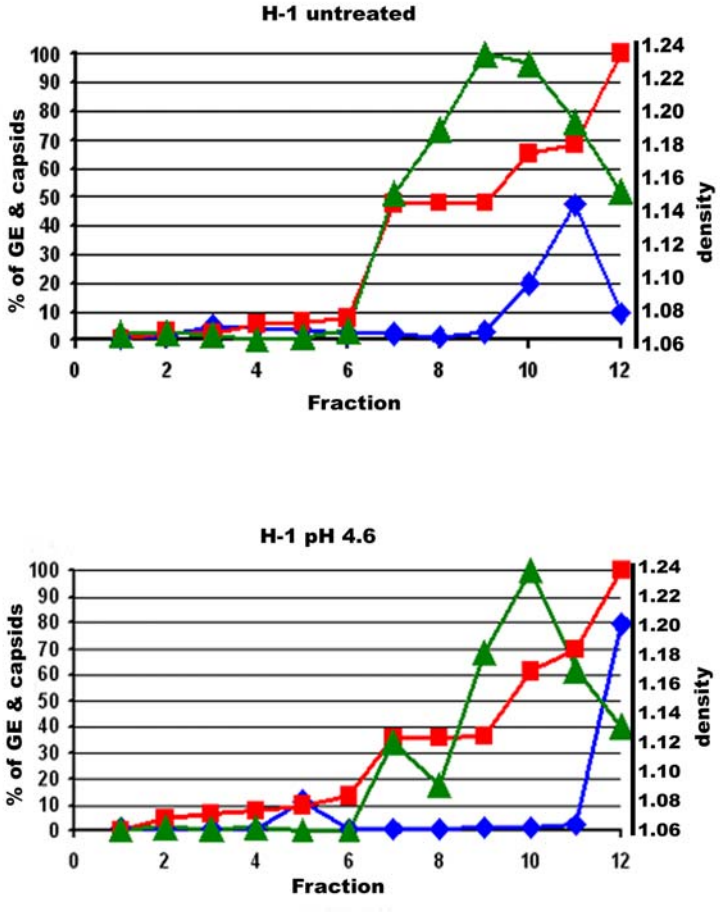

Figure 6B: Structural changes occurred due to pH treatment. pH 4.6 treated and untreated capsids after neutralization tris (0.5 M) after iodoxinal gradient centrifugation. No significant difference between the density of the capsid proteins were visible. Blue lines: PCR average (in triplates), red lines: density gradient, green lines: capsid protein.

5.7 Role of importin α on pH treated capsids

To analyse whether pH treatment indeed leads to NLS exposure as it was described to occur upon endocytotic acidification. Co-immune precipitations of the capsid were performed after addition of importin α/β. H-1 was treated with different pH (4.6, 5.2, and 6.0) for 10 min at 37°C then neutralised with tris base. Importin α and β were added in equimolar ratio to the pH treated capsids and incubated for 2 h at RT. Importin β was added as it stabilizes the NLS importin α binding in some cases (hepatitis B capsids, unpublished). After SDS PAGE, blotting and immune reactions the blot was developed with importin α and anti-capsid antibodies (figure 7).

By using an importin α antibody only those capsids which were treated with pH 4.6 revealed a co-precipitation being in accordance with the idea that acidification is required for importin α that initiates nuclear entry.

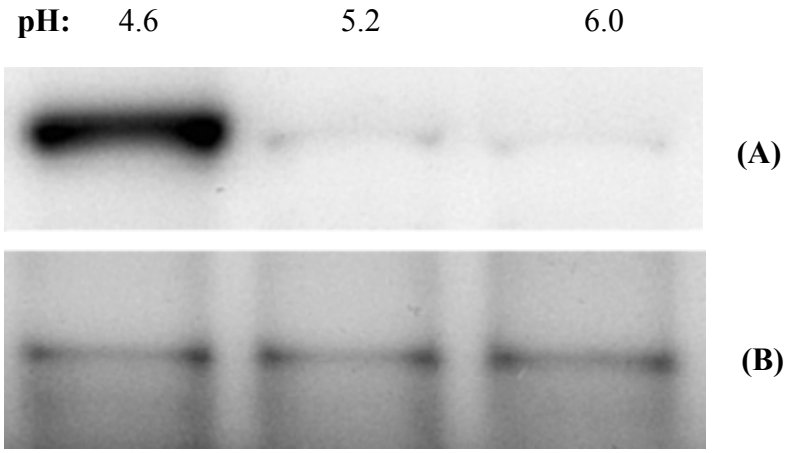

Figure 7: Co-immune-precipitation with anti- importin α and anti capsid antibody. H-1 was treated with different pH (4.6, 5.2, and 6.0) for 10 min at 37°C, neutralised with tris (0.5 M). pH treated capsids were incubated with importin α (50 ng) and β (90 ng). (A) Blot was developed with anti-importin α antibody, pH 4.6 treated capsids showing the band which represents that acidification is required and low pH treated capsids interact with importin α for nuclear entry. (B) Blot was developed with anti-capsid antibody, showed the same pattern of bands in all pH treated capsids.

5.8 Detection of pH treated H-1 capsids by immunofluorescence

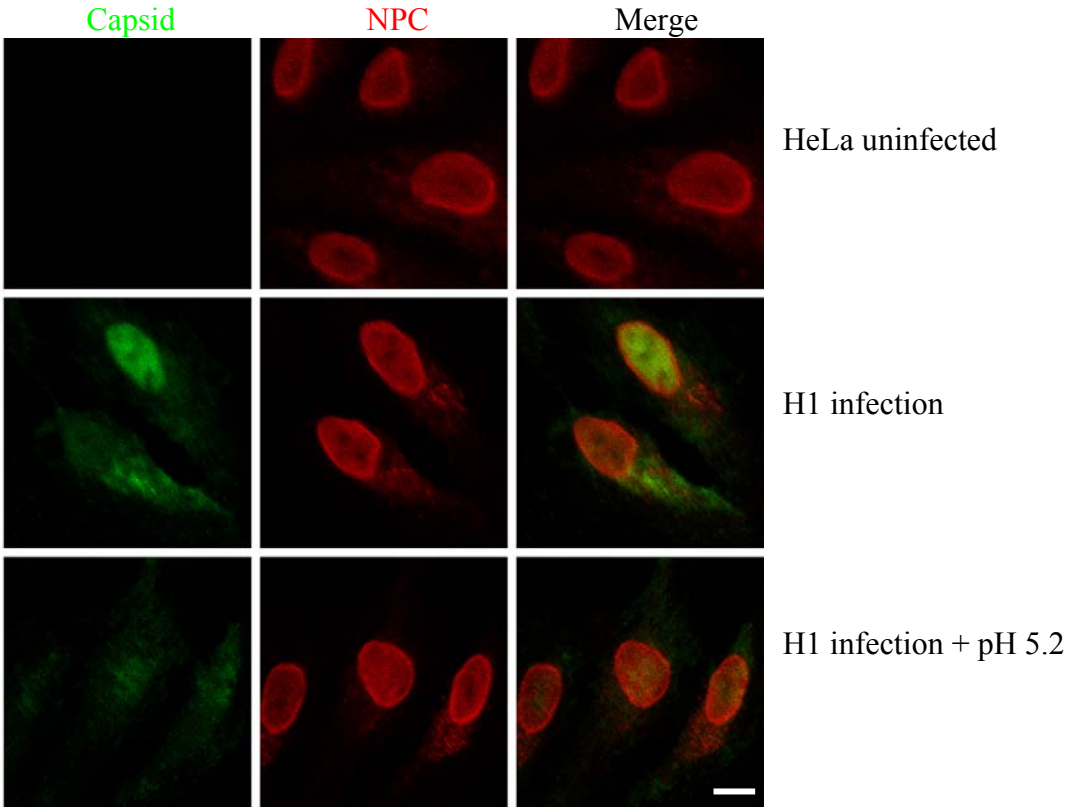

Figure 8: Effect of pH treated H-1 capsids on HeLa cells. (A) HeLa uninfected, NPC (red) no capsid (green) stain was observed. (B) H-1 infection at 37°C, showing the progeny capsids (C) pH (5.2) treated H-1 capsid showed reduced % of infection. Bar 10 µm.

Sample	Red (NPC stain)	Green (capsid stain)	% of infected cells
HeLa (negative control)	666	0	0 %
H-1 (positive control)	596	238	39.9 %
H-1 + pH 5.2	624	16	2.5 %

Acidification is frequently the cause why viruses- or subviral structures- entering the cell are different from the progeny viruses that are appointed to leave the cells. Thus the effect of acidification on infectivity was determined. Without treatment wt H-1 infected ~39.9% of HeLa cells as observed by indirect immunofluorescence, taking the progeny intranuclear capsids as determinant. In contrast pH 5.2 treated H-1 which was neutralised showed only 2.5% of infection rate. In negative control no infected cells were observed (figure 8).

In accordance with the distribution of endosomes/lysosomes in cells the appearence of the green capsid fluoresences was interpreted as binding of capsids or capsids that extend to the endosomal pathway. Thus we assumed that the pH treatment still allowed the exposure of the ligand domain on capsids surface but no nuclear import. From this experiment it has to be left open whether this block occurred upon escape from the endosome or at later stages of infection.

5.9 Kinetics of H-1 at different time course

To elucidate further possibilities of parvoviral nuclear import, high dose infections of HeLa cells (1000 capsids/cell) were performed allowing to follow the fate of the intracellular capsids by indirect immunofluorescence. Cells were infected for different time points (10, 30, 60, 120, 240 min and overnight). Figure 9A depicts that with increasing time more capsids (green) entered the cells and accumulated outside the nuclear envelope (blue) in the perinuclear region. Detailed views on the cells however, showed that in 11% of infected cells a local disruption of nuclear envelope occurred after over night (ON) incubation (figure 9B). The discontinuity was combined with a leakage of chromatin (red) out of the nucleus. Leakage of chromatin was restricted to those sites where H-1 capsids (green) accumulate and started over night post infection.

To verify whether this phenomenon is restricted just to the HeLa cells or a general phenomenon another cell line (HuH-7; human hepatocytes) was analyzed. In fact the local nuclear envelope disruption was also observed in 8.5% of the infected cells (figure 9C).

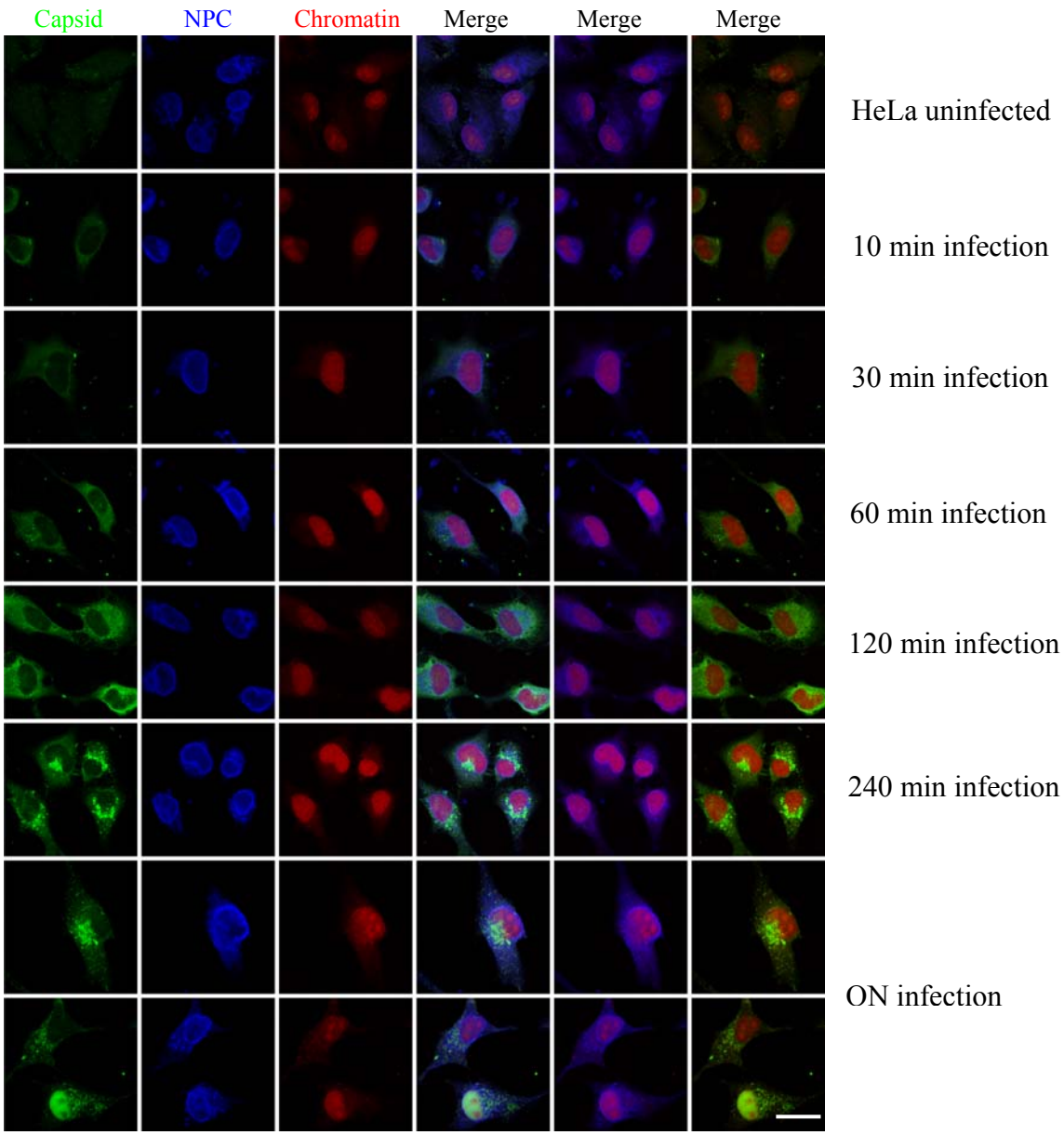

Figure 9A: Local disruption upon infection of HeLa cells with ~1000 H-1/cell. Analysis by confocal laser scanning microscopy at different time points given above. H-1 and NPC were stained by indirect immunofluorescence; the chromatin stained by propidium iodide. The colors above the panels show the corresponding structures. Bar 10 µm.

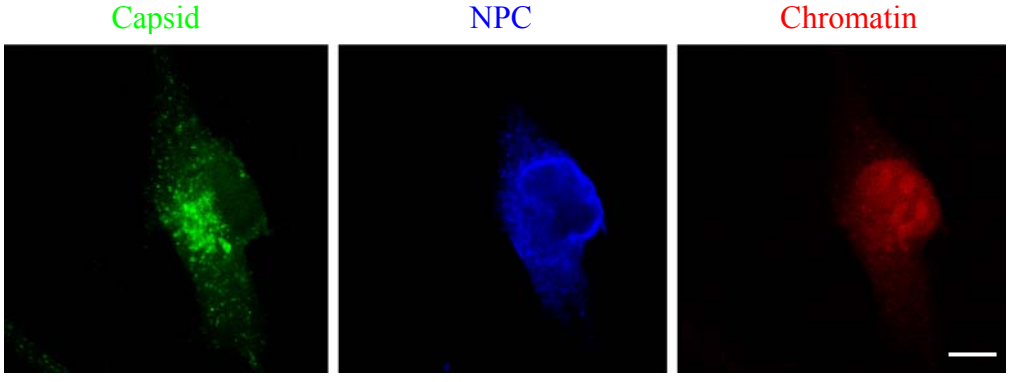

Figure 9B: Magnifying view of leakiness of nuclear envelope. Bar 10 µm

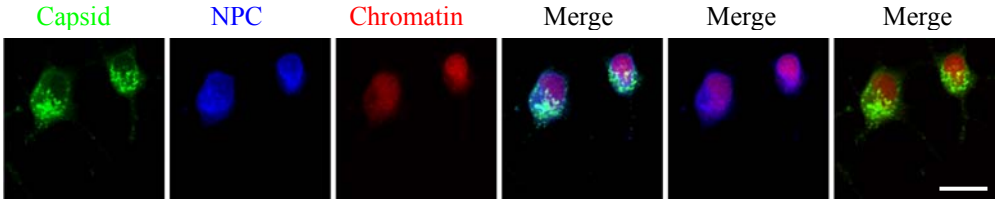

Figure 9C: NEBD upon infection of HuH-7 cells with ~1000 H-1/cell. Analyses by confocal laser scan microscopy at different time points given above. H-1 (green) and NPC (red) were stained by indirect immunofluorescence; the chromatin stained by propidium iodide (red). Bar 10 µm.

5.10 Live cell microscopy with mock purified virus

Previous studies on permeabilized cells showed that nuclei were hardly detectable after subjecting H-1 (Kann.M, unpublished). According to the nuclear disintegration observed before the loss of nuclei might be explained by the ability of H-1 to disintegrate them.

In order to verify this assumption, *in vitro* experiments were performed on permeabilized HeLa cells using live cell microscopy. In these assays, cells were permeabilized with digitonin, which solubilises only cholesterol-containing membranes as the plasma membrane, leaving e.g. ER and nuclear membrane unchanged.

Permeabilization was combined with chromatin stain using propidium iodide. Unincorporated stain, digitonin and soluble cytosolic proteins were removed upon the subsequent washing step. After addition of 1.6 x10^8 H-1 (300 capsids/cell) in buffer, nuclear disintegration was monitored by the loss of propidium iodide using confocal microscopy at defined time points.

In a first experiment, the effect of H-1 was compared with buffer and a mock-purified virus at 37°C. In the latter assay, a lysate was used from uninfected NBK cells being purified as it was done for purification of H-1.

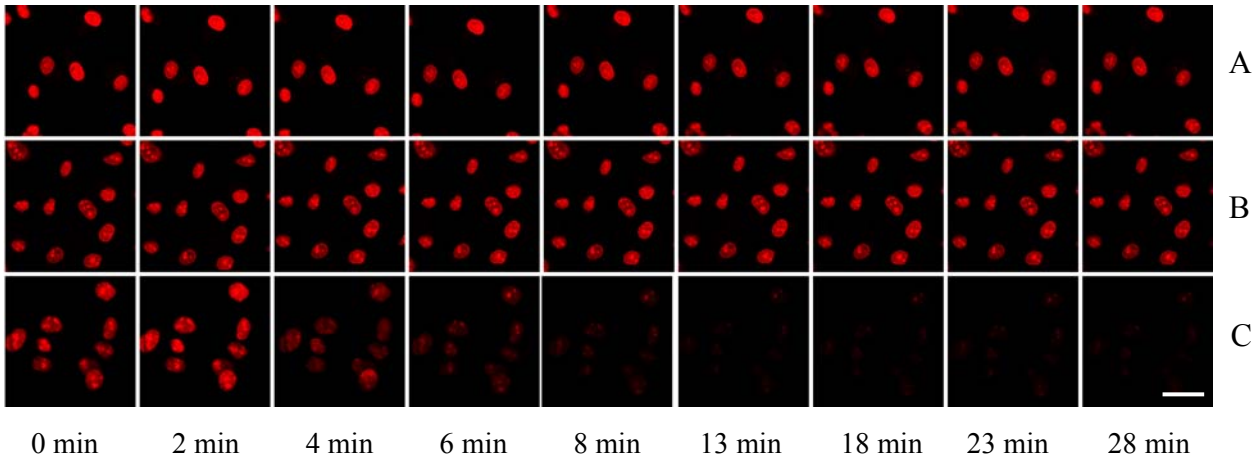

Figure 10A: Live cell confocal microscopy of the nuclear entry of mock treated cells and H-1 virus after permeabilization of HeLa cells. Nuclei were stained with propidium iodide. Pictures were taken at 0, 2, 4, 6, 8, 13, 18, 23 and 28 min. (A) In negative control (transport buffer) was added, no change in chromatin stain (B) mock purified virus (NBK cells), no change in chromatin stain (C) H-1 virus showed linear degradation of NE which represents that H-1 is causing degradation. Bar 10 µm.

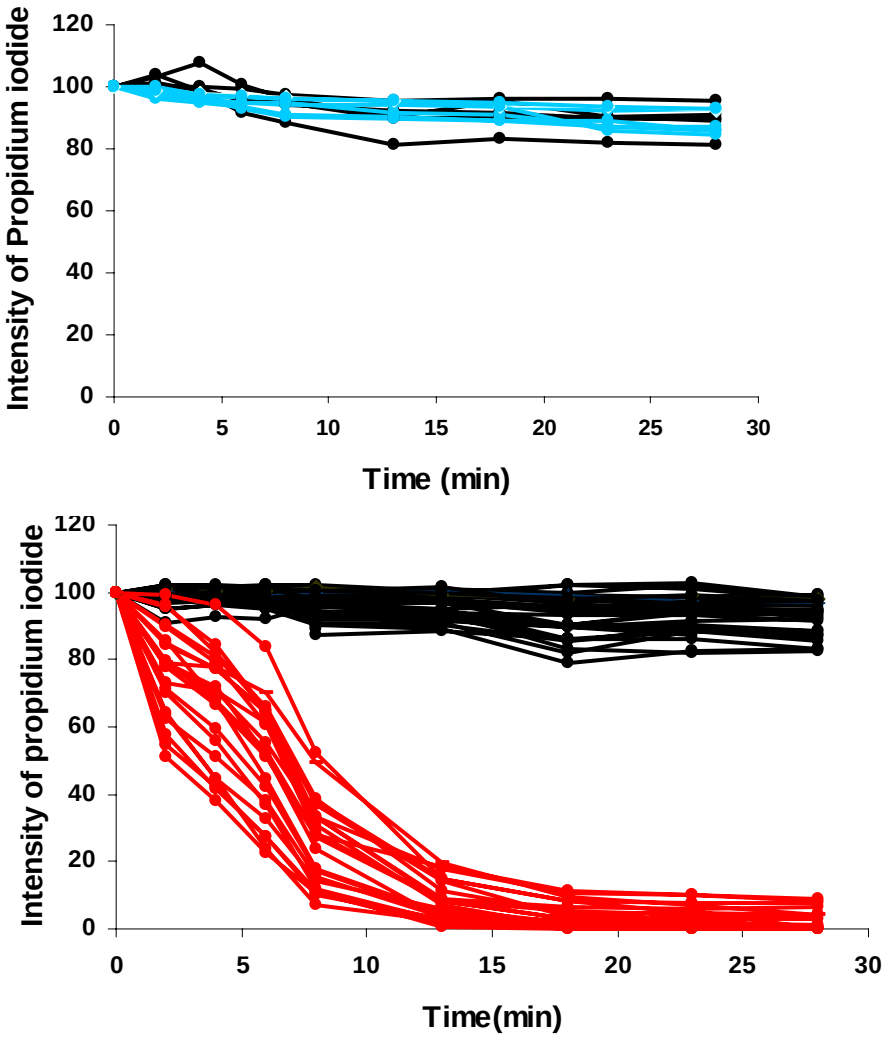

Figure 10B: Quantification data of mock and H-1 treated HeLa cells. Pictures were taken at 0, 2, 4, 6, 8, 13, 18, 23 and 28 min. Quantification was perofrmed for each cell. Intensity of propidium iodide was calculated at each time point. (1) Black lines: transport buffer (negative control), light blue lines: mock purified virus. (2) black lines: transport buffer, red lines: H-1 virus.

Figure 10A showed that in both buffer and mock exposed nuclei chromatin stain remained unchanged (half life not determinable). Addition of H-1 result a loss of chromatin as indicated by the PI stain (figure 10A) showing a loss of chromatin to 50% within 4-8 min (later on referred to be the "half-life"). The quantification was monitored in 13 different experiments and is depicted in figure 10B.

To verify whether this phenomenon was specific for H-1 or can be generally transferred to other parvoviruses we analyzed the degradation potential of the autonomous canine parvovirus (CPV) and the non-autonomous adeno-associated parvovirus (AAV).

5.11 Live cell microscopy of different parvoviruses

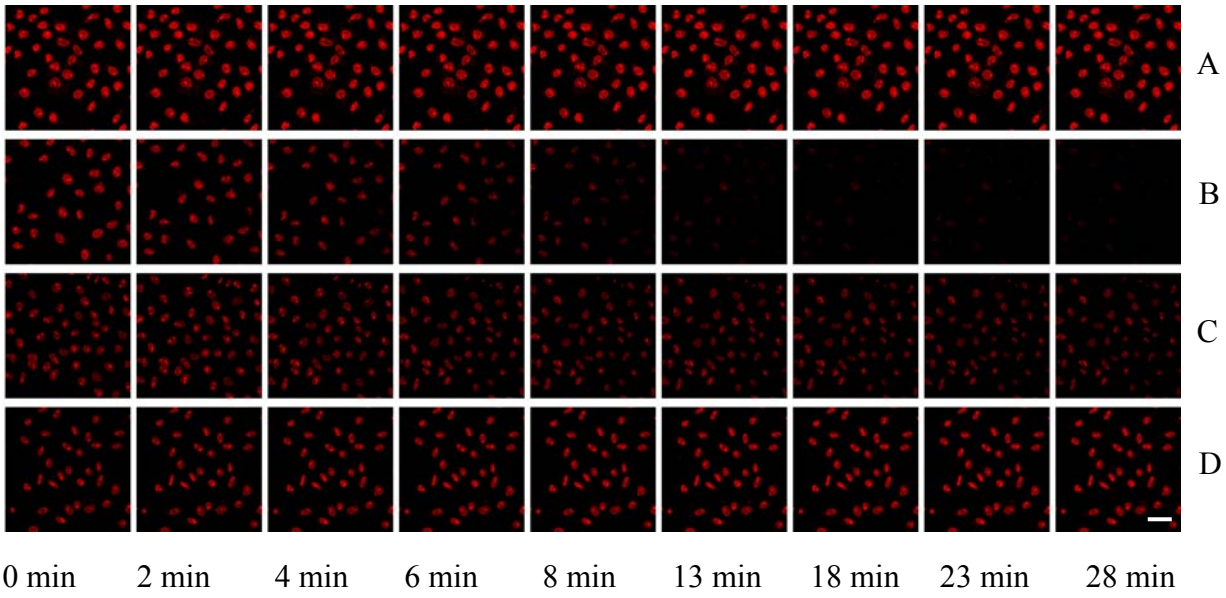

Figure 11A: Check out the nuclei degradation process on other parvoviruses. HeLa cells were permeabilized with digitonin. Washed and pre-incubated with transport buffer for 10 min at 37°C (A, B, C, D). Later cells were treated with different parvoviruses. Nuclei were stained with propidium iodide asdescribed earlier. (A) Transport buffer, no change in chromatin staining. (B) On H-1 treatment, degradation of chromatin (C) CPV treatment, same kind of degradation shown as in H-1 (D) AAV treated cells, no change in chromatin stain. Bar 5 µm.

As indicated in figures 11A, B and C, CPV caused a similar loss of propidium iodide stain as H-1. The reaction was somewhat slower showing the half-life of 8 min while H-1 exhibited a half-life of 6 min. It must be considered however that the half-life observed for H-1 mediated NEBD varied between the experiments so that a significant difference can not be concluded. In contrast, AAV did not affect the nuclei.

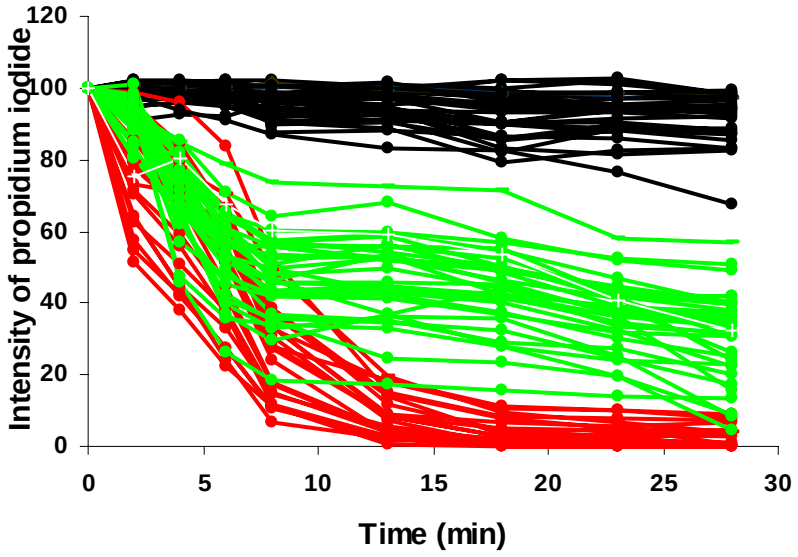

Figure11B: Quantification of the loss of chromatin stain induced by autonomous and non-autonomous parvoviruses. Black lines: transport buffer, red lines: H-1 virus, green lines: canine parvovirus.

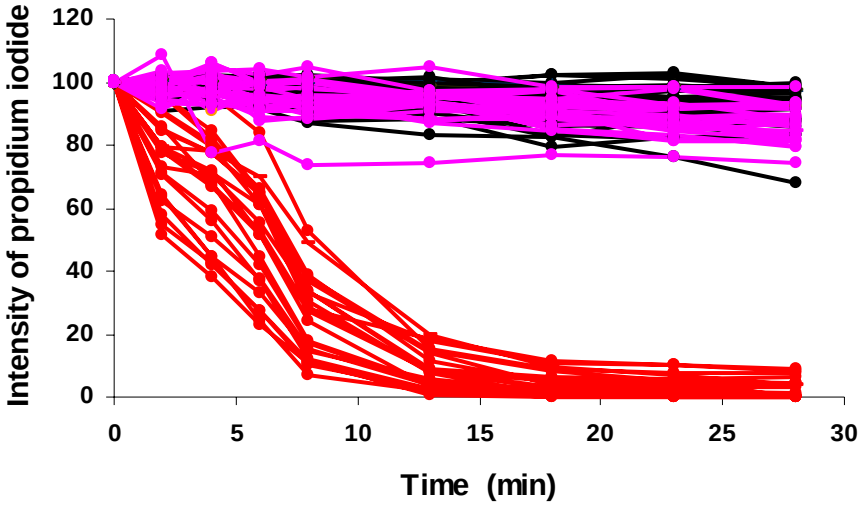

Figure11C: Quantification of the loss of chromatin stain induced by autonomous and non-autonomous parvoviruses. Black lines: transport buffer, red lines: H-1 virus, pink lines: adeno-associated virus.

5.12 Release of substrate after H-1 induction

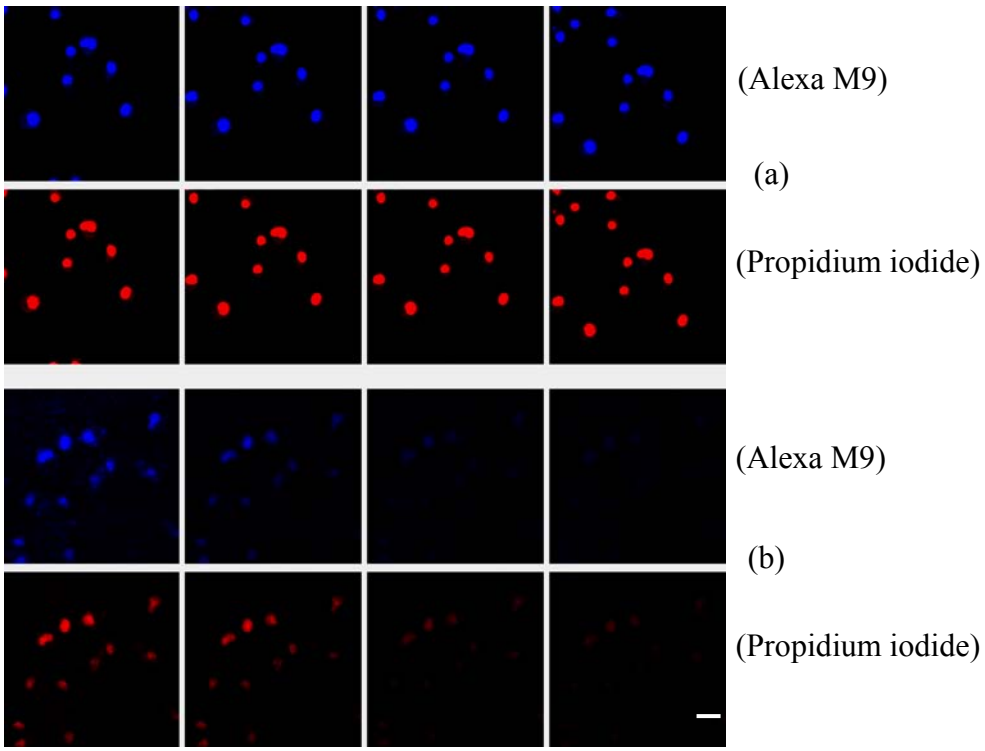

Figure 12A: H-1 induced release of substrates from digitonin-permeabilized cells. After permeabilization Alexa647-BSA conjugates with M9 domains were imported (blue). Chromatin was stained with propidium iodide. After washing **(a)** In negative control only transport buffer was added. **(b)** The release was initiated by addition of H-1 The fluorophores were monitored by confocal laser scan microscopy. Bar 5 µm.

The loss of chromatin stain indicated a disruption of the nuclear envelope. Accordingly not only chromatin, but also other substrates should be released. For prove of this hypothesis Alexa647-

BSA conjugated with a M9 domain, having a MW of ~97 kDa, was imported into the nuclei of digitonin-permeabilized cells. The 38-residue M9 domain of hnRNPA1 is sufficient to confer import into the nucleus. The import reaction is facilitated by the nuclear import receptor transportin that is a member of the importin ß superfamiliy. Thus the import reaction was performed in the presence of cytosol following the protocol of nuclear import analysis in digitonin-permeabilized cells. After washing steps to remove the cytosol and non-imported conjugate a propidium iodide stain was performed. Following subsequent washing, H-1 was added.

Figure 12A depicts an overlapping signal of imported M9-BSA (blue) and chromatin (red). In buffer-treated cells both intranuclear substances remained stable while addition of H-1 released M9-BSA with a half-life of 5.8 min (mean value of H-1 treated cells) followed by chromatin loss at 6.3 min (mean of all H-1 treated cells). These data indicate that once the nuclear envelope was showing small pores allowing the conjugate to leave the nuclei, the disintegration process proceeded rapidly leading to pores large enough to release even the chromatin.

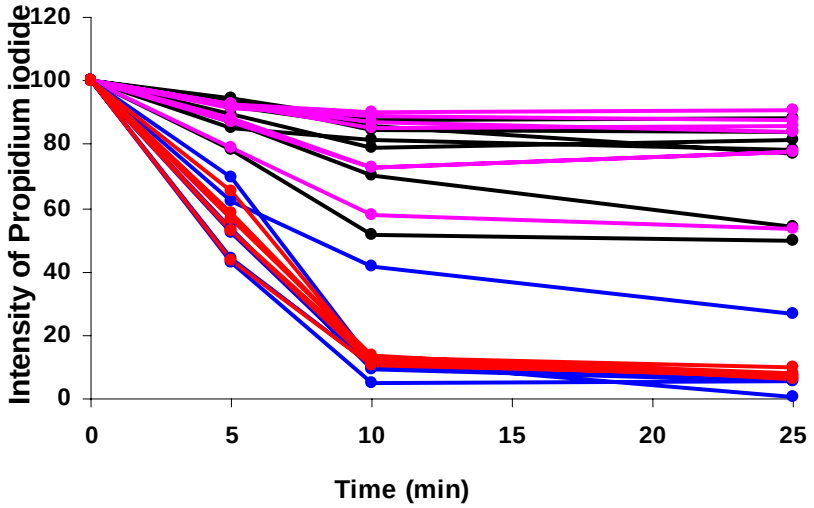

Figure 12B: Quantification of figure 12A. Black lines: negative control, Alexa647-BSA M9 conjugate. Pink lines: Negative control, chromatin determined by propidium iodide. Dark blue lines: H-1, Alexa647-BSA M9 conjugate. Red lines: H-1, chromatin determined by propidium iodide.

5.13 Analysis of nuclear degradation by EYFP lamin B receptor NRK cell line

Two integral proteins such as lamin B receptor (LBR) and lamin associated polypetide2 (LAP2) are present on inner nuclear membrane (Ellenberg.J, 1997). LBR is a chromatin-binding protein (Belmont.AS, et al, 1993, Broers.JL, et al, 1999), its isotypes are associated with the nuclear envelope (NE) and becomes disintegrated during mitosis (Ellenberg.J and Lippincott-Schwartz.J, 1999). In the following analysis, we used live-cell imaging of green fluorescent protein (EYFP)-tagged proteins in conjunction with LBR an INM protein to monitor the effect of H-1 virus.

Chromatin (red) and lamin B receptor staining (green) remained unchanged for the 28 min observation period in transport buffer treated nuclei (negative control). In contrast, loss of lamin B receptor and chromatin fluorescence was significantly detected when H-1 was added. Release of lamin B receptor was slightly faster than the escape of chromatin showing half-lives of 6 min versus 8 min being consistent with the assumption that the Lamin B is degraded first before the escape of the chromatin (figure 13A/B).

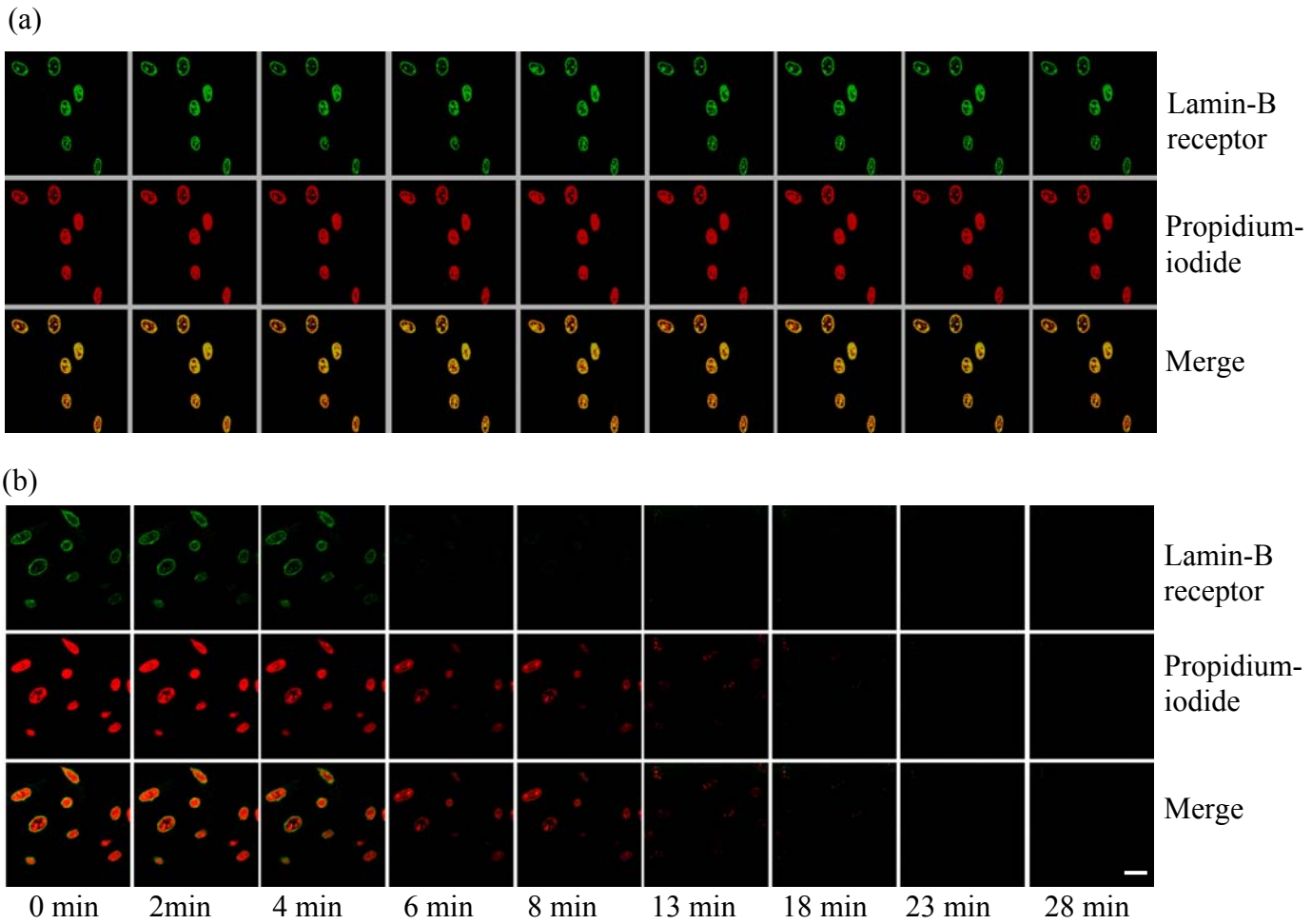

Figure 13A: Kinetic of nuclear envelope breakdown monitored by the fluorescence of the lamin B receptor and chromatin EYFP expressed NRK cells were permeabilized with digitonin. Lamin B receptor was visualized in green and chromatin in red. **(a)** No change in lamin B receptor and chromatin fluorescence was occurred when the nuclei were treated with buffer, **(b)** After H-1 treatment lamin B degraded first with a half life of 6 min while the half life of chromatin was 8 min. Bar 5 µm.

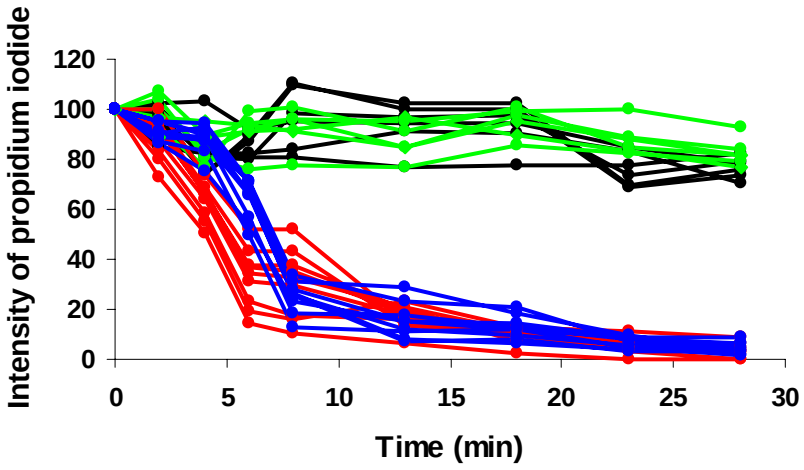

Figure 13B: Degradation of LBR upon H-1 treatment. Transport buffer (negative control): Black lines: lamin B receptor, green lines: propidium iodide, **H-1 virus:** red lines: lamin B receptor, blue lines: propidium iodide.

5.14 Analysis by wide field microscopy

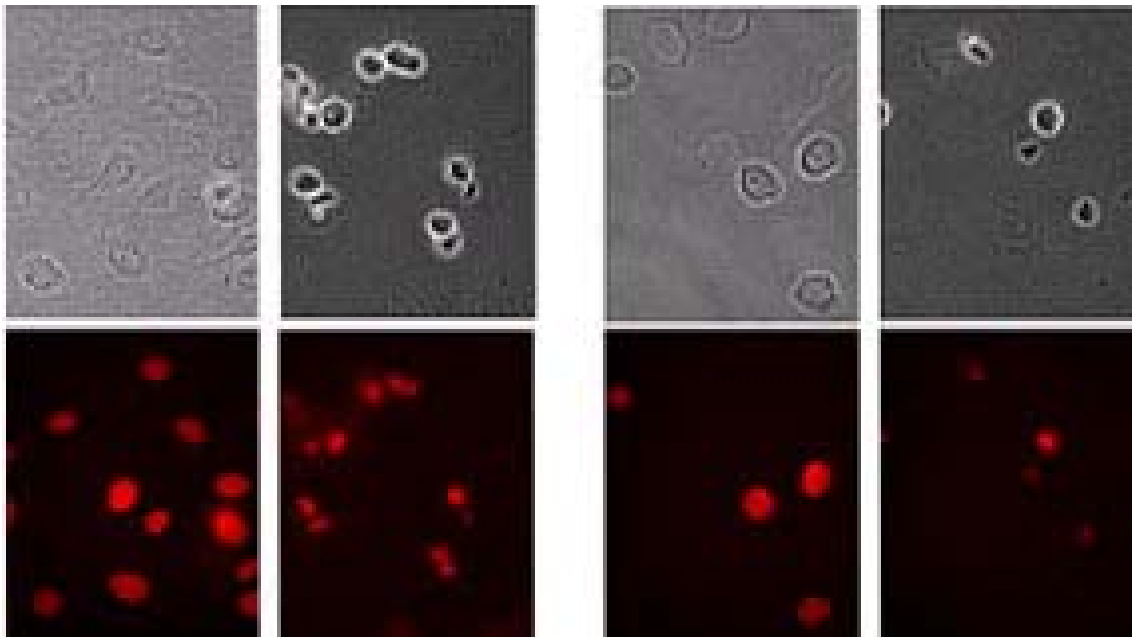

Figure 14A: Treatment of H-1 upon permeabilized HeLa cells. Pictures were taken from phase contrast microscopy. **(a)** Stained HeLa cells with buffer showing total chromatin stain but in H-1 treated cells some chromatin stain got lost. **(b)** In re-stained HeLa cells with buffer showing no difference and same phenomenon observed in H-1 treated cells.

After permeabilization (in the presence of propidium iodide), cells were treated with either transport buffer (negative control) or with H-1 virus for 30 min at 37°C in parallel assays (figure 14A). Cells were washed and one set was restained with propidium iodide solution (figure 14A (b)). This was performed to exclude whether the observed loss of fluoresence was infact caused by chromatin release or by a dissociation of the propidium iodide. Further analysis was done with wide field microscopy (WFM) because this microscope depicts the whole nuclei from top to bottom at one plane.

The infection experiments suggested that nuclear disintegration is a local process restricted to the site where H-1 has accumulated. In permeabilized cells however H-1 has access to the outside of the nuclei on all sites at the same time. An exception is the bottom of the nuclei where they are attached to the surface of the glass cover slip.

These results showed that, after H-1 treatment most of the propidium iodide staining was lost but some fluorescence was still present.

Quantitative ananlysis in figure 14B depicts that the concentration of propidium iodide remained the same in stained and restained nuclei. This latter finding shows that the loss of propidium iodide stain, observed in the experiments before was in fact caused by a release of chromatin and not by a destain of it. In the H-1 treated cells the concentration of the stain stayed identical but the area was significantly reduced implying that some chromosomes were lost. The remaining chromatin was not condensed upon H-1 treatment.

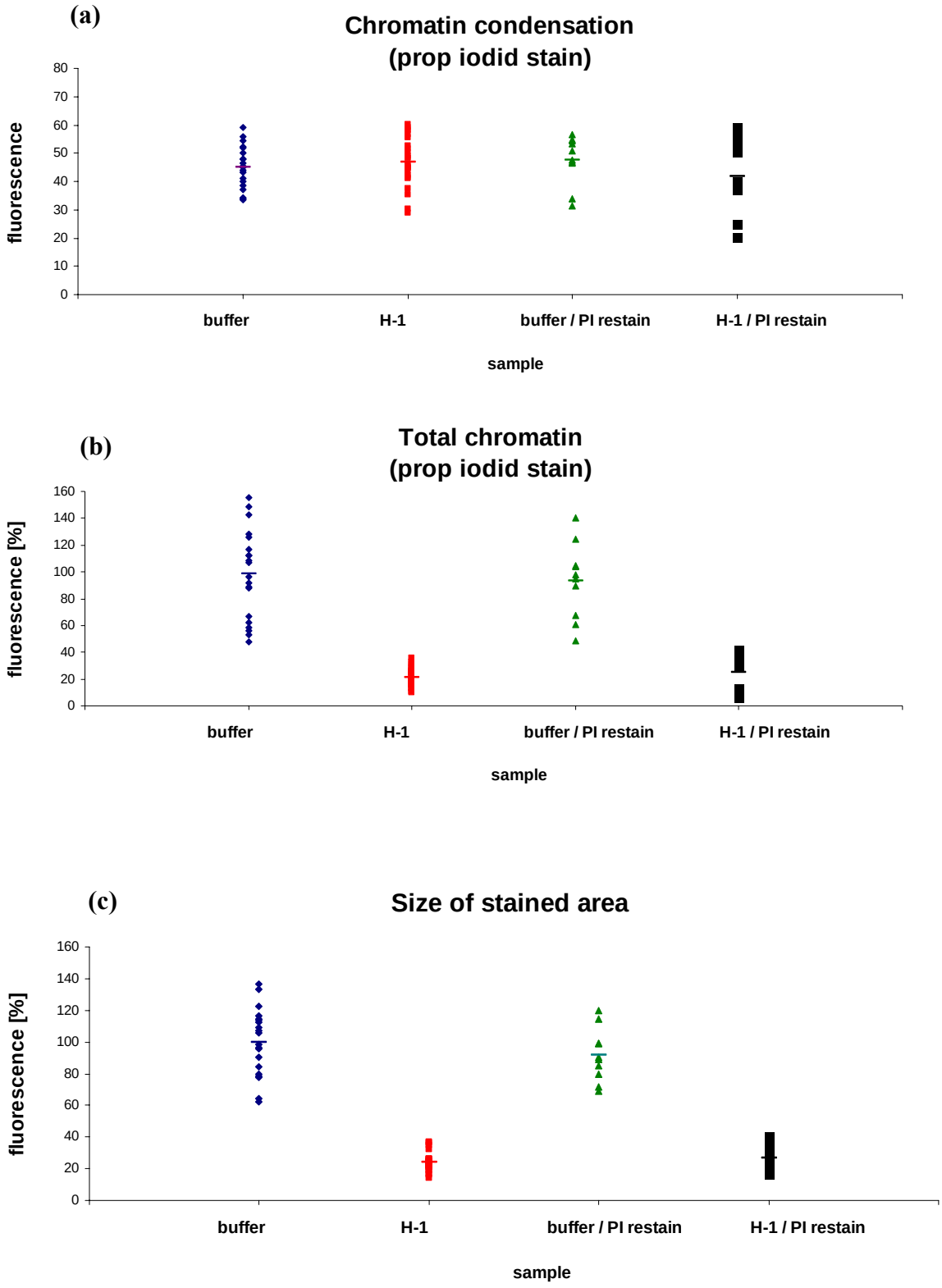

Figure 14B: Quantification analysis of HeLa cells upon H-1 treatment. (**a**) Propidium iodide concentration stayed same in stained and restained nuclei (intenstiy of stain calculated in single cell). **(b)** Total chromatin fluoresence was calculated in each cell which showed that loss of propidium iodide staining caused by a release of chormatin but not because of de-staining. **(c)** Size of stained area remained same in buffer (stained and restained) as well as in H-1 treated cells (stained and restained) only the area reduced. Bar represents the average.

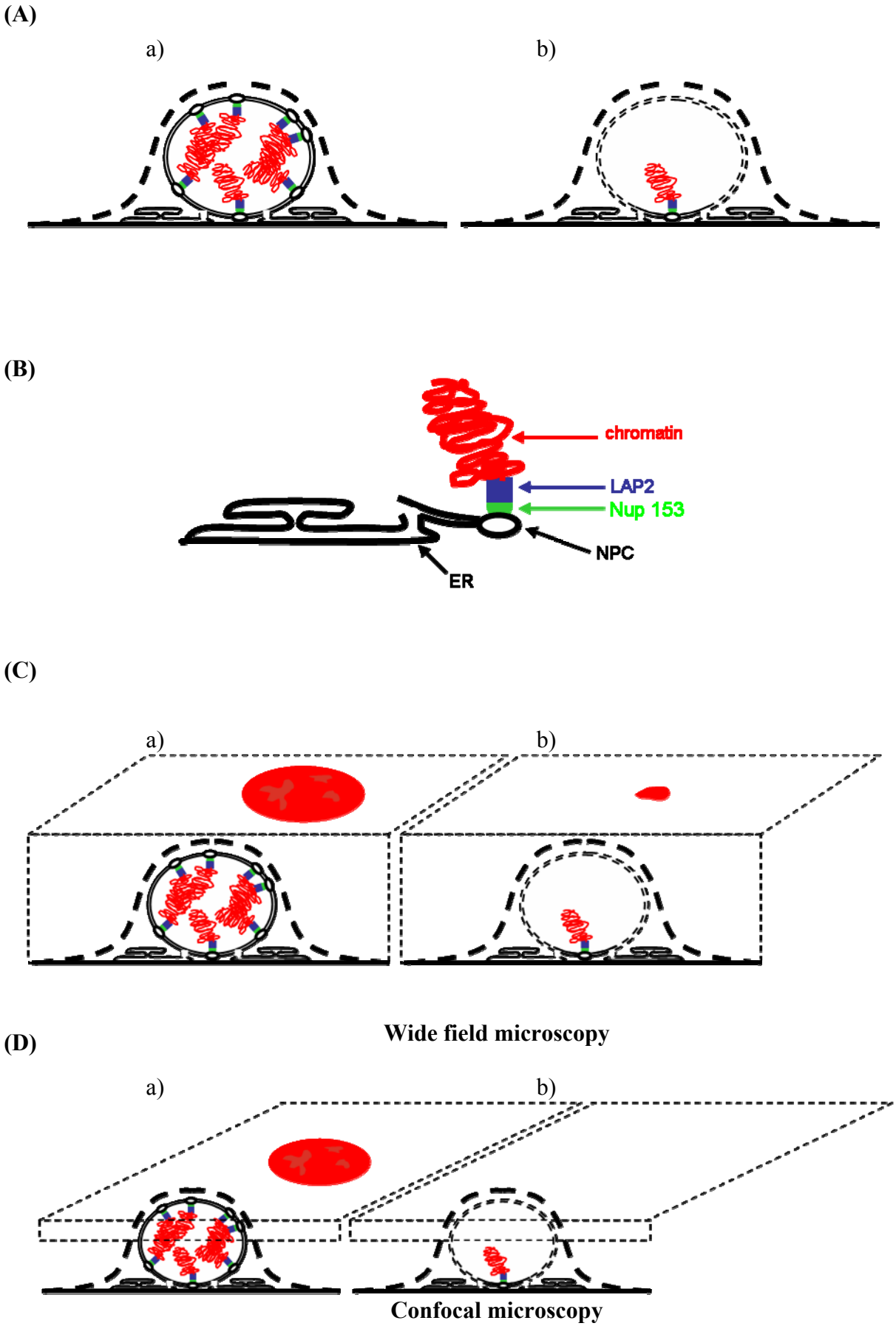

Figure 14C: Schematic diagram of H-1 treated cells by using different microscopes. (A) After permeabilization (a) in buffer (control) chromatin stayed attached. (b) After H-1 treatment chromatin leaked

out and few chromatin remained attached to the suface of the cell. **(B)** The adherence of the attached chromatin may be explained by the estabilished interaction between chromatin (red) and Nup 153 (green) via lamin associated protein (LAP, blue) **(C)** In wide field microscopy (WFM), pictures represents all levels of the nucleus (a) in the negative control (buffer) thus a wide fluoresence occurs while (b) in H-1 treated nuclei most of the chromatin had leaked out and only the remaining stain can be depicted. **(D)** In confocal analysis in contrast, only the fluoresence in equatorial section was recorded. (a) buffer treated cells showed thus a similar fluoresence as in WFM while (b) in H-1 treated cells, no chromatin staining was observed.

This assumption can be explained by the attachment of the chromatin with the nuclear envelope that stayed attached to the coverslip. Buendia.B and Courvalin.JC, (1997) reported that Lamin associated protein 2 (LAP2) – as depicted in figure14C (B) – connects the chromatin with the Nup153 that is part of the nuclear basket. The result thus implies that the Lamin was not entirely degraded but stayed integer at some parts of the nuclei.

This assumption explains the different outcome of the permeabilization when using different microscopes (for schematic presenatation see figure 14C): When confocal laser scan microscopy was used, the equatorial level of the cells was depicted while the wide field microscopy shows the nuclei in full depth. Remaining chromatin, attached to the bottom of each nucleus, closed to the surface of the glass cover slip can be thus detected (figure 14C (C).

According to this assumption phase contrast showed a degradation of nuclear shape upon H-1 treatment without a total loss of nuclear structure.

5.15 Effect of permeabilized YEFP lamin B receptor expressing cells upon H-1

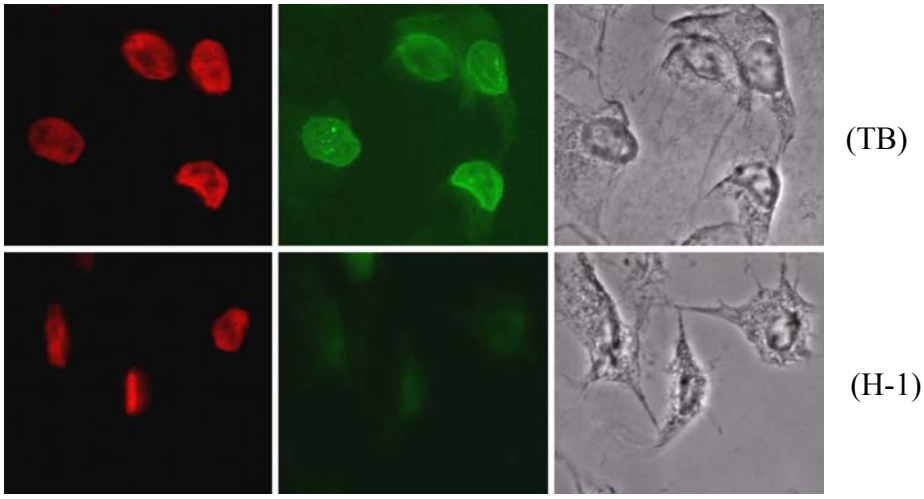

Figure 15: Effect of permeabilized YEFP lamin B receptor expressing cells upon H-1 treatment. Pictures were taken by wide field microscopy. (TB) No change observed in staining (red- chromatin stain, green- lamin B receptor). (H-1) Lamin B receptor stain was reduced but some fluorescence remained attached to those areas where phase contrast microscopy depicted residuals of the permeabilized cells.

For further support to this hypothesis, remaining EYFP lamin B receptor was recorded in wide field microscopy upon H-1 treatment. Figure 15 shows that in fact the area of lamin B receptor fluorescence was reduced but remained attached to those areas where phase contrast microscopy depicted residuals of the permeabilized cells.

5.16 H-1 treatment of non-permeabilized HeLa cells

If the observed phenomena of the nuclear envelope degradation reflect a physiological effect only the nucleus but not the plasma membrane should be affected. For control we thus evaluated the effect of H-1 on the plasma membrane of integer cells. As marker for permeabilization propidium iodide was used as this stain cannot pass the plasma membrane.

Figure 16A shows faint red signal in all cells irrespectively to the addition of H-1. Most likely these signals were derived from autofluorescence. One strong staining in the presence of H-1 but the irregular shape most likely indicates H-1-independent cell fragments, which is consistant by its appearance in phase contrast.

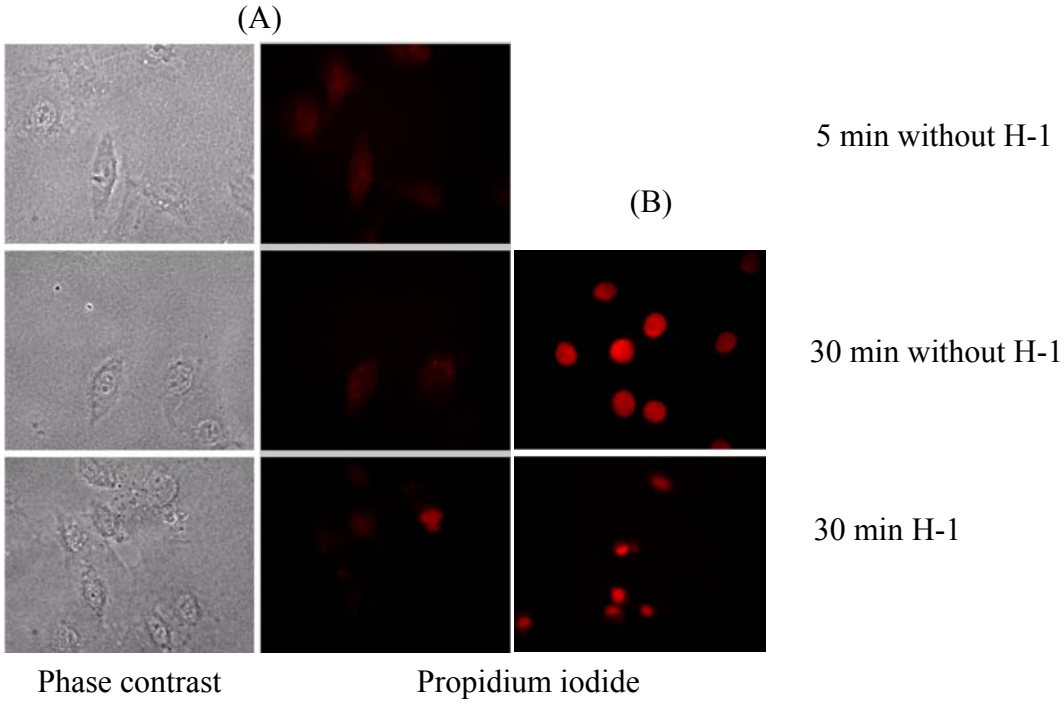

Figure 16: Effect of plasma membrane upon H-1 treatment. Pictures were taken with phase contrast microscopy. (A) Non-permeabilized HeLa cells 5 and 30 min without treated with H-1. 30 min treated with H-1 no change has been showed to plasma membrane. (B) Permeabilized HeLa cells.

5.17 Effect of NS1 protein on nuclear disruption

In order to evaluate the viral component that mediates the nuclear degradation and chromosomal escape we analysed the impact of different capsids and NS1. CPV and H-1 show high homology regarding all proteins. VP1 and VP2 both forming the capsid are identical in 51% and 52% of the amino acids respectively. The protein NS1 that is exposed on capsid surface on only genome-containing capsids is 73% identical. In contrast H-1 and AAV show identities of 30%, 29% for VP1 and 2 and only of 37% in a domain of 265 residues of the NS1 (termed Rep in AAV).

The extremely high homology of NS1 between CPV and H-1 might be a plausible reason why both parvoviruses disintegrated the nuclei while AAV showing a more limited Rep-homology does not. Thus first the role of NS1 was evaluated for nuclear disintegration. As NS1 is only present on DNA containing capsids (full capsids) but not in empty capsids both capsid types were compared for their potential to cause nuclear envelope breakdown (NEBD).

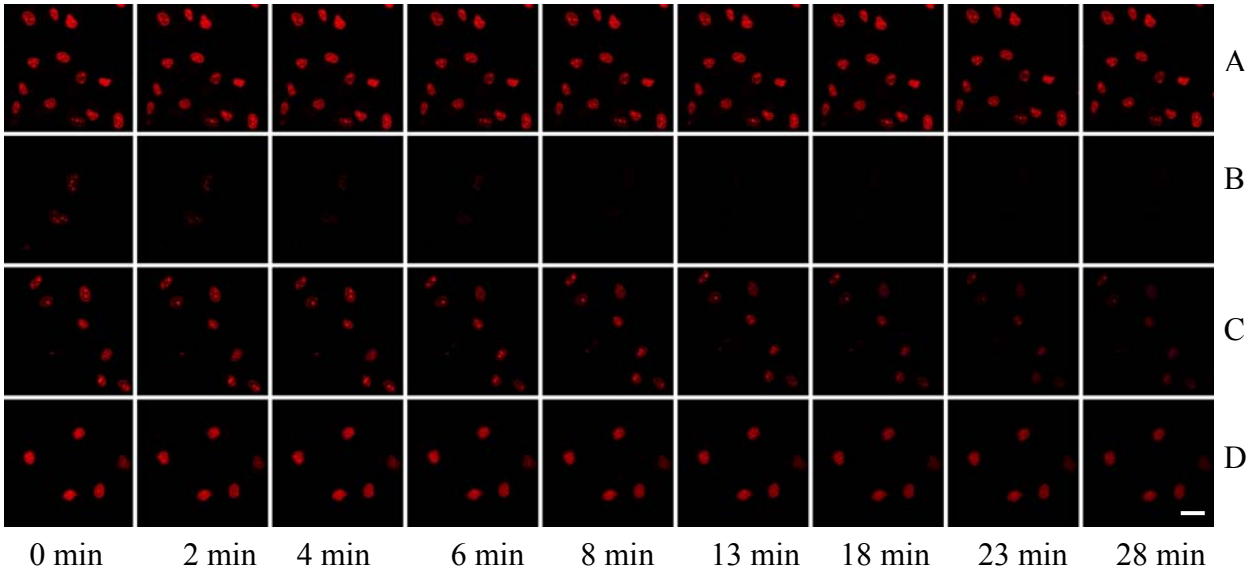

Figure 17A: Effect of NS1 protein on nuclear degradation. Live cell microscopy was performed by confocal laser scan on permeabilized HeLa cells. Chromatin was stained with propidium iodide. **(A)** No change in chromatin after treated with buffer. **(B)** On H-1 (full capsid) treatment loss of chromatin. **(C)** H-1 was pre-incubated with anti-NS1 antibody showed no change in chromatin. **(D)** Empty capsids (devoid of NS1) were unable to show any degradation. NS1 protein involves in nuclear degradation. Bar 5 µm.

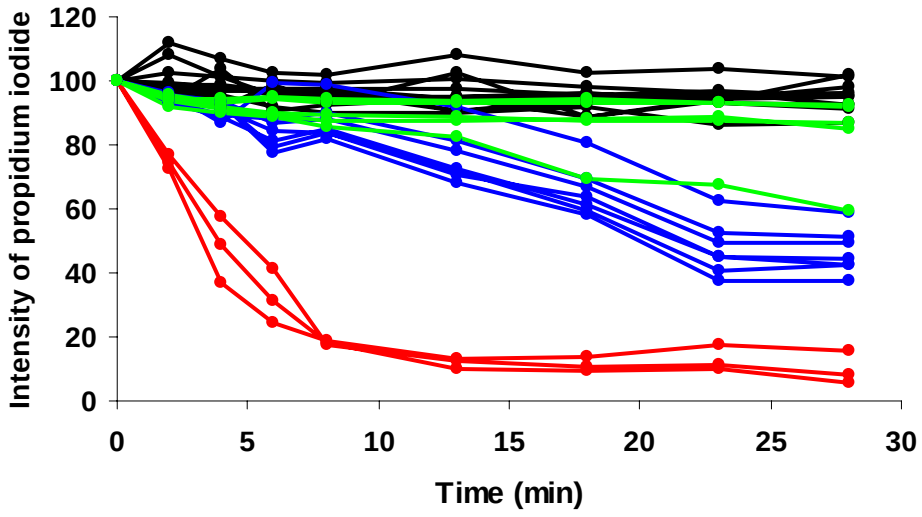

Figure 17B: Chromatin-release by H-1 under various conditions. The graphs show the quantification of experiments as in figure 18A. For every cell fluorescence's were standardized to the one at 0 min, which was set. Effect of NS1 on nuclear disruption. Black lines: negative controls with buffer. Red lines: H-1 in buffer. Blue lines: anti-NS1 pre-incubated H-1. Green lines: Empty H-1 (not harbouring NS1).

As depicted before, cells were treated with buffer (negative control) no loss of chromatin staining in between 0 to 30 min recorded in figure 17A. In contrast 1.6 x 10^8 full H-1 capsids caused a significant loss of chromatin staining (half-life 4 min) (figure 17A/B). Same amounts of empty capsids however, failed to induce nuclear disintegration.

Despite of the homologies structural differences on the capsid surface cannot be excluded to be responsible for the degradation. For differentiation between a capsid or an NS1 mediated process, full capsids were pre-incubated with an excess of anti-NS1 antibodies. This pre-incubation in fact

decreased disintegration to a half-life of the propidium iodide fluorescence to 30 min. The inhibition however was incomplete may be because of an incomplete saturation of NS1 by the antibody.

5.18 Kinetics of nuclear degradation at different temperatures

H-1 at Room temperature (a)

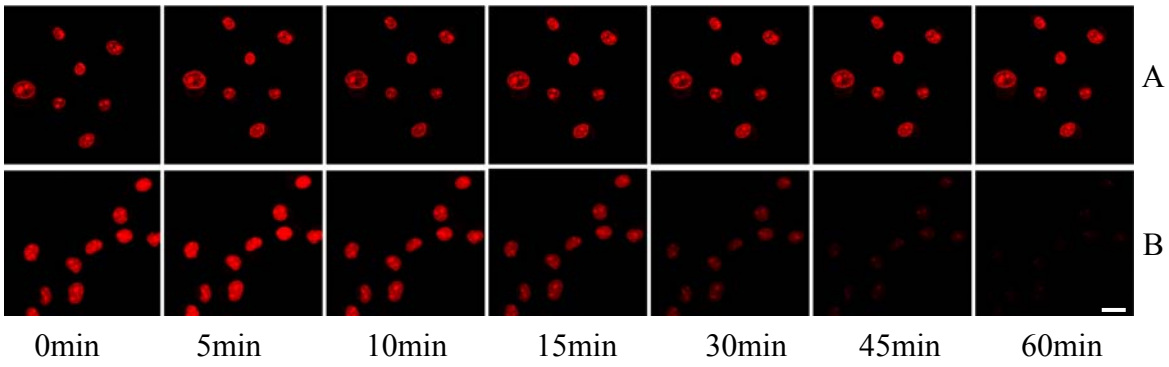

H-1 at 37°C (b)

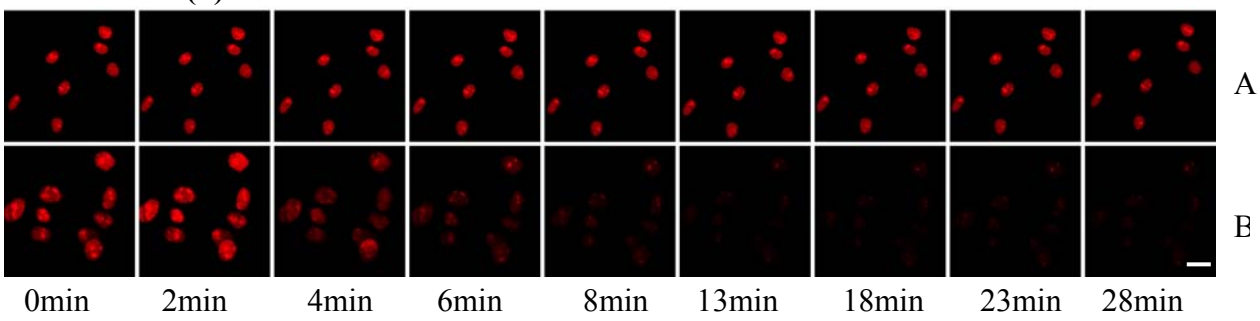

Figure 18A: Kinetics of propidium iodide loss upon H-1 treatment at room temperature and 37°C on permeabilized HeLa cells. **(a)** H-1 at RT: (A) No change in chromatin after treating with buffer. (B) Loss of chromatin seen after 30 min upon H-1 treatment. **(b)** H-1 at 37°C: (A) No chromatin loss seen after buffer treatment. (B) Degradation of chromatin showed after 6 min of H-1 treatment at 37°C which represents that nuclear disruption is temperature dependent process. Bar 5 µm.

The nuclear envelope break down (NEBD) observed for H-1 and CPV was should be an enzymatically triggered process. For further confirmation the effect of temperature was evaluated. H-1 capsids were subjected to HeLa cells at different temperatures (room temperature and 37°C) and the obtained results were compared with transport buffer treated cells (negative control). As shown by confocal live cell imaging, no effect was observed in the buffer treated cells (negative control) at room temperature and 37°C at all time points figure 18A. In contrast, loss of chromatin was observed with a half life of 30 min at room temperature (20°C) in H-1 (1.6×10^8 capsids) treated cells figure 18A (a). Cells exposed to H-1 (1.6×10^8 capsids) at 37°C, loss of chromatin was observed much faster (6 min) figure 18 A (b).

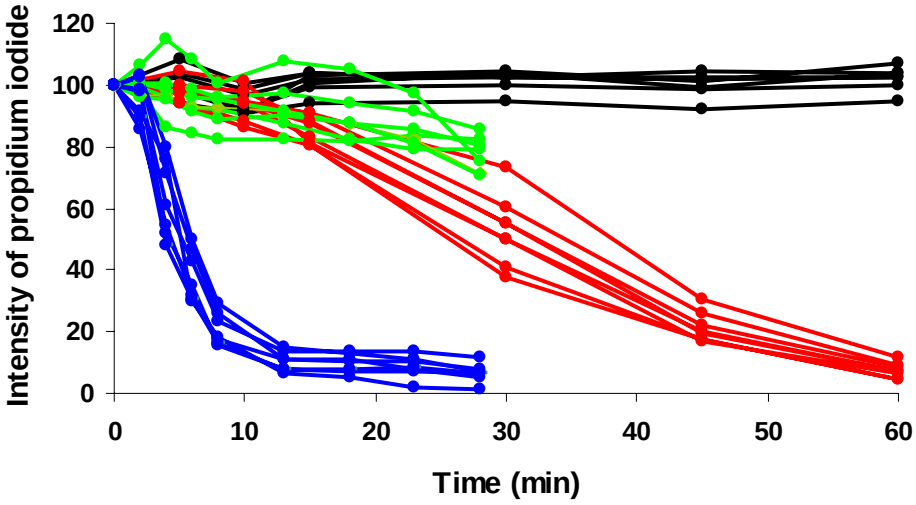

Figure 18B: Kinetics of nuclear disruption at room temperature versus 37°C. Black lines: negative control with buffer at room temperature. Red lines: H-1 in buffer at room temperature. Green lines: negative control with buffer at 37°C. Blue lines: H-1 in buffer at 37°C.

5.19 Role of ATP/ or GTP in NEBD

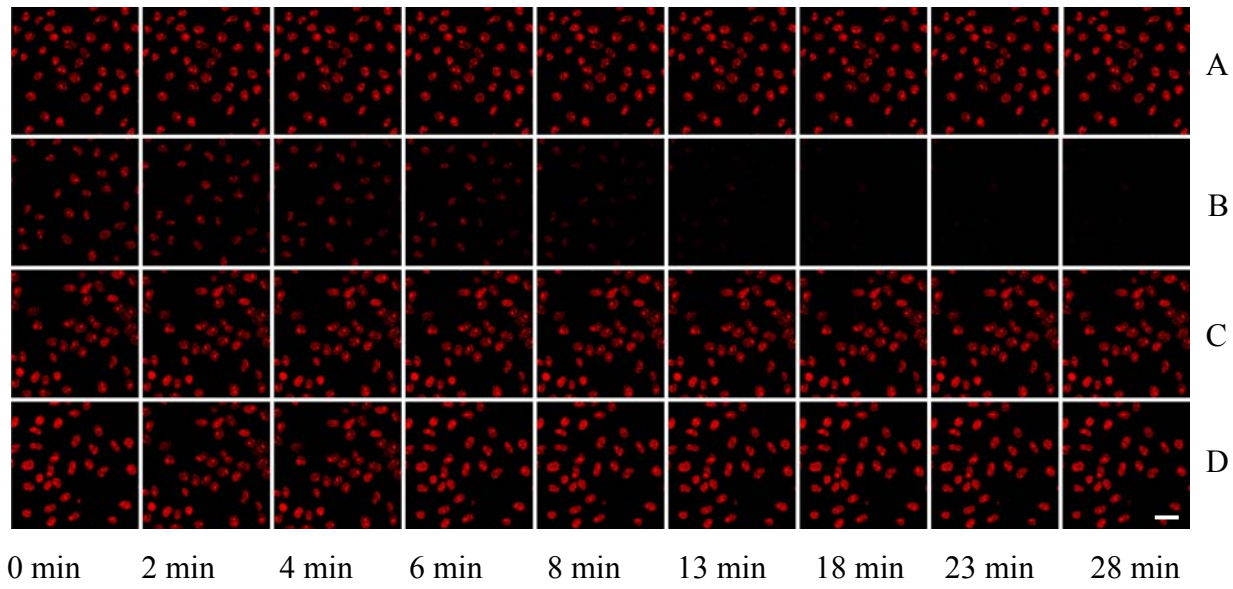

Figure 19A: Role of ATP/ or GTP in nuclear degradation. HeLa cells were permeabilized with digitonin. Washed the cells and pre-incubated in transport buffer for 10 min at 37°C (A and B). cells were pre-incubated with (C and D) hexokinase and glucose (ATP/GTP depletion). Nuclei were stained with propidium iodide **(A)** Transport buffer showed no change is chromatin staining. **(B)** On H-1 treatment degradation of chromatin staining were observed. **(C)** Pre-treated cells with hexokinase and glucose then transport buffer was added, no change in chromatin stain were shown. **(D)** Pre-treated cells with hexokinase and glucose then H-1 virus was added, no change in chromatin stain has been observed (blocked the nuclear degradation process) which shows that energy is required for nuclear degradation. Bar 5 µm.

An enzmatically driven NEBD should require energy generally derived from hydrolysis of triphosphates. Thus the requirement of ATP and/or GTP was investigated. This experiment was performed because although the permeabilized cells were washed some nucleotides were assumed to be present. In fact some protein kinases are known to be activated by only nano molar amount of

ATP. Permeabilized cells were treated with hexokinase/glucose prior to the addition of H-1. Hexokinase was of *Saccharomyces cerevisiae* origin that utilizes both ATP and GTP. The hexokinase/glucose system is well established for energy depletion in various nuclear import assays (Schwoebel.ED, et al, 2002, Nakamura.N and Wada.Y, 2000).

As depicted in figure 19A/B a gradual degradation of nuclei staining was observed upon H-1 virus treatment in permeabilized HeLa cells, but not after treatment with the ATP/GTP depleting system.

Taken together, all these observations suggest that NEBD is an enzymatic catalysed pathway requiring ATP and/or GTP. To explore the underlying enzymatic mechanism in more detail, we asked 1. Are apoptotic and mitotic key enzymes are involved? 2. Are cytosolic proteins involved in this process?

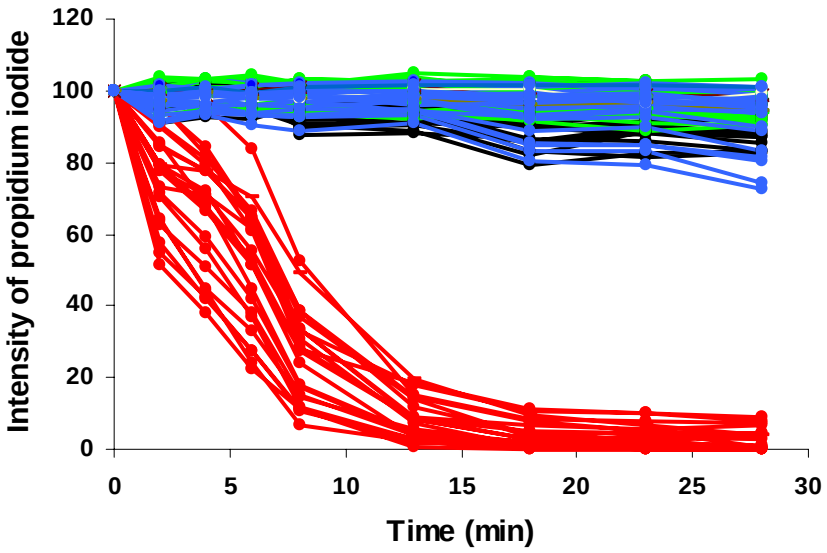

Figure 19B: Role of ATP/GTP in the loss of chromatin staining (quantification). Black lines: transport buffer (TB). Red lines: H-1 virus. Green lines: TB (hexokinase/glucose). Blue lines: H-1 (hexokinase/ glucose)

5.20 Role of apoptosis and mitosis in NEBD

Physiologically NEBD occurs during mitosis and apoptosis. The executing enzymes during these processes are casapase-3, cyclin-dependent kinase-2 (cdk-2) and protein kinase C (PKC). As described before, the lamina is a dynamic structure whose disassembly during mitosis is regulated primarily by phosphorylation of the lamins at conserved serine residues flanking the α-helical rod domain (Heald.R, and McKeon.F, 1990, Stuurman.N, et al, 1998). During apoptosis, one step in the irreversible disassembly of the nuclear lamina involves hyperphosphorylation of lamin B proteins by protein kinase C (PKC) (Brodie.C, and Blumberg.PM, 2003). Distinct from mitotic lamin phosphorylation, major PKC phosphorylation sites on lamin proteins have been mapped to serine residues located in close proximity to the nuclear localization signal in the C-terminal tail domain (Hocevar.BA, et al, 1993). Other cellular lamin kinases include mitogen-associated protein kinases and cyclic AMP-dependent protein kinase. During apoptosis, PKC has been shown to translocate to the nuclear membrane and to phosphorylate lamin B at the C-terminal domain, thereby inducing apoptotic lamina disassembly (Brodie.C, and Blumberg.PM, 2003**,** Buendia.B, et al, 1999).

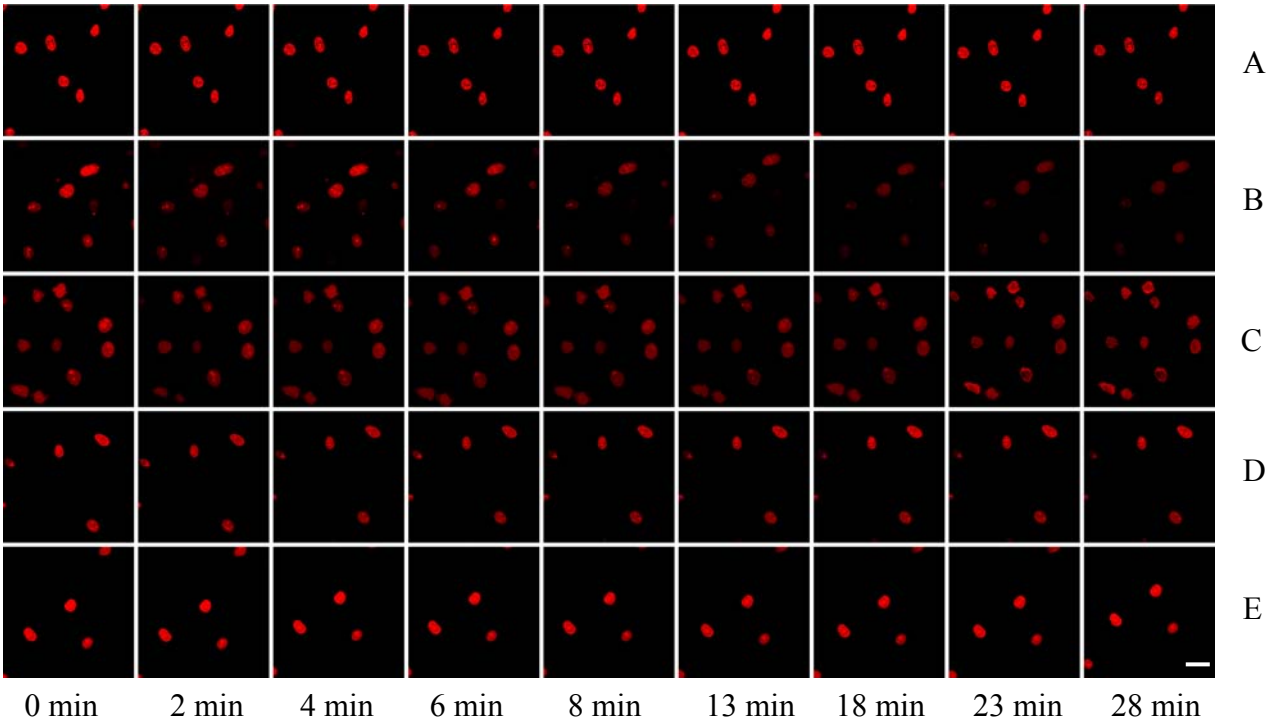

Figure 20A: Effect of mitotic and apoptotic inhibitors on pre-treated HeLa cells (permeabilized) later H-1 added. (A) No chromatin loss observed after buffer treatment (negative control). **(B)** Loss of chromatin showed after H-1 treatment. **(C)** Degradation blocked in those cells which were pre-incubated with H-89 inhibitor. **(D)** Roscovitine inhibitor. **(E)** Z-VAD-fmk inhibitor which showed phosphorylation, cdk2 and caspases are involved in nuclear degradation. Bar 5 µm.

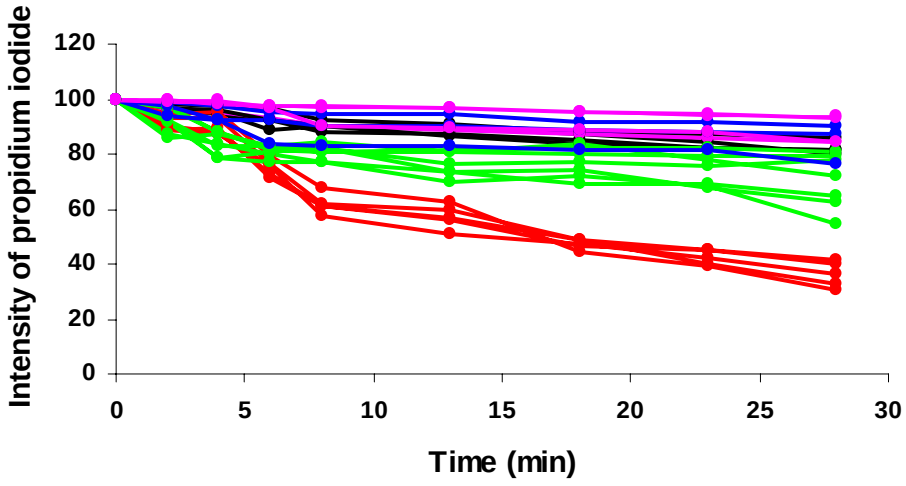

Figure 20B: Effect of mitotic and apoptotic inhibitors on H-1 treated cells. Black lines: transport buffer (negative control). Red lines: H-1 virus. Green lines: H-1 with H89 inhibitor. Blue lines: H-1 with roscovitine. Pink lines: H-1 with ZVAD-fmk.

To elucidate the involvement of apoptotic and mitotic enzymes during NEBD upon H-1 treatment, live cell inhibitory experiments were performed by using H-1 (1.6 x 10^8 capsids) as control and in the presence inhibitors H89 (PKC), roscovitine (cdk-2) and ZVAD fmk (caspase 3 and caspase 9). Results obtained from these experiments suggest that, cells treated with transport buffer sample were remained to be unchanged. Intact chromatin was observed in all time points figure 19A (A). Loss of chromatin was observed a half life of 8 min in H-1 treated group figure 20A (B). Cells treated with a H89 (10 µm) for a period of 45 min, inhibits the phosphorylation of protein kinase C

activity, did not observe any change towards chromatin staining and it remained to be integer figure 20A (C). Cells treated with roscovitine (50 µm) inhibit the cdk-2 activity, did not detect any significant changes in chromatin staining figure 20A (D). Cells treated with ZVAD-fmk (50 µm) inhibit caspase-3 and caspase-9 activity, were showing same observation as mentioned with H89 inhibitor figure 20A (E). These results were further supported by quantification data figure 20B. Taken together all these observations, we conclude that, apoptotic and mitotic inhibitors block H-1 mediated NEBD.

5.21 Involvement of cytosolic proteins in live cell microscopy

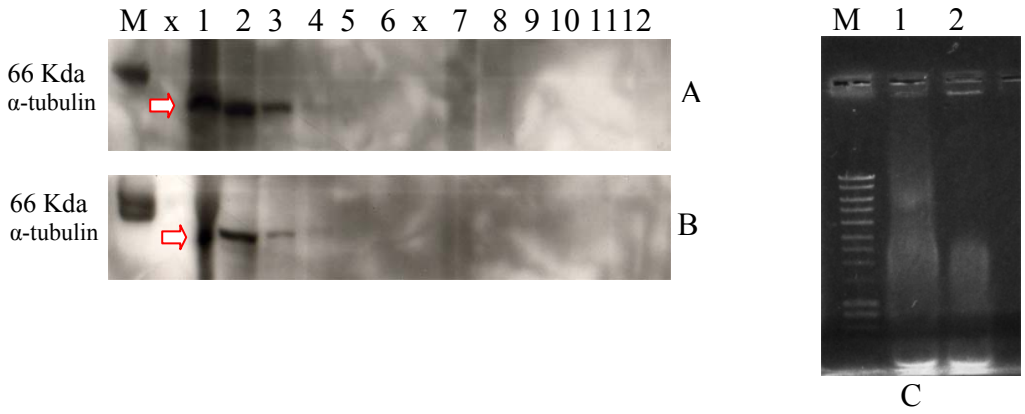

Figure 21: Immunoblotting done with α-tubulin antibody. SDS-PAGE (10-20% Tris glycine gels) and western blot performed for samples **(A)** Supernatant and **(B)** pellet, lane M is representing a rainbow protein marker showing band of 66 kDa. Lane 1 to 6 dilution series (1, 1/4, 1/16, 1/64, 1/256, 1/1024) of non-permeabilized HeLa cells showing the band of 50 kDa of α-tubulin. Lane 7 to 12 dilution series of (1, 1/4, 1/16, 1/64, 1/256, 1/1024) of permeabilized HeLa cells. **(C)** DNA gel (1% agarose) showed DNA ladder marker in lane M , lane 1 is non-permeabilized HeLa cells (pellet) and lane 2 is permeabilized HeLa cells (pellet).

Physiologically NEBD depends on cytosolic proteins (which ones) that enter the nucleus. Although the cells were washed after permeabilization it could not be excluded whether remaining cytosolic proteins were involved in H-1 mediated NEBD. In order to analyze the effect on washing the proportion of remaining cytosolic proteins was evaluated. As a marker tubulin was selected as the microtubules collapse upon permeabilization and washing. Figure 21A/B shows that in fact 98 % of the cellular tubulin was removed. As tubulin is fixed at insoluble structures it must be concluded that this number underestimates the release of other soluble proteins as e.g. nuclear transport receptors. Figure 21C shows that in both samples same amounts of DNA were present indicating that the same number of permeabilized cells was analyzed.

5.22 Role of WGA at NEBD process

As indicated by the previous experiments, H-1 need to contact with the outer part of the nuclear envelope to induce NEBD. Further full H-1 was determined to interact with proteins of the nuclear pore. For closer evaluation the effect of Wheat Germ Agglutinin (WGA) was evaluated. WGA is a lectin that binds to N-glycosylated proteins present on cytoplasmic face of the nuclear pore. Thereby WGA blocks active nuclear import reactions facilitated by nuclear transport receptors (Finlay.DR, et al, 1987). A pore glycoprotein thus appears to be either directly involved in nuclear transport or to be placed in such a position that WGA can, by binding to it, obstruct the passage of

nuclear proteins through the pore. The most likely candidate for the target of WGA binding is the 62 kDa pore glycoprotein observed by Davis.LI and Blobel.G (1986).

Figure 22A shows that addition of WGA has had poor effect on H-1-mediated NEBD. This observation implies that an active nuclear import of H-1 is not required. In fact this idea is in accordance with the observation that the permeabilized cells are devoid of significant amounts of soluble cytosolic proteins as e.g. the nuclear transport receptors. Quantification showed in figure 22B.

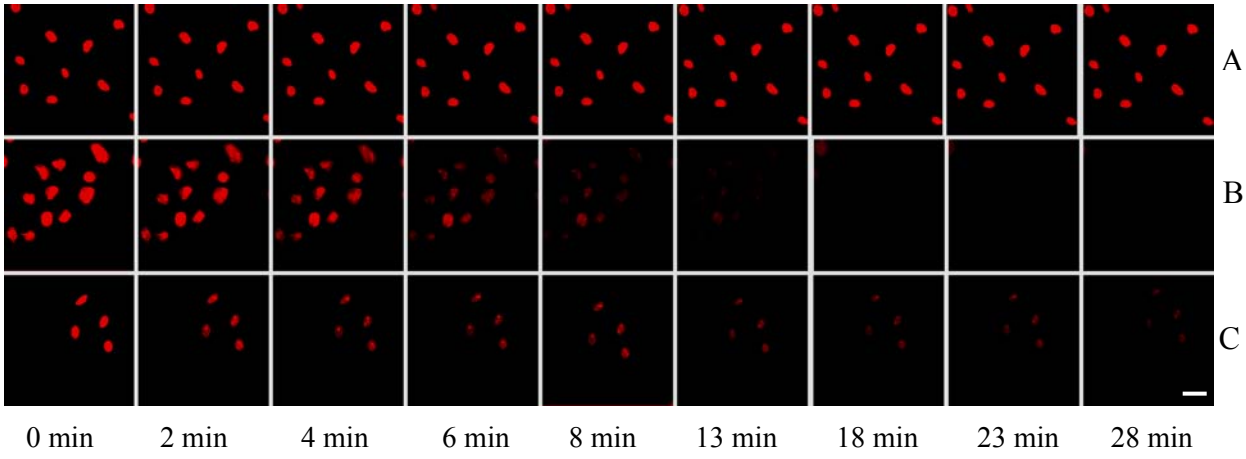

Figure 22A: Role of WGA at nuclear envelope breakdown upon H-1 treatment on permeabilized HeLa cells. Chromatin was stained with propidium iodide. **(A)** No change in chromatin stain upon buffer treatment. **(B)** Degradation of chromatin stain seen after H-1 treatment. **(C)** WGA (1mg/ml) treated cells upon addition of H-1 showed the degradation of chromatin. This result represents that WGA does not have any effect on nuclear degradation. Bar 5 µm.

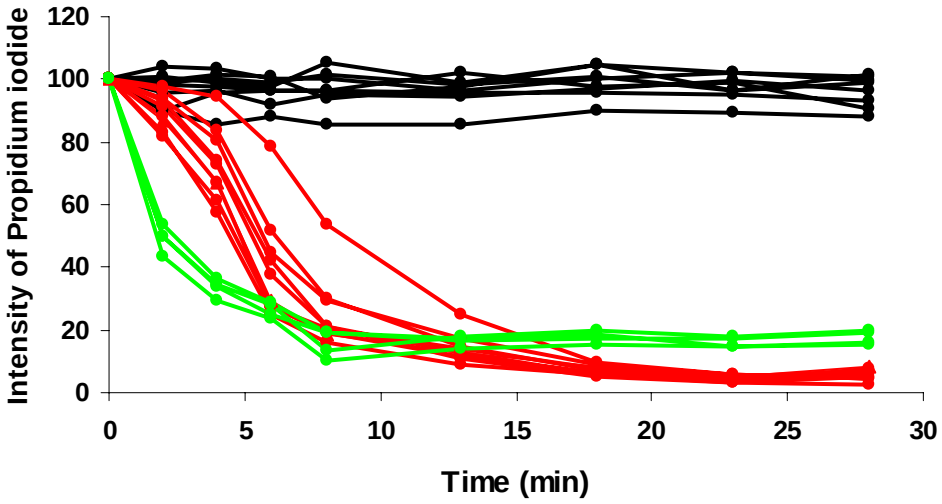

Figure 22B: Quantification of WGA treated cells upon H-1. Evaluation done by student t-test for each cell at each time point. Black lines: transport buffer (negative control). Green lines: H-1 in buffer. Red lines: H-1 with WGA.

5.23 Effect of phospholipase A_2 (PLA_2) on HeLa cells

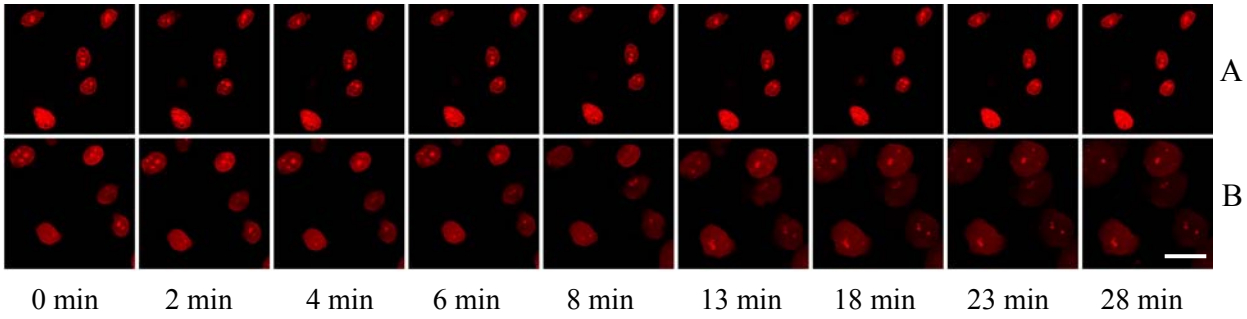

Figure 23A: Live cell confocal microscopy done on permeabilized HeLa cells to show the effect of PLA2 enzyme. Chromatin is shown in red. **(A)** No change in chromatin after treated with buffer. **(B)** After PLA2 enzyme treatment cells swelled up due to unknown reason. Bar 10 µm.

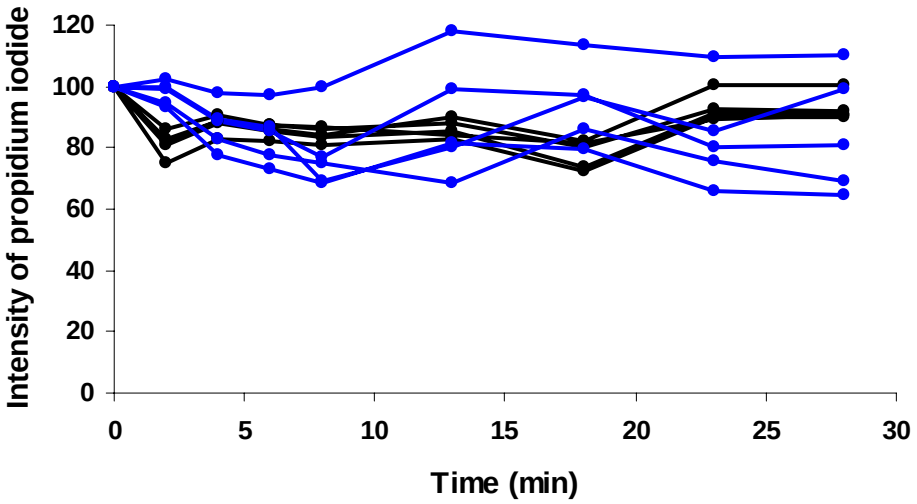

Figure 23B: Role of PLA_2 enzyme on HeLa cells. Quantification was performed with student t-test. Chromatin determined by propidium iodide. Black lines: transport buffer (negative control). Blue lines: PLA_2 enzyme in buffer.

Another possible mechanism of how H-1 may have mediated NEBD might be the phospholipase A_2 activity identified on the N-terminal domain of VP1 in a variety of parvoviruses. This region harbours a phospholipase A_2 (PLA_2) domain (Zadori.Z, 2001) that generates holes in membranes but, contradiction to the postulated role in nuclear transport allowing diffusion of small molecules of only ~3 kDa (Suikkanen.S, 2003). PLA_2 activity however was shown to be essential for release of the capsid from the endosomal compartment into the cytosol (Farr.GA, 2005, Suikkanen.S, 2003, Zadori.Z, 2001). Noteworthy, capsid release is inefficient and the majority of capsids end in the lysosomal compartment (Mani.B, 2006). However by unknown reasons the two evaluated PLA_2 inhibitors (Manoalide and AACOCF3) added caused an immediate nuclear disintegration irrespectively to the presence of H-1. For circumventing the problem the direct effect of PLA_2 on nuclei was evaluated.

Similar kind of live cell microscopy performed as described before instead of H-1 virus PLA_2 enzyme (1.6 $x10^8$ molecules) added to the cells to see the effect of PLA_2 enzyme on cells. Negative control (transfer buffer) remained unaffected (figure 23A) whereas cells treated with PLA_2 enzyme, showed that nuclei stayed integer but cells got swelled up (figure 23A). The cells were

certainly not only swollen in 2 dimensions but also in altitude. However, we measured the intensity based on pictures done with the same pinhole size. So for quantification, we used square root of area of each cell which was multiply by intensity of the propidium iodide for each cell to check that whether the cells were affected by PLA_2 enzyme or not. Plotting the calculated intensities of the nuclei (figure 23B) showed that PLA_2 enzyme did not cause any chromatin escape.

5.24 Live cell microscopy of phosphorylated HBV capsid

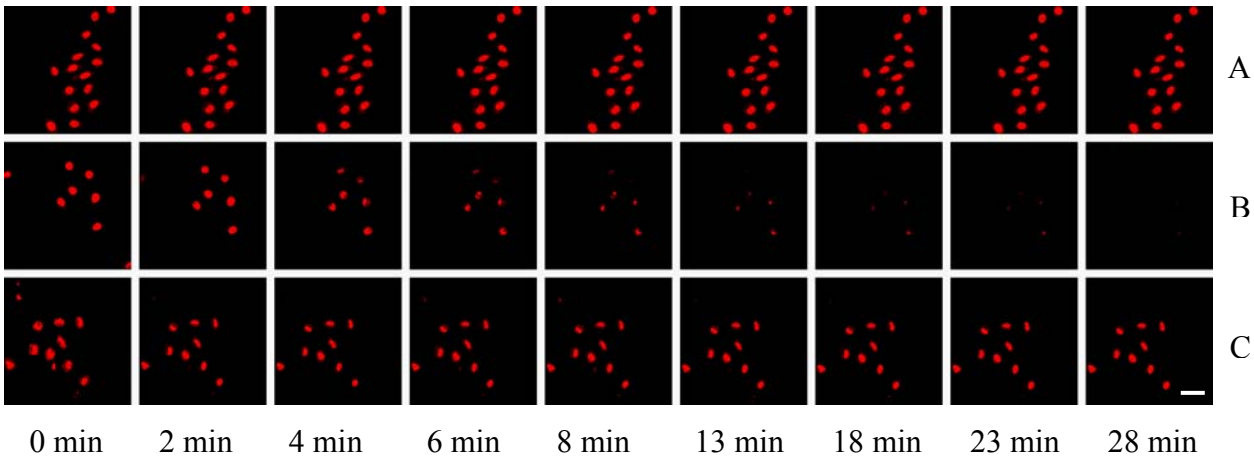

Figure 24A: Nuclear pore complex play a role in nuclear envelope breakdown. **(A)** Transport buffer showed no loss of chromatin staining. **(B)** H-1 virus, loss of chromatin staining observed. **(C)** Cells were pre-incubated with phosphorylated r-HBV capsids then H-1 was added, degradation process blocked. NPCs play an important role in nuclear envelop break down. Bar 5 µm.

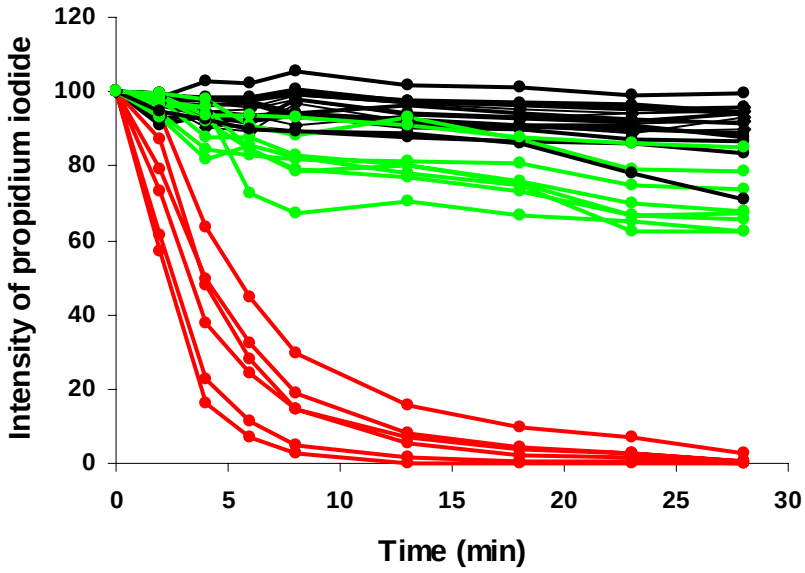

Figure 24B: Nuclear pore complex involved in nuclear envelope breakdown. Pictures were taken at 0, 2, 4, 6, 8, 13, 18, 23 and 28 min. Quantification was performed for each cell and intensity of propidium staining calculated at each time point. Black lines: transport buffer (negative control), red lines: H-1 virus, Green lines: HeLa cells pre-incubated with P-rHBC then treated with H-1 virus.

The missing inhibition of NEBD by WGA only exclude that an active nuclear import via transport receptors is a prerequisite for NEBD, it does not exclude that the parvoviruses that directly interact with the NPC causing this phenomenon. For further analysis if an interaction between H-1 and NPC is required for NEBD the pores were blocked with capsids of the hepatitis B virus (HBV).

In E.coli-expressed HBV capsids become imported into the nuclear basket via importin α and ß. Within the basket, they are arrested thereby blocking the nuclear pore. Permeabilized cells were pre-incubated with phosphorylated HBV capsids in the presence of cytosol before-after washing-H-1 (1.6 x 10^8 capsids) was added. As in previous experiments, the propidium iodide fluorescence was recorded. Chromatin staining stayed unchanged throughout the 30 min observation period in the negative control but disappeared in the H-1-exposed nuclei. Preloading of the NPCs by the HBV capsids in contrast blocked NEBD up to 80%, while the half-life of H-1 treated positive control was 6 minute (figure 24A/B). These data demonstrate that an H-1 NPC interaction triggers NEBD and suggests a direct interaction with nucleoporins as a cause for this phenomenon.

5.25 Role of apoptotic and mitotic markers on H-1 infected HeLa cells

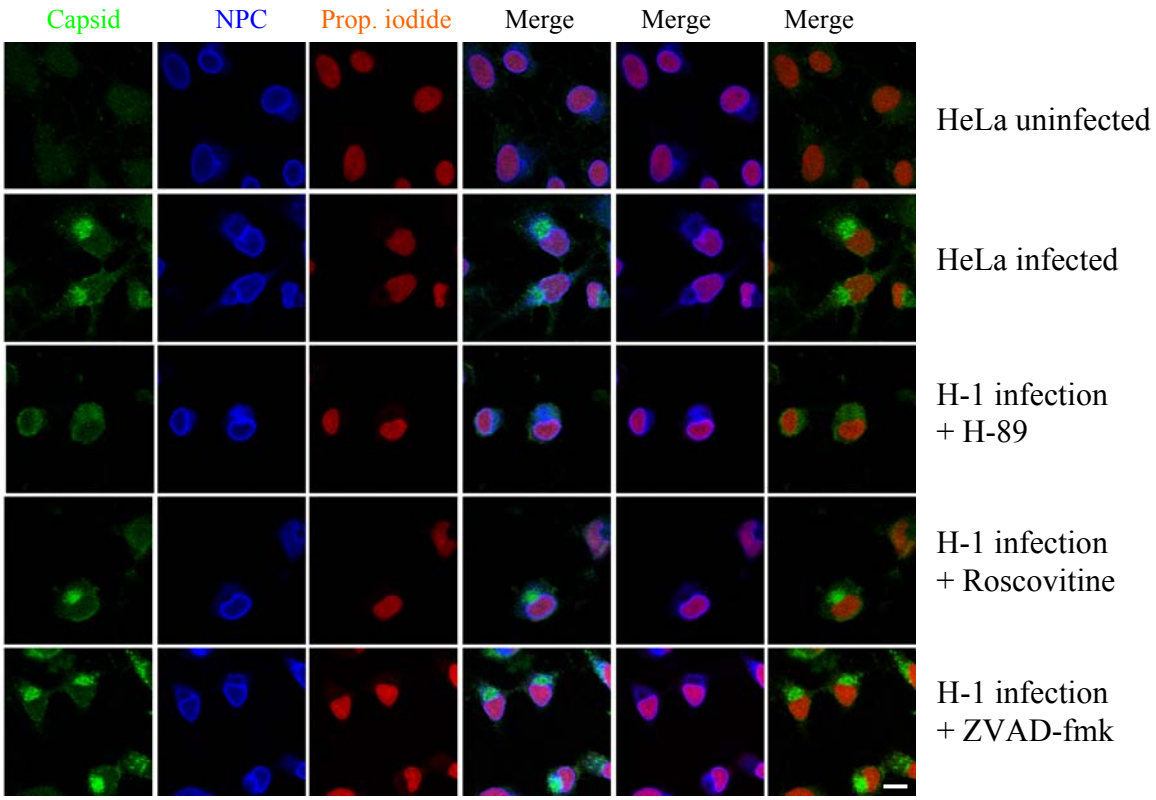

Figure 25A: Kinetic experiment by using different apoptotic inhibitors (2 h). Bar 5 µm.

Although NEBD was observed in permeabilized cells and upon infection it remained unclear, whether the same enzymes are essential in infection. To address this question kinetic infection experiments were performed by adding high doses of parvovirus H-1 (1000 capsids/cell) with the different inhibitors for the enzymes that execute NEBD. Discontinuous nuclear envelopes were analyzed 2, 4 and 8 h post infection. As depicted by confocal microscopy, uninfected HeLa cells displayed the integer NPC staining with no capsid staining (2, 4 and 8 h). In contrast, infected HeLa cells cause local disruption of the NE and the leakage of chromatin out of the nucleus in 10%

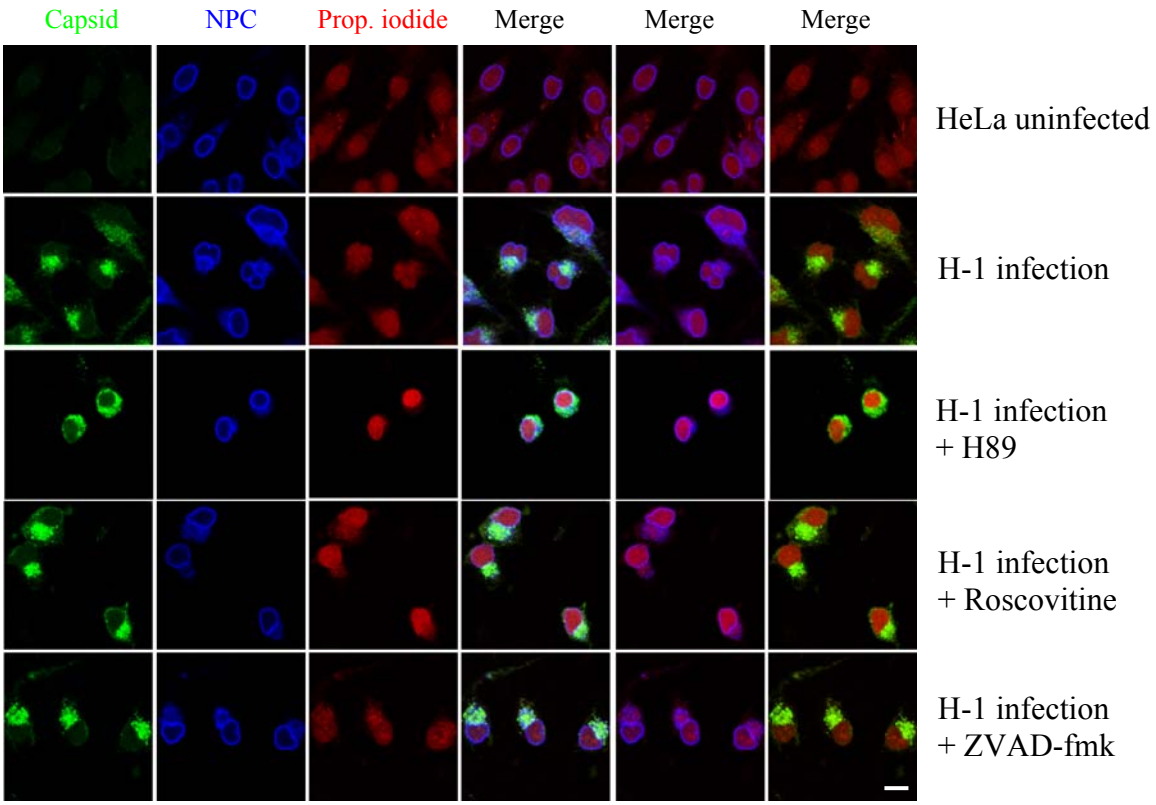

Figure 25B: Kinetic experiment by using different apoptotic inhibitors (4 h). Bar 5 µm.

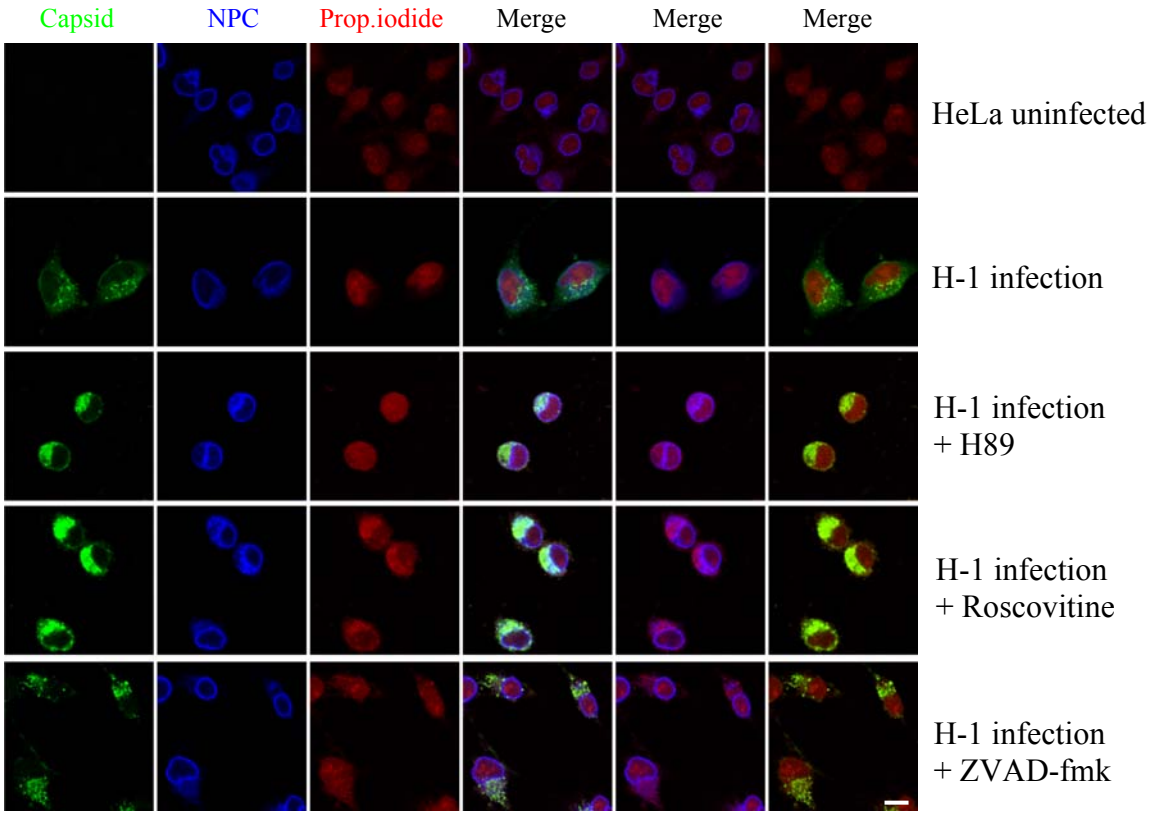

Figure 25C: Kinetic experiment by using different apoptotic inhibitors (8 h). Bar 5 µm.

of the cells only in 8 h incubation figure 25C. Leakage was restricted to those cells where H-1 was accumulated in the nuclear periphery in 2 and 4 h (figure 25A/B).

When cells were pre-incubated with H89, roscovitine and ZVAD-fmk (which inhibit PKC, cdk-2 and caspase-3 & 9 activities) no chromosomal leakage was observed, although capsids were accumulated at the perinuclear region.

To analyze the effect of the inhibitors on infection the incubation period was extended to over night. As described before, cells were treated with H89, roscovitine and ZVAD-fmk inhibitors (which inhibit PKC, cdk-2 and caspase-3 & 9 activities). Figure 25D shows that all inhibitors suppressed the generation of progeny capsids. Notheworthy H89 treated cells still allowed accumulation at the perinuclear region while roscovitine treated cells showed more a dispersed cytoplasmic or plasma membrane attached staining. Quantification table showed above (% of H-1 infected HeLa cells).

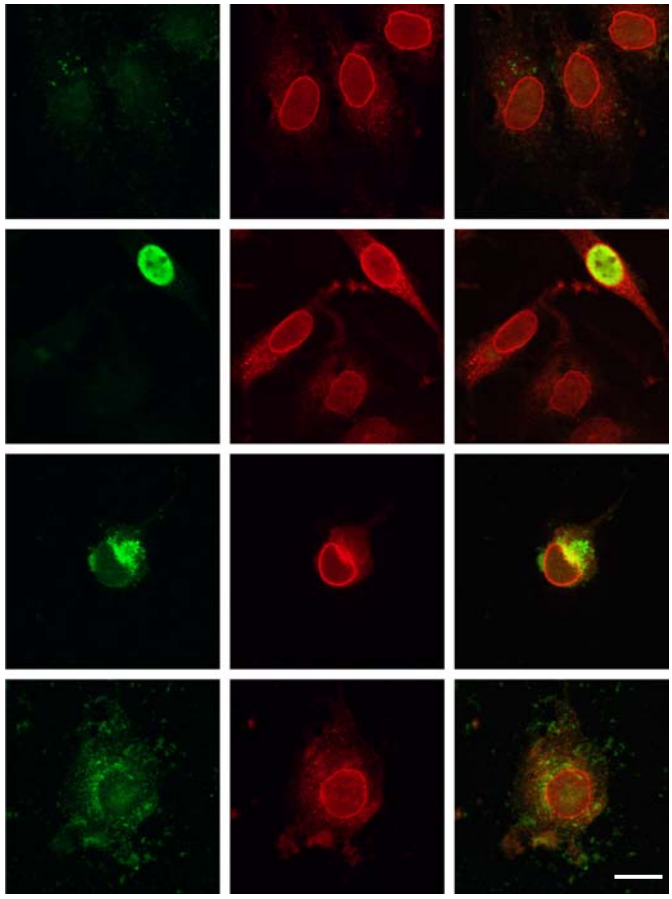

Figure 25D: Role of apoptotic inhibitors on H-1 infected HeLa cells at over night incubations. Capsids are in green and NPC is in red. Bar 10 µm.

Sample	Red (NPC stain)	Green (Capsid stain)	% of infected cells
HeLa (negative control)	595	0	0 %
H-1 (positive control)	673	210	32 %
H-1 + H89 (10 µm)	619	2	0.4 %
H-1 + Roscovitine (50 µm)	591	0	0 %

5.26 Effect of apoptotic and mitotic inhibitors on synthesis and transport of progeny H-1 capsid

However, the inhibitors may have interfered not only with the nuclear transport of the H-1 genome but with synthesis or nuclear transport of the progeny capsids. To differentiate the experimental protocol was modified. Cycloheximide was added during the uptake of H-1 followed by washing of the cells to remove the inhibitor. At this time H89, Roscovitin and ZVAD-fmk were added. This experimental design was performed to allow first the NEBD-dependent penetration of H-1 into the nucleus without allowing synthesis of progeny capsids followed by synthesis of progeny capsids from the nuclear H-1 DNA. Accordingly if H89, Roscovitine or ZVAD-fmk interferes with synthesis of progeny capsids, no nuclear progeny capsids should be generated.

Figure 26 and Table show that 70% of the cells showed progeny nuclear capsids in the positive control. Cycloheximide treatment reduced the number of successfully infected cells to 5.9%. The reason for this inhibition was not further evaluated but the block may occur on several levels for e.g. the requirement for new receptor synthesis for efficient entry or clathrin synthesis.

Irrespectively, H89 and Roscovitine treatment totally prevented generation of nuclear capsids although some cytoplasmic capsids were visible at least in PKC inhibited cells. As the capsid stain in cdk-2 inhibited cells was closed to the background in uninfected cells at least a strong reduction in capsid protein synthesis must be assumed.

In contrast, cells treated with ZVAD-fmk showed a similar proportion of nuclear capsids then in the only cycloheximide treated cells thus indicating that caspase-3 do not interfere with synthesis or transport of the progeny capsids. Thus its inhibitory function on infection must be carried by its action on preventing NEBD giving an evidence that NEBD is not a side effect but essential for the viral life cycle.

Sample	Total cells (NPC stain)	Nuclear capsids (green)	% of cells with nuclear capsids
HeLa (negative control)	1103	0	0 %
H-1 (positive control)	1023	720	70 %
H-1+ cycloheximide	1005	60	5.9 %
H-1+ cyclo+ H89	682	0	0 %
H-1+ cyclo+ Roscovitine	338	0	0 %
H-1+ cyclo+ ZVAD- fmk	980	40	4 %

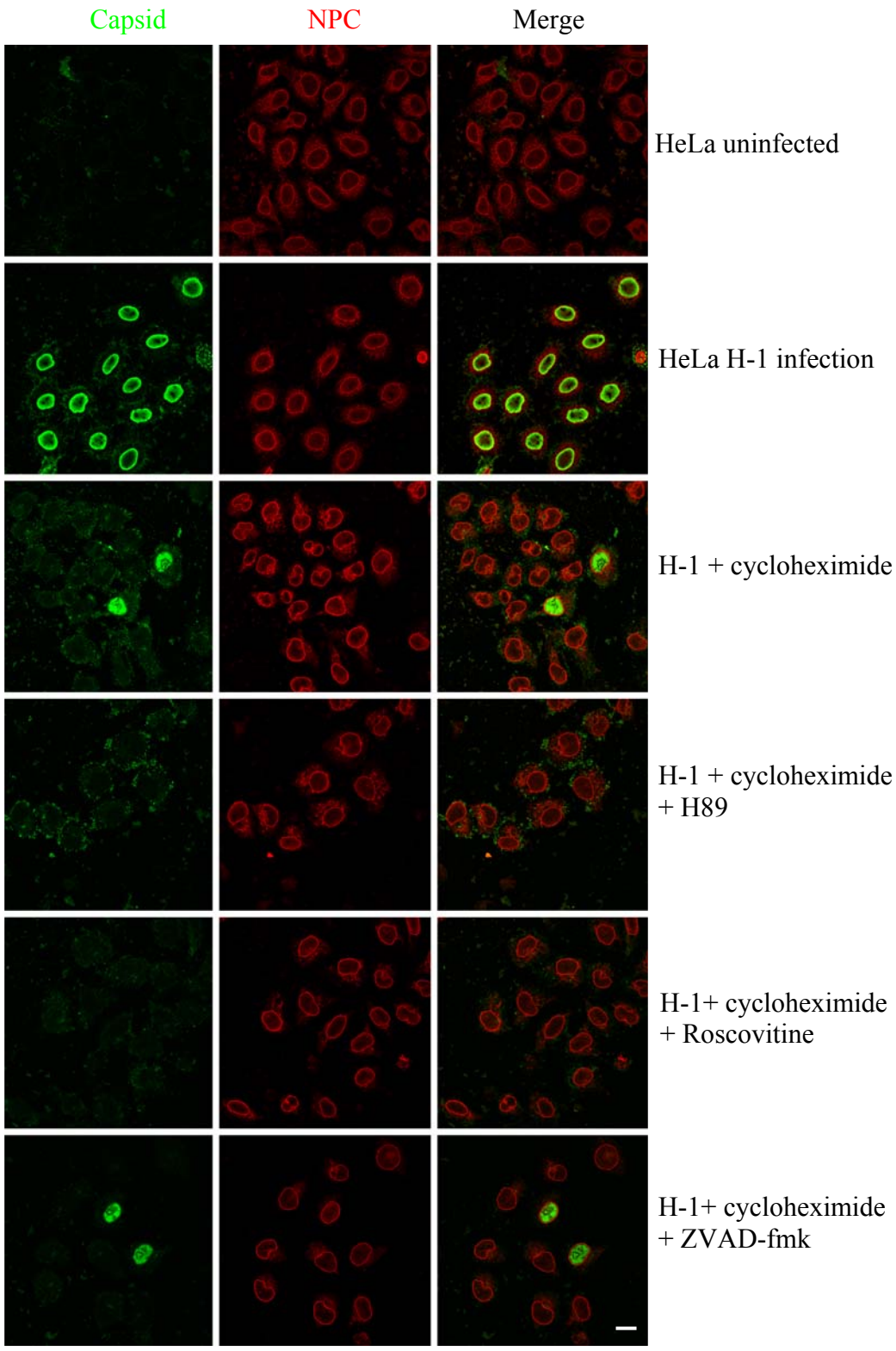

Figure 26: Confocal immunofluorescence images of H-1 infected HeLa cells treated with cycloheximide, showing capsids (green), NPC (red) by using different mitotic and apoptotic inhibitors H89 (PKC), roscovitine (cdk2) and ZVAD-fmk (caspase 3-9). To conclude this PKC and cdk-2 are required for nuclear import but not caspases. Bar 5 µm.

6. Discussion

The nuclear import of parvoviruses is a controversial topic. So far three different models of parvovirus nuclear entry have been proposed basing on NLS exposure or PLA_2 and NS1 activity. As our data are surprising and controversial, we searched for alternative pathways.

We observed that parvovirus capsids localised within the nucleus after overnight infection being inhibited by addition of hygromycin and cycloheximide (figure 3A/B). These findings suggest that mRNA translocation and protein synthesis are requirement for the generation of intranuclear capsids arguing against a direct entry of the capsids upon entry. Similarly, others showed that these inhibitors inhibit the productive infection in HIV (Gatti.PJ, et al, 1998) and coronavirus (Sawicki.SG and Sawicki.DL, 1986). In agreement with this assumption, high level infection is being clearly above the detection limit of the applied immunofluorescence (IF) did not demonstrate the nuclear entry within the first 2 h of post infection. Within such a time, endocytosis and nuclear transport should have been occurred as demonstrated for CPV (Vihinen-Ranta.M, et al, 2000) that uses the same import strategy. In case of CPV, the nuclear transport of the capsids was slow and with sufficient amount found in the nucleus only after 3 to 6 h after infection. Except parvoviruses some other viruses also use the endosomal pathway for entry e.g. Rubella virus, Vaccinia virus (Petruzziello.R, et al, 1996 and Townsley.AC, et al, 2006).

In-direct immunofluorescence showed co-staining of parvoviral capsids and proteins of the NPC within the nucleus. By using different secondary antibodies for detection of NPC and parvovirus capsids showed co-localization was not derived from bleed through of the filter but either by cross-reaction of the primary antibodies or by an interaction of progeny H-1 and NPC proteins (figure 4). Further experiments showed that in fact progeny capsids interact with nucleoporins explicitly with nups 358, 214 and 153 that bind to the anti-NPC antibody (figure 5) implying that the capsid can interact with the nuclear pore.

Acidification process is crucial for the entry of parvoviruses such as AAV and CPV (Barlett.JS, et al, 2000, Basak.S and Turner.H, 1992). These observations were also seen in parvovirus H-1, that requires acidification prior to penetration and thereby causes productive infection. Infact density gradient analysis of the acidified and untreated capsids did not show any significant difference corresponding to the co-immune precipitation of capsid proteins and viral genome (figure 6A/B). However, capsid structure was apparently changed as infection capacity was lost. According to the literature (Cotmore.SF, et al, 1999) this structural change should further lead to NLS exposure on the VP1up concomitantly as demonstrated for CPV.

Importin α should interact with this domain as it plays an essential role in nuclear import of protein exhibiting a classical NLS (Lange.A, et al, 2007). Infact these finding could be verified for H-1 in that acidification allowed coprecipitation of importin α (figure 7). However, incoming capsids did not extend the nucleus thus the effect on pH-driven disassembly was investigated. By iodoxinal gradient centrifugation no disintegration was observed as viral DNA and capsids migrated together, irrespectively to acid treatment (figure 6B).

As our results were not consistent with the proposed models of parvovirus nuclear import, we searched for an alternative nuclear import pathway and observed local disruption of the nuclear envelope in 11% HeLa cells (figure 9A). Disruption of the nuclear envelope was occurred only in that area where H-1 was accumulated and accompanied by chromatin leakage (figure 9B). Similar results were also obtained in Huh-7 cells (8.5%) suggesting that disruption was not cell line specific (figure 9C). The leakiness of the nuclear envelope was also observed in poliovirus

(Belov.GA, et al, 2004). In addition, our data on permeabilized cells, in which nuclei were hardly detectable after subjecting H-1 to the nuclei supports the notion. Furthermore, i*n vitro* experiments showed that H-1 was disintegrated with a half-life of 7 min (figure 10A/B). Half-life was defined to be a reduction of the chromatin to 50%. This loss was similar in all cells indicating an independent stage of the cell cycle in which the cell has been (but true for only those cells with nucleus). After 10 to 13 min, the nuclei appeared to be entirely disrupted. This was in agreement with the 10 min time span observed by (Lenart.P, et al, 2003) for NEBD upon mitosis in intact cells. Further, mock-purified virus did not show any effect on chromatin staining (figure 10A/B). Chromatin condensation was an indicator of mitosis observed in all experiments but did not help to differentiate between an apoptosis or mitosis like process at the time of permeabilization. Further, investigations were performed to obtain the evidence for generalization to other parvoviruses showed that CPV showed same kind of loss of chromatin staining as in case of H-1 (figure 11A/B). The observations were in accordance to the findings of Cohen.S, et al, (2006) who demonstrated that microinjection of MVM into the cytoplasm of *Xenopus oocytes* caused damage to the nuclear envelope (NE). This suggests that the nuclear-import mechanism of MVM involves disruption of the NE and import through the resulting breaks. While these data suggest that all parvoviruses follow the same strategy, our data on AAV which did not cause any nuclear envelope breakdown (NEBD) (figure 11A/C), imply that this phenomenon was particular for the autonomous parvoviruses.

Despite of the different amino acid sequences parvoviruses share a common capsid structure and more or less similar NS1 protein being attached. However, capsid structure was not only modified by acidification upon entry but also differ in empty and full capsids. Additionally, only full capsids exhibit the NS1 protein (Cotmore.SF and Tattersall.P, 1989). Although demonstrated to be cleaved off upon endocytosis (Cotmore.SF and Tattersall.P, 1989), analysis of the viral components that facilitate NEBD, should include NS1. First it has to be considered that not the entire protein is removed (Nuesch.JP, et al, 1993). Due to the low ratio of parvovirus particles versus infections units (< 200:1) it cannot be excluded that few capsids that represent the infectious ones still inhibit the entire NS1.

Our investigations thus included empty and full capsid as well as the necessity of NS1. In fact anti NS1 pre-incubation of the virions reduced the half-life of chromatin to ~25 min, six times more than in the positive control (figure 17A/B). Empty capsids did not exhibit any observable NEBD activity, seemingly supporting that NS1 is the viral partner that causes the degradation. In fact, homology search via BLAST showed that H-1 (NS1) and CPV (NS1) showed 73.2% identity in 671 residues showing the overlapping whereas, H-1(NS1) with AAV (Rep) showed 37.4% identity in 265 residues was overlapped. 36.6% similar identity was observed in CPV with AAV showing overlapping in 265 residues.

In NEBD, early spindle microtubules caused folds and invaginations in the NE up to 1 h prior to NEBD, creating mechanical tension in the nuclear lamina proteins. The first gap in the NE then appeared before lamin B depolymerization, at the site of maximal tension, by a tearing mechanism. Gap formation relaxed this tension and dramatically accelerated the rate of chromosome condensation. These produced holes in NE rapidly expanded over the nuclear surface. At last, NE fragments remaining on chromosomes were removed towards the centrosomes, which appeared to be a microtubule dependent manner. (Beaudouin.J, et al, 2002).

The time cause in mitosis was shown to be initialized by the formation of pores in the NE followed by a rapid condensation of the nuclear membranes allowing that larger macromolecules can escape (Lenart.P and Ellenberg.J, 2006). For analysing whether parvovirus-induced NE degradation follows the same kinetic we determined the half-life of two other parameters namely the escape of

M9-BSA–a 97 kDa conjugate (Kann.M, et al, 1999) that indicates the formation of small pores and the lamin B receptor that was inserted into the nuclear membrane upon expression of as EYFP fusion protein (Ellenberg.J, et al, 1997). To gain insight into the parvovirus NEBD, experiments were performed basing on kinetics. We observed LBR disappearance with a half-life of 6 min, chromatin loss 8 min in the same experiment (figure 14A/B) accompanied by 5.8 min of M9-BSA and 6.3 min (figure 12A/B) of propidium iodide (chromatin stain). Thus our data suggest loss of the LBR receptor fluorescence followed by the escape of the M9-BSA. Having the size of ~97 kDa (diameter of at least 7 nm), thus other latter result is in agreement of the natural NEBD upon mitosis as corresponding holes were described by Lenart.P and Ellenberg.J (2006) after onset of mitosis.

Membrane degradation could have been occurred by the PLA_2 activity that is encoded on VP1up (Zadori.Z, et al, 2001). As we could not entirely exclude that some parvoviruses expose this domain despite of pH treatment, we analysed the impact of PLA_2. Such an activity cleaves a phospholipids ester bond as demonstrate for the PLA_2 of cobra venome PLA_2 (Dennis.EA, 1997, Dennis.EA, et al, 1981). Thus only small holes should be generated being in accordance with findings of (Suikkanen.S, et al, 2003) that observed a permeability of endosomal membranes for molecules smaller than 3 kDa. To verify this finding for nuclear membranes, we incubated permeabilized nuclei with PLA_2 (bovine pancreas). In fact we observed a swelling of the nuclei at 8 min after subjection, which may indicate formation of small pores in the outer nuclear membrane from an osmotic swell. However at no time, even 28 min after onset of the experiment, chromatin loss was detected (figure 23A/B). PLA_2 of bovine pancreas and the parvoviruses may however exhibit other properties so that the swelling could be interpreted as a first stage in NE degradation. Subjection of known inhibitors (AACOCF3 and Manoalide) to permeabilized cells, however failed as both of them depleted the nuclei instantly after subjection. Nonetheless it must be considered that all studied parvoviruses exhibit such an activity including AAV that failed to cause NEBD.

Excluding such a general mechanism as the global membrane degradation, we asked which structure on the NE may have triggered NEBD. The microscopic finding showed that parvovirus interact with nucleoporins even with a hidden NLS led us to focus on the NPC.

WGA, a lectin has been shown to inhibit the accumulation of nuclear proteins by blocking the translocation step of the transport (Adam.EJ and Adam.SA, 1994, Finlay.DR, et al, 1987), probably by the interacting by O-gylcosylated nucleoporins (Finlay.DR, et al, 1987). Further WGA prevents nuclear apoptosis, suggesting that important mediators of apoptosis were not able to enter the nuclear compartment. Our findings from WGA treated cells upon H-1 virus showed similar degradation as observed on H-1 treatment (figure 22A/B). Thus, WGA does not affect the degradation of the nuclei by H-1. This observation indicates that no transport receptors are required in parvovirus NEBD, which is consistent with the absence of these factors in our assays. The interpretation however implies that parvovirus directly interacts with the nucleoporins but evidence has to be given experimentally. Seemingly failure of WGA to prevent NEBD is in divergence to the data of Vihinen-Ranta.M, et al, (2002) obtained after the microinjection of CPV. Keeping in mind that nuclear capsids represent imported progeny capsids, the finding may reflect that the progeny capsid subunits are imported into the nucleus by the classical import receptor-mediated pathway rather than the entering capsids pass the nuclear pore. Consistent with this hypothesis Riolobos.L, et al, (2006) showed that a trimeric complex of MVM VP1 and VP2 exhibit a nuclear translocation motif responsible for nuclear import of the complex via importins.

Based on the hypothesis that an NPC interaction is needed for NEBD we blocked the pores by pre-treating the permeabilized cells with an excess of phosphorylated hepatitis B virus capsid (P-HBc) (figure 24A/B). P-HBc interacts directly with nup 153 (Schmitz, unpublished) but depend upon

importin α and β for translocation into the nuclear basket (Kann.M, et al, 1999) where this nucleocapsid is anchored to the NPC. Due to this interaction the capsids become arrested allowing accumulation inside the pores. In fact investigation by electron microscopy showed up to seven P-HBc per NPC (Pante.N and Kann.M, 2002).

This preload of the pores in fact totally inhibited NEBD by H-1 supporting that nucleoporins – interaction triggered the reaction. Consistent with this idea nucleoporins (Nup 153, 358) are involved in initialisation of mitosis (Macaulay.C, et al, 1995, Salina .D, et al, 2003). Except mitosis, nucleoporins also play a central role in apoptosis (Fahrenkrog.B, 2006). The observation that the nuclear pores are involved and that these nucleoporins interact with H-1 capsids including nup 153 - however allows a further interpretation of inhibition by anti-NS1 antibody. This divalent antibody can cause a complex of two times 26 nm H-1 capsids connected a by 10 nm measuring antibody (NS1). Such a structure is at the limit size of the NPC which is 39 nm (Pante.N and Kann.M, 2002). The complex has thus poor excess to nucleoporins that are not exposed on the exterior of the NPC as e.g. nup 153. Consequently this experiment does not exclude that may be the structural differences between the empty and full capsids cause their different impact on NEBD.

The absence of soluble cytosolic factors in our assays (figure 21) implies the nuclei already contain the executing enzymes for NEBD that need to be activated. During apoptosis an activator apparently has to be imported through the nuclear pores as the WGA inhibition experiments mentioned earlier suggest (Buendia.B, et al, 1999). This implies that the imported activator is a "normal" karyophilic cargo that enters the lumen of the nucleus where it diffuses. Parvovirus however could not be seen inside the nucleus upon infection even when NEBD was visible. Moreover NEBD was a local phenomenon at those sides of the nucleus where the capsids accumulated. In agreement with these findings we found that NEBD in the permeabilized cells only took place at those parts of the nucleus that were accessible from the cytosolic side to the capsids.

Based on these data parvovirus mediated NEBD may thus use the same or a different activation pathway than that is described for apoptosis or mitosis. We thus added different apoptotic and mitotic inhibitors on HeLa cells which inhibit different enzymatic activity required during mitosis and apoptosis. These inhibitors were H89, roscovitine and ZVAD-fmk which inhibits protein kinase C (PKC), cyclin dependent 2 (cdk2) and caspase 3-9 activity. Cdk2 drives the G2 phase cells into mitosis within 30 minutes (Furuno.N, et al, 1999). Recent studies showed caspase 3 is activated immediately before the cells enter mitosis (Hsu.SL, et al, 2006). During apoptosis, caspase 3 is actively transported to the nucleus and increase the diffusion through the nuclear pores. This increase of the nuclear pores allow the passage to caspase 3 and other molecules which could not pass through the nuclear pore of the living cells in and out of the nucleus during apoptosis. Treatment of digitonin-permeabilized cells inhibited parvovirus-mediated NEBD demonstrating that the physiological degradation pathway was used. Moreover the applied inhibitors blocked the leakiness of the nuclear envelope in infection (figure 25) without affecting capsid accumulation at perinuclear region. In order to analyse the impact of these findings for infection we analysed the effect of inhibitor treatment on the appearance of nuclear progeny capsids. An interference with virus uptake was not observed but generation of nuclear capsids was totally inhibited. Nonetheless these findings could have been based on an inhibition of synthesis or an interference with nuclear import of the capsid subunits. In fact PKC as well as cdk-2 inhibition was shown to prevent the synthesis of nuclear capsids. While PKC inhibition apparently just interfered with translocation into the nucleus cdk-2 inhibition blocked the synthesis of the progeny capsids (figure 26). The latter observation is in accordance with cdk-2 participation in complimentary strand elongation (Bashir.T, et al, 2000). The effect of the PKC inhibition can be

explained by the unpublished data on MVM where phosphorylation of the VP1- (VP2) complex is essential for its nuclear import (Riolobos, unpublished). Nonetheless caspase-3 allowed capsids synthesis and nuclear entry leading to the conclusion that its inhibitory function on NEBD upon infection and inhibition of successful infection is correlated (figure 26).

Irrespectively to the obtained results on permeabilized cells and the impact on viral infection, the molecular mechanism of how parvovirus causes NEBD remains open. We hypothesize, for instance that PV may have a direct affinity or an indirect influence to caspase-3 activity through the modulation of the PDK/PKC pathway (figure A (3, 5)). The local enrichment may promote self-digestion of caspase-3 known to activate it (figure A (3)). However, our preliminary experiments could not give any evidence for a direct interaction favouring other models. Alternatively, PV may activate caspase-8 by promoting procaspase-8 dimerization that leads to activation (figure A (2)). Activated capsase-8 then could activate caspase-3 that cleaves different proteins of the NPC (nup153, RanBP2, nup214 and Tpr (Fahrenkrog.B, 2006, Ferrando-May.E, et al, 2001) and a PKC δ that becomes thereby activated; process that was described to occur during apoptosis (figure A (2, 3, 4). Active PKC δ activates cdk-2, and phosphorylates the lamin skeleton, leading to lamin depolymerization (figure A (5, 6, 8)). Indeed, PKC δ was shown to become activated upon MVM infection (Nüesch.P, unpublished).

Nonetheless, other pathways appear possible we can not exclude that parvoviruses directly activate cdk-2 with the consequences described before (figure A (7, 8). In this scenario, cleavage of nup153 by caspase-3 would not be involved. Another possibility is that H-1 recruits the PKC to the nuclear membrane to phosphorylate lamin B receptor and thereby permeabilize the lamina to facilitate the access of nuclear capsids to the inner nuclear membrane (figure A (5, 8)).

Despite of the yet not understood pathway that is caused by the lack of knowledge on physiological NEBD, the presented data may help to design the future experiments on NEBD without the interference of cytosolic signal cascades.

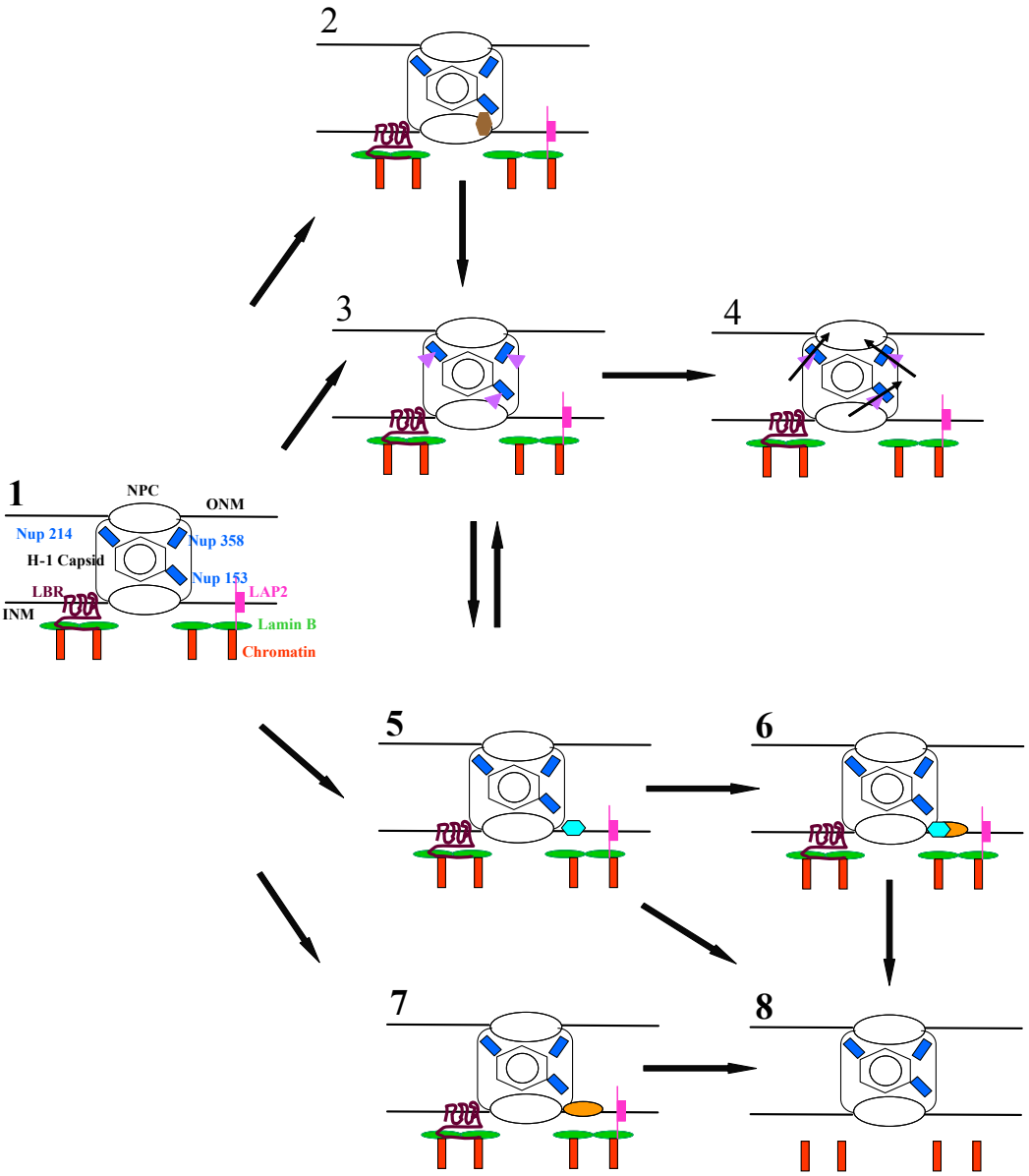

Figure A: Hypothetical possibilities how parvoviruses may induce local NEBD. (1) Parvoviruses (PV) interact with different nucleoporins (blue). (3) PV may cause either local enrichment of activated caspase-3 (violet) or may activate caspase-3 directly by an unknown mechanism. This activated or accumulated caspase may lead to cleavage (black arrows) of some nups (blue) (4) and /or cleave PKC embedded into the inner nuclear membrane (INM); which would result in an active PKC fragment (PKM) (sky blue) (5), PKM then leads to the activation of cdk-2 (orange) or according to the literature – may activate caspase-3 (Rosado.JA, et al, 2006) (6), Irrespectively PKM could then further phosphorylate the lamin structure (green) leading to lamin depolymerization (8). (2) Another possibility is that procaspase 8 promotes the caspase-8 (brown) activation and this activates caspase-3 (violet). (7) Following another scenario, LAP2 (pink) become phosphorylated by PV activated cdk-2 (orange) which disconnects the contact of NPC (black) and chromatin (red) (8). (5) Furthermore PKC (sky blue) may phosphorylate the LBR (maroon) which is present on INM resutling in lamin disassembly (green) (8).

7. Summary

The parvoviruses are among the smallest DNA viruses, which infects the vertebrates and insects. They are divided into dependoviruses and autonomous parvoviruses. The dependoviruses depend on helper adenovirus or herpes virus to provide functions needed for their replication, whereas the autonomous parvoviruses, Parvovirus and Erythrovirus, do not need any helper virus for their DNA multiplication.

Parvoviruses (PV) are non-enveloped, single stranded DNA viruses consisting of the structural proteins VP1 and VP2 and non-structural protein NS1. VP1 is the largest protein (83 kDa) contains NLS and a PLA_2 activity that is not exposed on viral capsids. NS1 protein acts as a transactivator, which is covalently bound to viral DNA, and which is exposed on capsids surface. It is believed to be cleaved from the capsid upon uptake into the cells. Parvoviruses enter via clathrin-mediated endocytosis and need a low pH for productive infection. Parvoviruses exhibit 18-24 nm diameter, which is small enough to pass the NPC without any disassembled form.

Accordingly some authors propose that NLS on VP1 that becomes exposed upon endosomal acidification mediates entry of the capsid into the nucleus. However microinjections, by passing the endosomes, generate progeny capsids being contradictory to this model. Other proposed that the PLA_2 actively allows the capsids to pass the nuclear membrane, while others suggest that this activity is required for endosomal release.

As the before mentioned models were based on the analysis of the autonomous parvoviruses MVM and CPV, we first evaluated whether our analysis done on parvovirus H-1 showed similar phenomenon. In fact we showed that acidification resulted in a structural change of the H-1 capsid resulting in the exposure of a NLS without leading to capsid disintegration. However nuclear entry did not occur upon infection but was shown to be caused by nuclear accumulation of progeny capsid or capsid subunits.

Analysing the early steps of infection we found that H-1 caused a local nuclear envelope breakdown (NEBD). This phenomenon was reproduced in digitonin-permeabilized cells even in the absence of cytosolic proteins. Corrseponding experiments with CPV confirmed that this phenomenon was not H-1 specific. Further investigation showed that parvovirus-mediated NEBD was an enzymatically driven process involving PKC, cdk-2 and caspase-3 that are the executing enzymes in physiological NEBD upon mitosis and apoptosis.

Inhibition experiments revealed that H-1 triggered NEBD by an interaction with the nulcear pores not requiring nuclear transport receptor that facilitate attachment. Infection experiments in the presence of PKC, cdk2 and caspase-3 inhibitors confirmed that all these enzymes were needed for PV-mediated NEBD upon infection. Further their inhibition blocked the appearance of progeny nuclear capsids. Further investigations revealed that PKC was however required for nuclear translocation of the progeny capsid subunits, cdk-2 for their synthesis while only caspase-3 did not affect these two steps.

Indirectly these finding thus indicate that NEBD is essential for the entry of the parvoviral capsids upon infection, which is a new import principle for viruses.

8. Zusammenfassung

Parvoviren (PV) gehören zu den kleinsten Viren überhaupt. Sie infizieren Vertebraten und Insekten und werden in Dependoviren und autonome PV unterteilt. Dependoviren benötigen die Hilfe von Herpes oder Adenoviren für Infektion oder Virusneusynthese, wohingegen die autonomen PV keinerlei Hilfe benötigen.

PV sind nicht-umhüllte einzelstränge DNA Viren, die aus den Strukturproteinen VP1 und VP2, sowie aus dem Nichtstrukturprotein NS1 bestehen. VP1 ist da größte der Proteine und enthält ein Kerntransportsignal (NLS), sowie eine Phosholipase A_2 (PLA_2) Aktivität. Beide Aktivitäten, die auf dem N-Terminus des VP1 Proteins kodiert sind, sind jedoch nicht auf der Oberfläche der Virionen exponiert. NS1 ist ein Transaktivator, der kovalent an die Virus DNA gebunden auf der Oberfläche der Viren exponiert ist. Es wird angenommen, dass dieses Protein während des Eintritts in die Zelle abgespalten wird.

PV werden über Endozytose in die Zelle aufgenommen und bedürfen eines niedrigen pH für eine produktive Infektion. Sie weisen einen Durchmesser von 18 – 24 nm auf, welcher klein genug ist, um einen Transport als intakte Partikel durch die Kernporen zu erlauben.

Damit übereinstimmend postulieren einige Autoren, dass das NLS, welches im Zuge der endosomalen Ansäuerung exponiert wird, den Transport des intakten Capsides in den Zellkern vermittelt. Dementgegengesetzt belegten jedoch Mikroinjektionsversuche – bei denen die Ansäuerung umgangen wird – ebenfalls die Synthese von Nachkommenviren. Andere Autoren postulierten, dass die PLA_2 Aktivität die Passage der Capside durch die Kernmembran vermitteln, wohingegen wieder andere Publikationen die PLA_2 Aktivität dem Freisetzen der Capside aus den Endosomen zuordnen.

Da die aufgezeigten Modelle auf der Analyse der autonomen PV MVM und CPV basieren, wurde in dieser Arbeit zunächst untersucht, ob die Analysen, die mit dem PV H-1 durchgeführt wurden, übertragbar sind. Tatsächlich konnte eine pH-bedingte Strukturänderung der Viruscapside beobachtet werden, die eine Exposition des NLS hervorrief, ohne jedoch die Capsidstruktur zu zerstören. Dessen ungeachtet konnte jedoch keinerlei nukleärer Import der infizierenden Capside in den Zellkern beobachtet werden. Einzig die Synthese von neuen Capsiduntereinheiten führte zu einer Akkumulation dieser, oder von kompletten Capsiden im Zellkern.

Während der Analyse des frühen Infektionsvorganges konnte beobachtet werden, dass die Kernmembran lokal an den Stellen desintegriert wurde, an denen PV auf der cytosolischen Seite akkumulierten. Dieses Phänomen konnte ebenfalls in Abwesenheit cytosolischer Proteine in Digitonin-permeabilisierten Zellen beobachtet werden. Korrespondierende Experimente mit dem PV CPV bestätigte, dass dieses Phänomen nicht H-1-spezifisch war. Weitere Analysen zeigten, dass die PV-vermittelte Kernmembranzerstörung (nuclear envelope break-down, NEBD) ein enzymatisch katalysierter Prozess war, der PKC, Cdk 2 Kinase und Caspase 3, also die ausführenden Enzyme dieses Vorganges während Apoptose und Mitose, benötigte.

Inhibitionsexperimente demonstrierten, dass der NEBD durch einen Kontakt zwischen H-1 und den Kernporen vermittelt wurde. Inhibitionen der PKC, Cdk 2 und Caspase 3 während Infektionen zeigten weiterhin, dass alle diese Enzyme auch dort den NEBD vermittelten und die Entstehung von nukleären neusynthetisierten Capsiden verhinderten. Nähere Charakterisierungen belegten jedoch, dass PKC den nukleären Import der Capsiduntereinheiten in den Zellkern verhinderten, Cdk-2 die Neusynthese blockierte, aber Caspase-3 weder mit Synthese oder Transport der

neusynthetisierten Intermediate interferierte. Indirekt implizieren diese Resultate also, dass der NEBD für das Eindringen der Capside in den Zellkern während der Infektion notwendig sind, welches ein völlig neues Prinzip für den Kerntransport von Viren darstellt.

9. References

Adam, E. J. and S. A. Adam. "Identification of cytosolic factors required for nuclear location sequence-mediated binding to the nuclear envelope." J.Cell Biol. 125.3 (1994): 547-55.

Alam, A., et al. "Early activation of caspases during T lymphocyte stimulation results in selective substrate cleavage in nonapoptotic cells." J.Exp.Med. 190.12 (1999): 1879-90.

Al-Awqati, Q. "Proton-translocating ATPases." Annu.Rev.Cell Biol. 2 (1986): 179-99.

Alnemri, E. S., et al. "Human ICE/CED-3 protease nomenclature." Cell 87.2 (1996): 171.

Authier, F., B. I. Posner, and J. J. Bergeron. "Endosomal proteolysis of internalized proteins." FEBS Lett. 389.1 (1996): 55-60.

Ball-Goodrich, L. J., et al. "Rat parvovirus type 1: the prototype for a new rodent parvovirus serogroup." J.Virol. 72.4 (1998): 3289-99.

Ball-Goodrich, L. J., et al. "Immune responses to the major capsid protein during parvovirus infection of rats." J.Virol. 76.19 (2002): 10044-49.

Baptiste, D. C., et al. "An investigation of the neuroprotective effects of tetracycline derivatives in experimental models of retinal cell death." Mol.Pharmacol. 66.5 (2004): 1113-22.

Bartlett, J. S., R. Wilcher, and R. J. Samulski. "Infectious entry pathway of adeno-associated virus and adeno-associated virus vectors." J.Virol. 74.6 (2000): 2777-85.

Basak, S. and H. Turner. "Infectious entry pathway for canine parvovirus." Virology 186.2 (1992): 368-76.

Bashir, T., et al. "Cyclin A activates the DNA polymerase delta -dependent elongation machinery in vitro: A parvovirus DNA replication model." Proc.Natl.Acad.Sci.U.S.A 97.10 (2000): 5522-27.

Beaudouin, J., et al. "Nuclear envelope breakdown proceeds by microtubule-induced tearing of the lamina." Cell 108.1 (2002): 83-96.

Belmont, A. S., Y. Zhai, and A. Thilenius. "Lamin B distribution and association with peripheral chromatin revealed by optical sectioning and electron microscopy tomography." J.Cell Biol. 123.6 Pt 2 (1993): 1671-85.

Belov, G. A., et al. "Bidirectional increase in permeability of nuclear envelope upon poliovirus infection and accompanying alterations of nuclear pores." J.Virol. 78.18 (2004): 10166-77.

Berns, K. I. and C. Giraud. "Biology of adeno-associated virus." Curr.Top.Microbiol.Immunol. 218 (1996): 1-23.

Besselsen, D. G., et al. "Detection of H-1 parvovirus and Kilham rat virus by PCR." J.Clin.Microbiol. 33.7 (1995): 1699-703.

Blumenthal, R., R. D. Klausner, and J. N. Weinstein. "Voltage-dependent translocation of the asialoglycoprotein receptor across lipid membranes." Nature 288.5789 (1980): 333-38.

Blumenthal, R., M. Henkart, and C. J. Steer. "Clathrin-induced pH-dependent fusion of phosphatidylcholine vesicles." J.Biol.Chem. 258.5 (1983): 3409-15.

Brodie, C. and P. M. Blumberg. "Regulation of cell apoptosis by protein kinase c delta." Apoptosis. 8.1 (2003): 19-27.

Broers, J. L., et al. "Dynamics of the nuclear lamina as monitored by GFP-tagged A-type lamins." J.Cell Sci. 112 (Pt 20) (1999): 3463-75.

Brown, K. E., S. M. Anderson, and N. S. Young. "Erythrocyte P antigen: cellular receptor for B19 parvovirus." Science 262.5130 (1993): 114-17.

Bucci, C., et al. "The small GTPase rab5 functions as a regulatory factor in the early endocytic pathway." Cell 70.5 (1992): 715-28.

Buendia, B. and J. C. Courvalin. "Domain-specific disassembly and reassembly of nuclear membranes during mitosis." Exp.Cell Res. 230.1 (1997): 133-44.

Buendia, B., A. Santa-Maria, and J. C. Courvalin. "Caspase-dependent proteolysis of integral and peripheral proteins of nuclear membranes and nuclear pore complex proteins during apoptosis." J.Cell Sci. 112 (Pt 11) (1999): 1743-53.

Bullough, P. A., et al. "Structure of influenza haemagglutinin at the pH of membrane fusion." Nature 371.6492 (1994): 37-43.

Burger, K. N., et al. "Dynamin is membrane-active: lipid insertion is induced by phosphoinositides and phosphatidic acid." Biochemistry 39.40 (2000): 12485-93.

Caillet-Fauquet, P., et al. "Programmed killing of human cells by means of an inducible clone of parvoviral genes encoding non-structural proteins." EMBO J. 9.9 (1990): 2989-95.

Cain, C. C., D. M. Sipe, and R. F. Murphy. "Regulation of endocytic pH by the Na+,K+-ATPase in living cells." Proc.Natl.Acad.Sci.U.S.A 86.2 (1989): 544-48.

Chapman, R. E. and S. Munro. "Retrieval of TGN proteins from the cell surface requires endosomal acidification." EMBO J. 13.10 (1994): 2305-12.

Chaudhary, N. and J. C. Courvalin. "Stepwise reassembly of the nuclear envelope at the end of mitosis." J.Cell Biol. 122.2 (1993): 295-306.

Chipman, P. R., et al. "Cryo-electron microscopy studies of empty capsids of human parvovirus B19 complexed with its cellular receptor." Proc.Natl.Acad.Sci.U.S.A 93.15 (1996): 7502-06.

Clague, M. J., et al. "Vacuolar ATPase activity is required for endosomal carrier vesicle formation." J.Biol.Chem. 269.1 (1994): 21-24.

Cohen, S. and N. Pante. "Pushing the envelope: microinjection of Minute virus of mice into Xenopus oocytes causes damage to the nuclear envelope." J.Gen.Virol. 86.Pt 12 (2005): 3243-52.

Cohen, S., et al. "Parvoviral nuclear import: bypassing the host nuclear-transport machinery." J.Gen.Virol. 87.Pt 11 (2006): 3209-13.

Corbau, R., et al. "Regulation of MVM NS1 by protein kinase C: impact of mutagenesis at consensus phosphorylation sites on replicative functions and cytopathic effects." Virology 278.1 (2000): 151-67.

Cornelis, J. J., et al. "Susceptibility of human cells to killing by the parvoviruses H-1 and minute virus of mice correlates with viral transcription." J.Virol. 64.6 (1990): 2537-44

Cotmore, S. F. and P. Tattersall. "The autonomously replicating parvoviruses of vertebrates." Adv.Virus Res. 33 (1987): 91-174.

Cotmore, S. F. and P. Tattersall. "A genome-linked copy of the NS-1 polypeptide is located on the outside of infectious parvovirus particles." J.Virol. 63.9 (1989): 3902-11.

Cotmore, S. F., et al. "The NS2 polypeptide of parvovirus MVM is required for capsid assembly in murine cells." Virology 231.2 (1997): 267-80.

Cotmore, S. F. and P. Tattersall. "High-mobility group 1/2 proteins are essential for initiating rolling-circle-type DNA replication at a parvovirus hairpin origin." J.Virol. 72.11 (1998): 8477-84.

Cotmore, S. F., et al. "Controlled conformational transitions in the MVM virion expose the VP1 N-terminus and viral genome without particle disassembly." Virology 254.1 (1999): 169-81.

Courvalin, J. C., et al. "The lamin B receptor of the inner nuclear membrane undergoes mitosis-specific phosphorylation and is a substrate for p34cdc2-type protein kinase." J.Biol.Chem. 267.27 (1992): 19035-38.

Cullen, B. R. "Journey to the center of the cell." Cell 105.6 (2001): 697-700.

Dabauvalle, M. C., et al. "Distribution of emerin during the cell cycle." Eur.J.Cell Biol. 78.10 (1999): 749-56.

Daro, E., et al. "Rab4 and cellubrevin define different early endosome populations on the pathway of transferrin receptor recycling." Proc.Natl.Acad.Sci.U.S.A 93.18 (1996): 9559-64.

Dautry-Varsat, A., A. Ciechanover, and H. F. Lodish. "pH and the recycling of transferrin during receptor-mediated endocytosis." Proc.Natl.Acad.Sci.U.S.A 80.8 (1983): 2258-62.

Davis, C. G., et al. "Acid-dependent ligand dissociation and recycling of LDL receptor mediated by growth factor homology region." Nature 326.6115 (1987): 760-65.

Davis, L. I. and G. Blobel. "Identification and characterization of a nuclear pore complex protein." Cell 45.5 (1986): 699-709.

Dennis, E. A., et al. "Cobra venom phospholipase A2: a review of its action toward lipid/water interfaces." Mol.Cell Biochem. 36.1 (1981): 37-45.

Dennis, E. A. "The growing phospholipase A2 superfamily of signal transduction enzymes." Trends Biochem.Sci. 22.1 (1997): 1-2.

DiPaola, M., et al. "Loss of alpha 2-macroglobulin and epidermal growth factor surface binding induced by phenothiazines and naphthalene sulfonamides." J.Cell Physiol 118.2 (1984): 193-202.

DiPaola, M. and F. R. Maxfield. "Conformational changes in the receptors for epidermal growth factor and asialoglycoproteins induced by the mildly acidic pH found in endocytic vesicles." J.Biol.Chem. 259.14 (1984): 9163-71.

Dorsch, S., et al. "The VP1 unique region of parvovirus B19 and its constituent phospholipase A2-like activity." J.Virol. 76.4 (2002): 2014-18.

Douar, A. M., et al. "Intracellular trafficking of adeno-associated virus vectors: routing to the late endosomal compartment and proteasome degradation." J.Virol. 75.4 (2001): 1824-33.

Dreger, M., et al. "Identification of phosphorylation sites in native lamina-associated polypeptide 2 beta." Biochemistry 38.29 (1999): 9426-34.

Duband-Goulet, I., J. C. Courvalin, and B. Buendia. "LBR, a chromatin and lamin binding protein from the inner nuclear membrane, is proteolyzed at late stages of apoptosis." J.Cell Sci. 111 (Pt 10) (1998): 1441-51.

Eichwald, V., et al. "The NS2 proteins of parvovirus minute virus of mice are required for efficient nuclear egress of progeny virions in mouse cells." J.Virol. 76.20 (2002): 10307-19.

Ellenberg, J., et al. "Nuclear membrane dynamics and reassembly in living cells: targeting of an inner nuclear membrane protein in interphase and mitosis." J.Cell Biol. 138.6 (1997): 1193-206.

Ellenberg, J. and J. Lippincott-Schwartz. "Dynamics and mobility of nuclear envelope proteins in interphase and mitotic cells revealed by green fluorescent protein chimeras." Methods 19.3 (1999): 362-72.

Ellis, J. A., et al. "Aberrant intracellular targeting and cell cycle-dependent phosphorylation of emerin contribute to the Emery-Dreifuss muscular dystrophy phenotype." J.Cell Sci. 111 (Pt 6) (1998): 781-92.

Enari, M., et al. "A caspase-activated DNase that degrades DNA during apoptosis, and its inhibitor ICAD." Nature 391.6662 (1998): 43-50.

Fahrenkrog, B. "The nuclear pore complex, nuclear transport, and apoptosis." Can.J.Physiol Pharmacol. 84.3-4 (2006): 279-86.

Falcieri, E., et al. "Nuclear pores in the apoptotic cell." Histochem.J. 26.9 (1994): 754-63.

Falcieri, E., et al. "The behaviour of nuclear domains in the course of apoptosis." Histochemistry 102.3 (1994): 221-31.

Falnes, P. O. and K. Sandvig. "Penetration of protein toxins into cells." Curr.Opin.Cell Biol. 12.4 (2000): 407-13.

Fan, T. J., et al. "Caspase family proteases and apoptosis." Acta Biochim.Biophys.Sin.(Shanghai) 37.11 (2005): 719-27.

Farr, G. A., L. G. Zhang, and P. Tattersall. "Parvoviral virions deploy a capsid-tethered lipolytic enzyme to breach the endosomal membrane during cell entry." Proc.Natl.Acad.Sci.U.S.A 102.47 (2005): 17148-53.

Favreau, C., et al. "Cell cycle-dependent phosphorylation of nucleoporins and nuclear pore membrane protein Gp210." Biochemistry 35.24 (1996): 8035-44.

Fernandes-Alnemri, T., et al. "In vitro activation of CPP32 and Mch3 by Mch4, a novel human apoptotic cysteine protease containing two FADD-like domains." Proc.Natl.Acad.Sci.U.S.A 93.15 (1996): 7464-69.

Ferrando-May, E., et al. "Caspases mediate nucleoporin cleavage, but not early redistribution of nuclear transport factors and modulation of nuclear permeability in apoptosis." Cell Death.Differ. 8.5 (2001): 495-505.

Finlay, D. R., et al. "Inhibition of in vitro nuclear transport by a lectin that binds to nuclear pores." J.Cell Biol. 104.2 (1987): 189-200.

Foisner, R. and L. Gerace. "Integral membrane proteins of the nuclear envelope interact with lamins and chromosomes, and binding is modulated by mitotic phosphorylation." Cell 73.7 (1993): 1267-79.

Fuchs, R., S. Schmid, and I. Mellman. "A possible role for Na+,K+-ATPase in regulating ATP-dependent endosome acidification." Proc.Natl.Acad.Sci.U.S.A 86.2 (1989): 539-43.

Furuno, N., Elzen N. den, and J. Pines. "Human cyclin A is required for mitosis until mid prophase." J.Cell Biol. 147.2 (1999): 295-306.

Gatti, P. J., et al. "Inhibition of HIV type 1 production by hygromycin B." AIDS Res.Hum.Retroviruses 14.10 (1998): 885-92.

Giese, N. A., et al. "Suppression of metastatic hemangiosarcoma by a parvovirus MVMp vector transducing the IP-10 chemokine into immunocompetent mice." Cancer Gene Ther. 9.5 (2002): 432-42.

Gilchrist, D., B. Mykytka, and M. Rexach. "Accelerating the rate of disassembly of karyopherin.cargo complexes." J.Biol.Chem. 277.20 (2002): 18161-72.

Gillooly, D. J., et al. "Localization of phosphatidylinositol 3-phosphate in yeast and mammalian cells." EMBO J. 19.17 (2000): 4577-88.

Gluck, S. L. "The vacuolar H(+)-ATPases: versatile proton pumps participating in constitutive and specialized functions of eukaryotic cells." Int.Rev.Cytol. 137C (1993): 105-37.

Goldenthal, K. L., I. Pastan, and M. C. Willingham. "Serial section analysis of clathrin-coated pits in rat liver sinusoidal endothelial cells." Exp.Cell Res. 161.2 (1985): 342-52.

Gorlich, D., et al. "Identification of different roles for RanGDP and RanGTP in nuclear protein import." EMBO J. 15.20 (1996): 5584-94.

Grewe, C., A. Beck, and H. R. Gelderblom. "HIV: early virus-cell interactions." J.Acquir.Immune.Defic.Syndr. 3.10 (1990): 965-74.

Griffiths, G., et al. "Ultrastructural localization of the regulatory (RII) subunit of cyclic AMP-dependent protein kinase to subcellular compartments active in endocytosis and recycling of membrane receptors." J.Cell Sci. 96 (Pt 4) (1990): 691-703.

Griffiths, G. and J. Gruenberg. "The arguments for pre-existing early and late endosomes." Trends Cell Biol. 1.1 (1991): 5-9.

Gruenbaum, Y., et al. "The nuclear lamina comes of age." Nat.Rev.Mol.Cell Biol. 6.1 (2005): 21-31.

Gruenberg, J. and F. R. Maxfield. "Membrane transport in the endocytic pathway." Curr.Opin.Cell Biol. 7.4 (1995): 552-63.

Gruenberg, J. "The endocytic pathway: a mosaic of domains." Nat.Rev.Mol.Cell Biol. 2.10 (2001): 721-30.

Gyllensten, K., et al. "Parvovirus B19 infection in HIV-1 infected patients with anemia." Infection 22.5 (1994): 356-58.

Hanahan, D. and R. A. Weinberg. "The hallmarks of cancer." Cell 100.1 (2000): 57-70.

Haraguchi, T., et al. "Live fluorescence imaging reveals early recruitment of emerin, LBR, RanBP2, and Nup153 to reforming functional nuclear envelopes." J.Cell Sci. 113 (Pt 5) (2000): 779-94.

Harbour, J. W., S. Ahmad, and M. El-Bash. "Rate of resolution of exudative retinal detachment after plaque radiotherapy for uveal melanoma." Arch.Ophthalmol. 120.11 (2002): 1463-69.

Heald, R. and F. McKeon. "Mutations of phosphorylation sites in lamin A that prevent nuclear lamina disassembly in mitosis." Cell 61.4 (1990): 579-89.

Hinshaw, J. E., B. O. Carragher, and R. A. Milligan. "Architecture and design of the nuclear pore complex." Cell 69.7 (1992): 1133-41.

Hocevar, B. A., D. J. Burns, and A. P. Fields. "Identification of protein kinase C (PKC) phosphorylation sites on human lamin B. Potential role of PKC in nuclear lamina structural dynamics." J.Biol.Chem. 268.10 (1993): 7545-52.

Holtta-Vuori, M., et al. "Modulation of cellular cholesterol transport and homeostasis by Rab11." Mol.Biol.Cell 13.9 (2002): 3107-22.

Hood, J. K. and P. A. Silver. "Cse1p is required for export of Srp1p/importin-alpha from the nucleus in Saccharomyces cerevisiae." J.Biol.Chem. 273.52 (1998): 35142-46.

Hsu, S. L., et al. "Caspase 3, periodically expressed and activated at G2/M transition, is required for nocodazole-induced mitotic checkpoint." Apoptosis. 11.5 (2006): 765-71.

Hueffer, K., et al. "Combinations of two capsid regions controlling canine host range determine canine transferrin receptor binding by canine and feline parvoviruses." J.Virol. 77.18 (2003): 10099-105.

Jacoby, R. O., et al. "Rodent parvovirus infections." Lab Anim Sci. 46.4 (1996): 370-80.

Jahraus, A., et al. "Evidence for retrograde traffic between terminal lysosomes and the prelysosomal/late endosome compartment." J.Cell Sci. 107 (Pt 1) (1994): 145-57.

Janik, J. E., M. M. Huston, and J. A. Rose. "Locations of adenovirus genes required for the replication of adenovirus-associated virus." Proc.Natl.Acad.Sci.U.S.A 78.3 (1981): 1925-29.
Johnson, L. S., et al. "Endosome acidification and receptor trafficking: bafilomycin A1 slows receptor externalization by a mechanism involving the receptor's internalization motif." Mol.Biol.Cell 4.12 (1993): 1251-66.

Jost, M., et al. "Phosphatidylinositol-4,5-bisphosphate is required for endocytic coated vesicle formation." Curr.Biol. 8.25 (1998): 1399-402.

Kaiser, J., R. J. Stockert, and A. W. Wolkoff. "Effect of monensin on receptor recycling during continuous endocytosis of asialoorosomucoid." Exp.Cell Res. 174.2 (1988): 472-80.

Kaludov, N., et al. "Adeno-associated virus serotype 4 (AAV4) and AAV5 both require sialic acid binding for hemagglutination and efficient transduction but differ in sialic acid linkage specificity." J.Virol. 75.15 (2001): 6884-93.

Kann, M., et al. "Phosphorylation-dependent binding of hepatitis B virus core particles to the nuclear pore complex." J.Cell Biol. 145.1 (1999): 45-55.

Kaufmann, B., A. A. Simpson, and M. G. Rossmann. "The structure of human parvovirus B19." Proc.Natl.Acad.Sci.U.S.A 101.32 (2004): 11628-33.

Kennedy, N. J., et al. "Caspase activation is required for T cell proliferation." J.Exp.Med. 190.12 (1999): 1891-96.

Kielian, M. and A. Helenius. "pH-induced alterations in the fusogenic spike protein of Semliki Forest virus." J.Cell Biol. 101.6 (1985): 2284-91.

Kielian, M. "Membrane fusion and the alphavirus life cycle." Adv.Virus Res. 45 (1995): 113-51.

Kobe, B. "Autoinhibition by an internal nuclear localization signal revealed by the crystal structure of mammalian importin alpha." Nat.Struct.Biol. 6.4 (1999): 388-97.

Kotin, R. M., et al. "Site-specific integration by adeno-associated virus." Proc.Natl.Acad.Sci.U.S.A 87.6 (1990): 2211-15.

Kornfeld, S. and I. Mellman. "The biogenesis of lysosomes." Annu.Rev.Cell Biol. 5 (1989): 483-525.

Kumar, S. and M. F. Lavin. "The ICE family of cysteine proteases as effectors of cell death." Cell Death.Differ. 3.3 (1996): 255-67

Kutay, U., et al. "Export of importin alpha from the nucleus is mediated by a specific nuclear transport factor." Cell 90.6 (1997): 1061-71.

Lang, S. "[Experimental research on gene therapy and transfer on head and neck cancer in the course of a multimodal therapy concept]." Laryngorhinootologie 81.7 (2002): 534-35.

Lange, A., et al. "Classical nuclear localization signals: definition, function, and interaction with importin alpha." J.Biol.Chem. 282.8 (2007): 5101-05.

Launay, S., et al. "Vital functions for lethal caspases." Oncogene 24.33 (2005): 5137-48.

Lazebnik, Y. A., et al. "Nuclear events of apoptosis in vitro in cell-free mitotic extracts: a model system for analysis of the active phase of apoptosis." J.Cell Biol. 123.1 (1993): 7-22.

Lazebnik, Y. A., et al. "Studies of the lamin proteinase reveal multiple parallel biochemical pathways during apoptotic execution." Proc.Natl.Acad.Sci.U.S.A 92.20 (1995): 9042-46.

Lee, S. J., et al. "Structural basis for nuclear import complex dissociation by RanGTP." Nature 435.7042 (2005): 693-96.

Lenart, P., et al. "Nuclear envelope breakdown in starfish oocytes proceeds by partial NPC disassembly followed by a rapidly spreading fenestration of nuclear membranes." J.Cell Biol. 160.7 (2003): 1055-68.

Lenart, P. and J. Ellenberg. "Monitoring the permeability of the nuclear envelope during the cell cycle." Methods 38.1 (2006): 17-24.

Leopold, P. L., et al. "Dynein- and microtubule-mediated translocation of adenovirus serotype 5 occurs after endosomal lysis." Hum.Gene Ther. 11.1 (2000): 151-65.

Li, X. and S. L. Rhode, III. "Mutation of lysine 405 to serine in the parvovirus H-1 NS1 abolishes its functions for viral DNA replication, late promoter trans activation, and cytotoxicity." J.Virol. 64.10 (1990): 4654-60.

Li, Y., et al. "Genome organization of the densovirus from Bombyx mori (BmDNV-1) and enzyme activity of its capsid." J.Gen.Virol. 82.Pt 11 (2001): 2821-25.

Lin, F. T., et al. "Clathrin-mediated endocytosis of the beta-adrenergic receptor is regulated by phosphorylation/dephosphorylation of beta-arrestin1." J.Biol.Chem. 272.49 (1997): 31051-57.

Lombardo, E., et al. "Complementary roles of multiple nuclear targeting signals in the capsid proteins of the parvovirus minute virus of mice during assembly and onset of infection." J.Virol. 76.14 (2002): 7049-59.

MacaUlay, C., E. Meier, and D. J. Forbes. "Differential mitotic phosphorylation of proteins of the nuclear pore complex." J.Biol.Chem. 270.1 (1995): 254-62.

Mallard, F., et al. "Direct pathway from early/recycling endosomes to the Golgi apparatus revealed through the study of shiga toxin B-fragment transport." J.Cell Biol. 143.4 (1998): 973-90.

Marsh, M. and A. Helenius. "Virus entry into animal cells." Adv.Virus Res. 36 (1989): 107-51.

Marsh, M. and D. Cutler. "Taking the Rabs off endocytosis." Curr.Biol. 3.1 (1993): 30-32.

Marsh, M. and R. Bron. "SFV infection in CHO cells: cell-type specific restrictions to productive virus entry at the cell surface." J.Cell Sci. 110 (Pt 1) (1997): 95-103.

Marsh, M. and A. Pelchen-Matthews. "Endocytosis in viral replication." Traffic. 1.7 (2000): 525-32.

Mani, B., et al. "Low pH-dependent endosomal processing of the incoming parvovirus minute virus of mice virion leads to externalization of the VP1 N-terminal sequence (N-VP1), N-VP2 cleavage, and uncoating of the full-length genome." J.Virol. 80.2 (2006): 1015-24.

Martin, D. A., et al. "Membrane oligomerization and cleavage activates the caspase-8 (FLICE/MACHalpha1) death signal." J.Biol.Chem. 273.8 (1998): 4345-49.

Matlin, K. S., et al. "Infectious entry pathway of influenza virus in a canine kidney cell line." J.Cell Biol. 91.3 Pt 1 (1981): 601-13.

Matsuura, Y., et al. "Structural basis for Nup2p function in cargo release and karyopherin recycling in nuclear import." EMBO J. 22.20 (2003): 5358-69.

Matsuura, Y. and M. Stewart. "Structural basis for the assembly of a nuclear export complex." Nature 432.7019 (2004): 872-77.

Matsuura, Y. and M. Stewart. "Nup50/Npap60 function in nuclear protein import complex disassembly and importin recycling." EMBO J. 24.21 (2005): 3681-89.

Maxwell, I. H., K. L. Terrell, and F. Maxwell. "Autonomous parvovirus vectors." Methods 28.2 (2002): 168-81.

McKenna, R., et al. "Three-dimensional structure of Aleutian mink disease parvovirus: implications for disease pathogenicity." J.Virol. 73.8 (1999): 6882-91.

Mellman, I. and H. Plutner. "Internalization and degradation of macrophage Fc receptors bound to polyvalent immune complexes." J.Cell Biol. 98.4 (1984): 1170-77.

Mellman, I. "Endocytosis and molecular sorting." Annu.Rev.Cell Dev.Biol. 12 (1996): 575-625.

Minc, E., et al. "Localization and phosphorylation of HP1 proteins during the cell cycle in mammalian cells." Chromosoma 108.4 (1999): 220-34.

Moehler, M., et al. "Effective infection, apoptotic cell killing and gene transfer of human hepatoma cells but not primary hepatocytes by parvovirus H1 and derived vectors." Cancer Gene Ther. 8.3 (2001): 158-67.

Moehler, M., et al. "Oncolytic parvovirus H1 induces release of heat-shock protein HSP72 in susceptible human tumor cells but may not affect primary immune cells." Cancer Gene Ther. 10.6 (2003): 477-80.

Montesano, R., et al. "Non-coated membrane invaginations are involved in binding and internalization of cholera and tetanus toxins." Nature 296.5858 (1982): 651-53.

Mukherjee, S., R. N. Ghosh, and F. R. Maxfield. "Endocytosis." Physiol Rev. 77.3 (1997): 759-803.

Muzio, M., et al. "An induced proximity model for caspase-8 activation." J.Biol.Chem. 273.5 (1998): 2926-30.

Nadler, S. G., et al. "Differential expression and sequence-specific interaction of karyopherin alpha with nuclear localization sequences." J.Biol.Chem. 272.7 (1997): 4310-15.

Naeger, L. K., J. Cater, and D. J. Pintel. "The small nonstructural protein (NS2) of the parvovirus minute virus of mice is required for efficient DNA replication and infectious virus production in a cell-type-specific manner." J.Virol. 64.12 (1990): 6166-75.

Nakamura, N. and Y. Wada. "Properties of DNA fragmentation activity generated by ATP depletion." Cell Death.Differ. 7.5 (2000): 477-84.

Neamati, N., et al. "Degradation of lamin B1 precedes oligonucleosomal DNA fragmentation in apoptotic thymocytes and isolated thymocyte nuclei." J.Immunol. 154.8 (1995): 3788-95.

Nelson, N. "The vacuolar proton-ATPase of eukaryotic cells." Bioessays 7.6 (1987): 251-54.

Nicholson, D. W., et al. "Identification and inhibition of the ICE/CED-3 protease necessary for mammalian apoptosis." Nature 376.6535 (1995): 37-43.

Nicholson, D. W. and N. A. Thornberry. "Caspases: killer proteases." Trends Biochem.Sci. 22.8 (1997): 299-306.

Nikolakaki, E., et al. "Mitotic phosphorylation of the lamin B receptor by a serine/arginine kinase and p34(cdc2)." J.Biol.Chem. 272.10 (1997): 6208-13.

Nuesch, J. P. and P. Tattersall. "Nuclear targeting of the parvoviral replicator molecule NS1: evidence for self-association prior to nuclear transport." Virology 196.2 (1993): 637-51.

Nuesch, J. P., et al. "Biochemical activities of minute virus of mice nonstructural protein NS1 are modulated In vitro by the phosphorylation state of the polypeptide." J.Virol. 72.10 (1998): 8002-12.

Nunez, M. T. and J. Glass. "Iron uptake in reticulocytes. Inhibition mediated by the ionophores monensin and nigerisin." J.Biol.Chem. 260.27 (1985): 14707-11.

Oberhammer, F. A., et al. "Chromatin condensation during apoptosis is accompanied by degradation of lamin A+B, without enhanced activation of cdc2 kinase." J.Cell Biol. 126.4 (1994): 827-37.

Orth, K., et al. "The CED-3/ICE-like protease Mch2 is activated during apoptosis and cleaves the death substrate lamin A." J.Biol.Chem. 271.28 (1996): 16443-46.

Pante, N. and U. Aebi. "Molecular dissection of the nuclear pore complex." Crit Rev.Biochem.Mol.Biol. 31.2 (1996): 153-99.

Pante, N. and M. Kann. "Nuclear pore complex is able to transport macromolecules with diameters of about 39 nm." Mol.Biol.Cell 13.2 (2002): 425-34.

Parker, J. S. and C. R. Parrish. "Cellular uptake and infection by canine parvovirus involves rapid dynamin-regulated clathrin-mediated endocytosis, followed by slower intracellular trafficking." J.Virol. 74.4 (2000): 1919-30.

Parker, J. S., et al. "Canine and feline parvoviruses can use human or feline transferrin receptors to bind, enter, and infect cells." J.Virol. 75.8 (2001): 3896-902.

Petruzziello, R., et al. "Pathway of rubella virus infectious entry into Vero cells." J.Gen.Virol. 77 (Pt 2) (1996): 303-08.

Pfaller, R., C. Smythe, and J. W. Newport. "Assembly/disassembly of the nuclear envelope membrane: cell cycle-dependent binding of nuclear membrane vesicles to chromatin in vitro." Cell 65.2 (1991): 209-17.

Pfaller, R. and J. W. Newport. "Assembly/disassembly of the nuclear envelope membrane. Characterization of the membrane-chromatin interaction using partially purified regulatory enzymes." J.Biol.Chem. 270.32 (1995): 19066-72.

Pyrpasopoulou, A., et al. "The lamin B receptor (LBR) provides essential chromatin docking sites at the nuclear envelope." EMBO J. 15.24 (1996): 7108-19.

Rabe, B., et al. "Nuclear import of hepatitis B virus capsids and release of the viral genome." Proc.Natl.Acad.Sci.U.S.A 100.17 (2003): 9849-54.

Rabinowitz, J. E. and R. J. Samulski. "Building a better vector: the manipulation of AAV virions." Virology 278.2 (2000): 301-08.

Rao, K., et al. "Separation of Fe+3 from transferrin in endocytosis. Role of the acidic endosome." FEBS Lett. 160.1-2 (1983): 213-16.

Rao, L., D. Perez, and E. White. "Lamin proteolysis facilitates nuclear events during apoptosis." J.Cell Biol. 135.6 Pt 1 (1996): 1441-55.

Rayet, B., et al. "Induction of programmed cell death by parvovirus H-1 in U937 cells: connection with the tumor necrosis factor alpha signalling pathway." J.Virol. 72.11 (1998): 8893-903.

Reguera, J., et al. "Role of interfacial amino acid residues in assembly, stability, and conformation of a spherical virus capsid." Proc.Natl.Acad.Sci.U.S.A 101.9 (2004): 2724-29.

Riezman, H., et al. "Molecular mechanisms of endocytosis." Cell 91.6 (1997): 731-38.

Riolobos, L., et al. "Nuclear transport of trimeric assembly intermediates exerts a morphogenetic control on the icosahedral parvovirus capsid." J.Mol.Biol. 357.3 (2006): 1026-38.

Rhode, S. L., III. "trans-Activation of parvovirus P38 promoter by the 76K noncapsid protein." J.Virol. 55.3 (1985): 886-89.

Rommelaere, J. and J. J. Cornelis. "Antineoplastic activity of parvoviruses." J.Virol.Methods 33.3 (1991): 233-51.

Rosado, J. A., et al. "Early caspase-3 activation independent of apoptosis is required for cellular function." J.Cell Physiol 209.1 (2006): 142-52.

Rubino, M., et al. "Selective membrane recruitment of EEA1 suggests a role in directional transport of clathrin-coated vesicles to early endosomes." J.Biol.Chem. 275.6 (2000): 3745-48.

Rudel, T. and G. M. Bokoch. "Membrane and morphological changes in apoptotic cells regulated by caspase-mediated activation of PAK2." Science 276.5318 (1997): 1571-74.

Sahara, S., et al. "Acinus is a caspase-3-activated protein required for apoptotic chromatin condensation." Nature 401.6749 (1999): 168-73.

Sakahira, H., M. Enari, and S. Nagata. "Cleavage of CAD inhibitor in CAD activation and DNA degradation during apoptosis." Nature 391.6662 (1998): 96-99.

Salina, D., et al. "Nup358 integrates nuclear envelope breakdown with kinetochore assembly." J.Cell Biol. 162.6 (2003): 991-1001.

Samulski, R. J., et al. "Targeted integration of adeno-associated virus (AAV) into human chromosome 19." EMBO J. 10.12 (1991): 3941-50.

Sanlioglu, S., et al. "Endocytosis and nuclear trafficking of adeno-associated virus type 2 are controlled by rac1 and phosphatidylinositol-3 kinase activation." J.Virol. 74.19 (2000): 9184-96.

Sato, S. B. and S. Toyama. "Interference with the endosomal acidification by a monoclonal antibody directed toward the 116 (100)-kD subunit of the vacuolar type proton pump." J.Cell Biol. 127.1 (1994): 39-53.

Sawicki, S. G. and D. L. Sawicki. "Coronavirus minus-strand RNA synthesis and effect of cycloheximide on coronavirus RNA synthesis." J.Virol. 57.1 (1986): 328-34.

Schwoebel, E. D., T. H. Ho, and M. S. Moore. "The mechanism of inhibition of Ran-dependent nuclear transport by cellular ATP depletion." J.Cell Biol. 157.6 (2002): 963-74.

Shah, S., S. Tugendreich, and D. Forbes. "Major binding sites for the nuclear import receptor are the internal nucleoporin Nup153 and the adjacent nuclear filament protein Tpr." J.Cell Biol. 141.1 (1998): 31-49.

Shisheva, A., et al. "Localization and insulin-regulated relocation of phosphoinositide 5-kinase PIKfyve in 3T3-L1 adipocytes." J.Biol.Chem. 276.15 (2001): 11859-69.

Simonsen, A., et al. "EEA1 links PI(3)K function to Rab5 regulation of endosome fusion." Nature 394.6692 (1998): 494-98.

Simonsen, A., et al. "The role of phosphoinositides in membrane transport." Curr.Opin.Cell Biol. 13.4 (2001): 485-92.

Sipe, D. M. and R. F. Murphy. "High-resolution kinetics of transferrin acidification in BALB/c 3T3 cells: exposure to pH 6 followed by temperature-sensitive alkalinization during recycling." Proc.Natl.Acad.Sci.U.S.A 84.20 (1987): 7119-23.

Sodeik, B. "Mechanisms of viral transport in the cytoplasm." Trends Microbiol. 8.10 (2000): 465-72.

Somsel, Rodman J. and A. Wandinger-Ness. "Rab GTPases coordinate endocytosis." J.Cell Sci. 113 Pt 2 (2000): 183-92.

Strasser, A., L. O'Connor, and V. M. Dixit. "Apoptosis signaling." Annu.Rev.Biochem. 69 (2000): 217-45.

Suikkanen, S., et al. "Release of canine parvovirus from endocytic vesicles." Virology 316.2 (2003): 267-80.

Suikkanen, S., et al. "Exploitation of microtubule cytoskeleton and dynein during parvoviral traffic toward the nucleus." J.Virol. 77.19 (2003): 10270-79.

Summerford, C. and R. J. Samulski. "Membrane-associated heparan sulfate proteoglycan is a receptor for adeno-associated virus type 2 virions." J.Virol. 72.2 (1998): 1438-45.

Susin, S. A., et al. "Two distinct pathways leading to nuclear apoptosis." J.Exp.Med. 192.4 (2000): 571-80.

Srivastava, A. "Parvovirus-based vectors for human gene therapy." Blood Cells 20.2-3 (1994): 531-36.

Srinivasula, S. M., et al. "Molecular ordering of the Fas-apoptotic pathway: the Fas/APO-1 protease Mch5 is a CrmA-inhibitable protease that activates multiple Ced-3/ICE-like cysteine proteases." Proc.Natl.Acad.Sci.U.S.A 93.25 (1996): 14486-91.

Srinivasula, S. M., et al. "Generation of constitutively active recombinant caspases-3 and -6 by rearrangement of their subunits." J.Biol.Chem. 273.17 (1998): 10107-11.

Stuurman, N., S. Heins, and U. Aebi. "Nuclear lamins: their structure, assembly, and interactions." J.Struct.Biol. 122.1-2 (1998): 42-66.

Tabas, I., et al. "Endocytosed beta-VLDL and LDL are delivered to different intracellular vesicles in mouse peritoneal macrophages." J.Cell Biol. 111.3 (1990): 929-40.

Tabas, I., et al. "The influence of particle size and multiple apoprotein E-receptor interactions on the endocytic targeting of beta-VLDL in mouse peritoneal macrophages." J.Cell Biol. 115.6 (1991): 1547-60.

Tattersall, P., et al. "Three structural polypeptides coded for by minite virus of mice, a parvovirus." J.Virol. 20.1 (1976): 273-89.

Tattersall, P., A. J. Shatkin, and D. C. Ward. "Sequence homology between the structural polypeptides of minute virus of mice." J.Mol.Biol. 111.4 (1977): 375-94.

Thacker, T. C. and F. B. Johnson. "Binding of bovine parvovirus to erythrocyte membrane sialylglycoproteins." J.Gen.Virol. 79 (Pt 9) (1998): 2163-69.

Thornberry, N. A. and Y. Lazebnik. "Caspases: enemies within." Science 281.5381 (1998): 1312-16.

Toolan, H. W., et al. "H-1 virus viremia in the Human." Proc.Soc.Exp.Biol.Med. 119 (1965): 711-15.

Townsley, A. C., et al. "Vaccinia virus entry into cells via a low-pH-dependent endosomal pathway." J.Virol. 80.18 (2006): 8899-908.

Tran, D., et al. "Ligands internalized through coated or noncoated invaginations follow a common intracellular pathway." Proc.Natl.Acad.Sci.U.S.A 84.22 (1987): 7957-61

Trowbridge, I. S., J. F. Collawn, and C. R. Hopkins. "Signal-dependent membrane protein trafficking in the endocytic pathway." Annu.Rev.Cell Biol. 9 (1993): 129-61.

Tullis, G. E., L. R. Burger, and D. J. Pintel. "The minor capsid protein VP1 of the autonomous parvovirus minute virus of mice is dispensable for encapsidation of progeny single-stranded DNA but is required for infectivity." J.Virol. 67.1 (1993): 131-41.

Turkewitz, A. P., A. L. Schwartz, and S. C. Harrison. "A pH-dependent reversible conformational transition of the human transferrin receptor leads to self-association." J.Biol.Chem. 263.31 (1988): 16309-15.

van Weert, A. W., et al. "Transport from late endosomes to lysosomes, but not sorting of integral membrane proteins in endosomes, depends on the vacuolar proton pump." J.Cell Biol. 130.4 (1995): 821-34.

Vigers, G. P. and M. J. Lohka. "Regulation of nuclear envelope precursor functions during cell division." J.Cell Sci. 102 (Pt 2) (1992): 273-84.

Vihinen-Ranta, M., et al. "Characterization of a nuclear localization signal of canine parvovirus capsid proteins." Eur.J.Biochem. 250.2 (1997): 389-94.

Vihinen-Ranta, M., et al. "Intracellular route of canine parvovirus entry." J.Virol. 72.1 (1998): 802-06.

Vihinen-Ranta, M., W. Yuan, and C. R. Parrish. "Cytoplasmic trafficking of the canine parvovirus capsid and its role in infection and nuclear transport." J.Virol. 74.10 (2000): 4853-59.

Vihinen-Ranta, M., et al. "The VP1 N-terminal sequence of canine parvovirus affects nuclear transport of capsids and efficient cell infection." J.Virol. 76.4 (2002): 1884-91.

Vihinen-Ranta, M., S. Suikkanen, and C. R. Parrish. "Pathways of cell infection by parvoviruses and adeno-associated viruses." J.Virol. 78.13 (2004): 6709-14.

Vilhardt, F., et al. "Urokinase-type plasminogen activator receptor is internalized by different mechanisms in polarized and nonpolarized Madin-Darby canine kidney epithelial cells." Mol.Biol.Cell 10.1 (1999): 179-95.

Villa, P., S. H. Kaufmann, and W. C. Earnshaw. "Caspases and caspase inhibitors." Trends Biochem.Sci. 22.10 (1997): 388-93.

Walker, N. P., et al. "Crystal structure of the cysteine protease interleukin-1 beta-converting enzyme: a (p20/p10)2 homodimer." Cell 78.2 (1994): 343-52.

Walters, R. W., et al. "Binding of adeno-associated virus type 5 to 2,3-linked sialic acid is required for gene transfer." J.Biol.Chem. 276.23 (2001): 20610-16.

Weaver, V. M., et al. "Degradation of nuclear matrix and DNA cleavage in apoptotic thymocytes." J.Cell Sci. 109 (Pt 1) (1996): 45-56.

Weis, K., C. Dingwall, and A. I. Lamond. "Characterization of the nuclear protein import mechanism using Ran mutants with altered nucleotide binding specificities." EMBO J. 15.24 (1996): 7120-28.

Whittaker, G. R., M. Kann, and A. Helenius. "Viral entry into the nucleus." Annu.Rev.Cell Dev.Biol. 16 (2000): 627-51.

Willwand, K. and B. Hirt. "The major capsid protein VP2 of minute virus of mice (MVM) can form particles which bind to the 3'-terminal hairpin of MVM replicative-form DNA and package single-stranded viral progeny DNA." J.Virol. 67.9 (1993): 5660-63.

Wilson, K. P., et al. "Structure and mechanism of interleukin-1 beta converting enzyme." Nature 370.6487 (1994): 270-75.

Wu, J., et al. "Nup358, a cytoplasmically exposed nucleoporin with peptide repeats, Ran-GTP binding sites, zinc fingers, a cyclophilin A homologous domain, and a leucine-rich region." J.Biol.Chem. 270.23 (1995): 14209-13.

Wyllie, A. H., J. F. Kerr, and A. R. Currie. "Cell death: the significance of apoptosis." Int.Rev.Cytol. 68 (1980): 251-306.

Yamashiro, D. J., et al. "Segregation of transferrin to a mildly acidic (pH 6.5) para-Golgi compartment in the recycling pathway." Cell 37.3 (1984): 789-800.

Yuan, C. Q., Y. N. Li, and X. F. Zhang. "Down-regulation of apoptosis-inducing factor protein by RNA interference inhibits UVA-induced cell death." Biochem.Biophys.Res.Commun. 317.4 (2004): 1108-13.

Zadori, Z., et al. "A viral phospholipase A2 is required for parvovirus infectivity." Dev.Cell 1.2 (2001): 291-302.

Zhou, W., et al. "Protein kinase C-mediated bidirectional regulation of DNA synthesis, RB protein phosphorylation, and cyclin-dependent kinases in human vascular endothelial cells." J.Biol.Chem. 268.31 (1993): 23041-48.

10. Acknowledgements

This research was performed in the *Institute of Medical Virology*, *Justus-Liebig-University, Gießen*, *Germany* and some part was also performed in *REGER, Bordeaux 2 University, Bordeaux, France.* During the laboratory research and thesis writing, many colleagues, scientists and friends supported and encouraged me to finish my work. Therefore, I will take this opportunity to acknowledge those persons.

I take this opportunity with pride and immense pleasure in expressing my deep regards to **Prof. Dr. Michael Kann** for giving me the chance to work on this thesis. I am very thankful for the work possibilities he gave me during my stay as well as for his close and effective supervision and very stimulating discussions.

I would also like to sincerely thank **Prof. Dr. Alfred M Pingoud**, for my reviewer from *Institute for Biochemistry and Nuclear Protein Complexes*, *Justus-Liebig-University, Gießen*, Germany for his friendly and excellent guidance during the seminars, critical correction of my thesis and for financial support (DFG scholarship).

I am especially grateful to **Prof. Dr. rer. nat Karl-Heinz Kogel**, for my reviewer from *Institute for Phytopathology and Applied Zoology*, *Justus-Liebig-University, Gießen*, Germany to be one of the member of my examination committee.

I wish to particularly acknowledge and express my sincere gratitude to **Prof. Dr. Wolfram H. Gerlich,** director for *Institute for Medical Virology*, *Justus-Liebig-University, Gießen*, Germany for his help and support to do research work in his department.

I am especially grateful to **Prof. Simon Litvik**, a director, *REGER, Bordeaux 2 University, Bordeaux, France* for giving me an opportunity to work such a renound laboratory and special thanks to **Dr. Jan Cornelis, Dr. Christiane Dinsart & Dr. Derrick Robinson** for providing the H-1 virus and antibodies.

I would like to appreciate to **Deutsche Forschungsgemeinschaft (DFG)** for the financial support for 3 years of my Ph.D work in Germany and the **Universite de Bordeaux 2** for supporting my work in France.

I cannot refrain from especially thanking my colleagues **Dr. Andre Schmitz, Dr. Birgit Rabe, Dr. Holger Arends, Dr. Aris Haryanto, Alexandra Schwarz, Michael Foss, Dr. Sebastian Laine, Dr. Therese Erin-Astier** and other lab members (whose name are not mentioned) for their inspiring discussions and stimulating cooperation, leading to a most pleasant research work as well as for the nice atmosphere in and outside the lab. Also i would like to express thanks to **Nathali Sanant** to help me in using confocal microscope **and Dr. Jamilah Michel & Isabelle Dewor** for the administration work.

Specially, I would like to address my special thanks to my dear husband **Srikanth Karnati** for his immense love, support, suggestion and patience. Finally, I would like to acknowledge my parents **Dr. R.K. Porwal, Mrs. Renu Porwal**, my sister **Mayuri Porwal**, my parent in-laws and all family members and friends for their continuous support and encouragement through out my thesis work.

11. Curriculum Vitae

Manvi Porwal
164 cours de L'Argonne, CDU; 33000 - Bordeaux, France
Home: +33-557 598 552; Mobile-+33-616 551 610
Email: porwalmanvi@yahoo.co.in

Nationality: Indian
Family Status: Married
Date of Birth: 01 July 79

Education

2005- till to date	**Assistante Associée -** "Transport mechanisms of Parvovirus H-1" **CNRS-MCMP, Universite Bordeaux 2, Bordeaux, France.**
2003-2005	**PhD research - "**Analysing the nuclear import of parvoviruses- Effect of parvovirus H-1 on NE". **Justus Liebig University Giessen, Germany.**
1999-2001	**Master of Science in Microbiology** **Barkatullah University, Bhopal, India. (74% - First division)**
1996-1999	**Bachelor of Science- Chemistry, Botany & Zoology.** **Rohillkhand University, Bareilly, India. (82% - First division)**
1995	**Intermediate Education – Biology, Physics& Chemistry, S.M.I.C, Chandausi, India, India. (75% - First Division)**
1993	**Secondary School Education** **B.M.G.I.C, Chandausi, India. (72% - First Division)**

Relevant Training & Experience

10/2002-12/2002	**Internship -** "Expression and purification of a DNA methyl-transferase from *E. coli*" at the Institute for crystallography, **Freie University, Berlin, Germany.**
02/2002-09/2002	**Research Chemist -** "Recombinant protein expression" in the multinational company "**Ranbaxy Research Laboratories" NewDelhi, India.**
01/2001-06/ 2001	**Diploma work** - "Cloning and characterization of genome of rice *Tungro baciliform* virus from Tamil Nadu", Dept. of Molecular biology, **Delhi University, New Delhi, India**.

Scholarships/Prizes Awarded

- Gold Medal for securing ***top position in B.Sc. biology stream*** by Rohillkhand University Bareilly, U.P, India.

- Six month scholarship to complete r***esearch training in Delhi University, New Delhi.*** Obtained by the Institute Of Microbiology & Biotechnology, Barkatullah University, Bhopal, M.P., India.

- Three months scholarship from the DAAD (German Academic Exchange Service) to complete the ***research internship*** in the Institute of Crystallography at the Freie University, Berlin, Germany.

Conferences & Workshops

Active participation in **"Conference on Bioinformatics"** held at Bhopal conducted by **National Academy of Sciences India,** 11-13 November 1999, Bhopal, India.

Attended workshop on **"Plant Diversity, Inventorisation and Conservation**" held at **Central Institute for Medicinal and Aromatic Plants (CIMAP),** 16 Jan - 04 Feb 2000, Lucknow, India.

Poster on the meeting of the study group "**Cell biology of viral infections**" within the Society of Virology, 15-17 September 2003**,** Zeilitzheim, Germany**.**

Poster on the "**International meeting for virology"** organized by the IUMS (International Union of Microbiological Societies), 23-28 July 2005, San Francisco, U.S.A

Publications

Manvi Porwal, Sarah Cohen, Nelly Panté, Maija Vihinen-Ranta, Michael Kann. An interaction between parvoviral capsids and the nuclear pore induce mitosis-like nuclear envelope breakdown in the absence of cytosolic factors. (in preparation).

Holger Ahrens, **Manvi Porwal**, Birgit Rabe and Michael Kann**.** Evaluation of the nuclear entry of parvovirus H-1. (in preparation).